

AD-A048 981

MCDONNELL DOUGLAS RESEARCH LABS ST LOUIS MO
STUDY OF THE CLASS TRANSITION IN CROSSLINKED POLYMERS USING NUC--ETC(U)
DEC 77 I M BROWN, A C LIND
MDC-Q0633

F/G 7/3

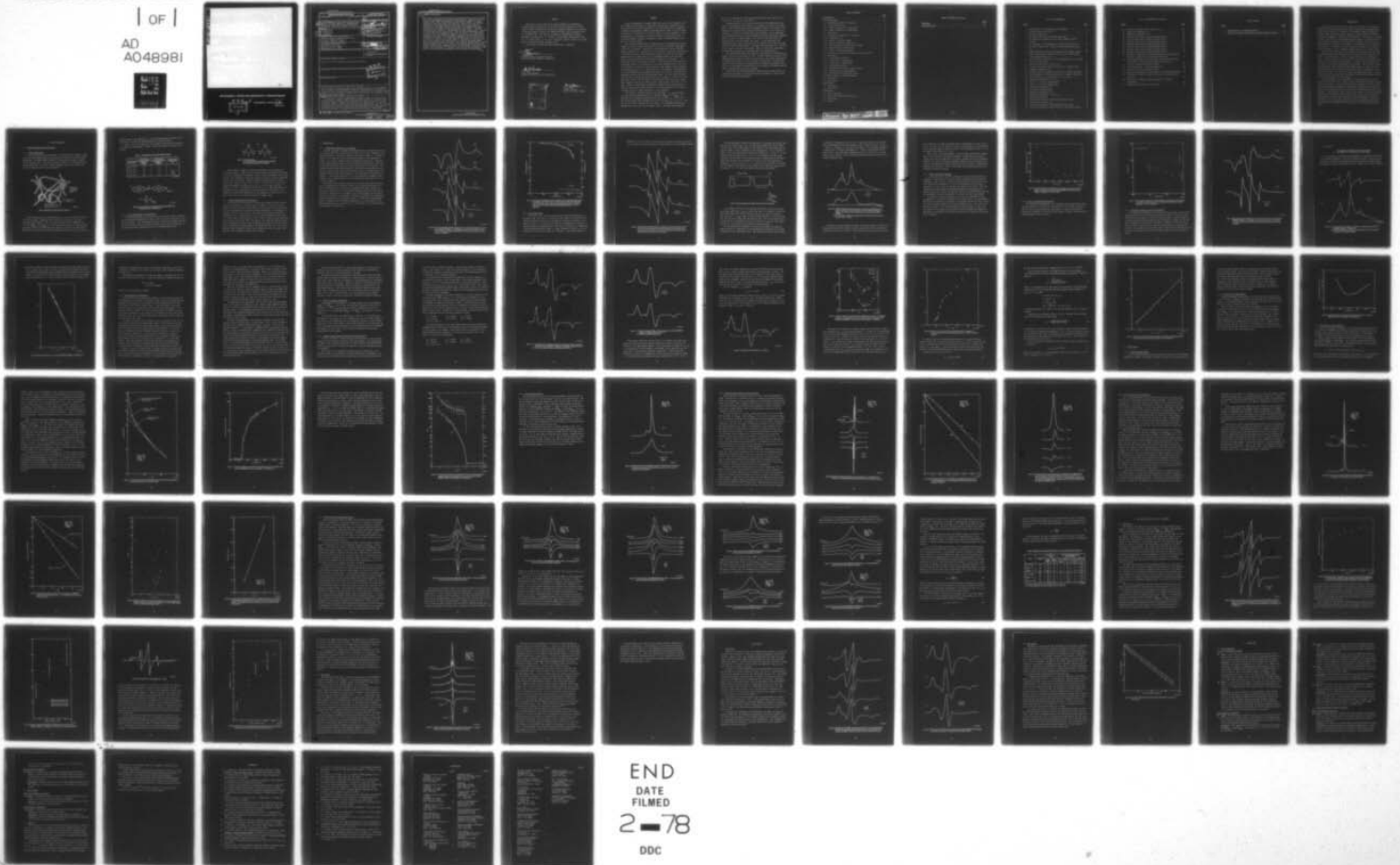
N00019-76-C-0565

NL

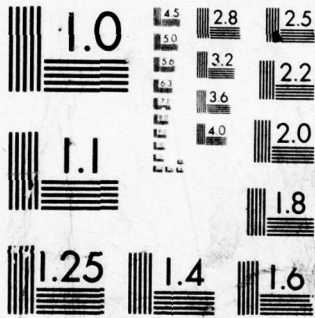
UNCLASSIFIED

1 of 1

AD
A048981



END
DATE
FILMED
2-78
DDC



MICROCOPY RESOLUTION TEST CHART
NATIONAL BUREAU OF STANDARDS-1963-A

AD-4048981

MCDONNELL DOUGLAS RESEARCH LABORATORIES

DDG
RECEIVED
JAN 23 1978
F



UNCLASSIFIED

SECURITY CLASSIFICATION OF THIS PAGE (When Data Entered)

REPORT DOCUMENTATION PAGE		READ INSTRUCTIONS BEFORE COMPLETING FORM
1. REPORT NUMBER	2. GOVT ACCESSION NO.	3. RECIPIENT'S CATALOG NUMBER
4. TITLE (and Subtitle) STUDY OF THE GLASS TRANSITION IN <u>CROSSLINKED</u> POLYMERS USING NUCLEAR AND ELECTRON MAGNETIC RESONANCE.		5. TYPE OF REPORT & PERIOD COVERED Final Report. 6 Sep 76-6 Dec 77,
7. AUTHOR(s) I. M./Brown A. C./Lind		6. PERFORMING ORG. REPORT NUMBER MDC-Q0633
9. PERFORMING ORGANIZATION NAME AND ADDRESS McDonnell Douglas Research Laboratories McDonnell Douglas Corporation St. Louis, Missouri 63166		8. CONTRACT OR GRANT NUMBER(s) N00019-76-C-0565 new
11. CONTROLLING OFFICE NAME AND ADDRESS Department of the Navy Naval Air Systems Command Washington, D. C. 20361		10. PROGRAM ELEMENT, PROJECT, TASK AREA & WORK UNIT NUMBERS
14. MONITORING AGENCY NAME & ADDRESS (if different from Controlling Office)		12. REPORT DATE 6 Dec 77
		13. NUMBER OF PAGES 87 (12) 86p.
		15. SECURITY CLASS. (if this report) Unclassified
16. DISTRIBUTION STATEMENT (of this Report) Approved for public release; distribution unlimited.		15a. DECLASSIFICATION/DOWNGRADING SCHEDULE
17. DISTRIBUTION STATEMENT (of the abstract entered in Block 20, if different from Report)		
18. SUPPLEMENTARY NOTES		
19. KEY WORDS (Continue on reverse side if necessary and identify by block number) Glass transition temperature, Main-chain segmental motion, Electron paramagnetic resonance, Nuclear magnetic resonance, Dimethylsiloxane, Bisphenol-A carbonate, Block copolymer, Phases, Electron and nuclear spin relaxation times, Domain, Plasticizer, Computer simulations, Electron spin echo, Motional correlation times, Epoxy resin		
20. ABSTRACT (Continue on reverse side if necessary and identify by block number) Pulsed and cw electron paramagnetic resonance (EPR) and pulsed proton nuclear magnetic resonance (NMR) techniques were applied to the study of the main-chain segmental motions associated with the glass transitions in block copolymers and the influence of plasticizers on these motions. In the EPR experiments, both cw and electron spin echo measurements were made of a stable nitroxide radical which was used as an EPR spin probe of its environment in the block copolymer. The proton NMR experiments included conventional		

DDC
 RECEIVED
 JAN 23 1978
 F

405 315 Au

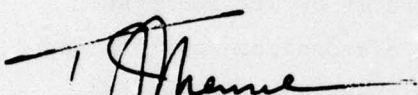
20. ABSTRACT (Continued)

spin-lattice and spin-spin relaxation time measurements along with broadline and multiple-pulsed partially-relaxed spectra. Samples of polydimethylsiloxane (DMS) and bisphenol-A polycarbonate (BPAC) of varying composition and block length were examined. Above 220 K, the radicals exhibited both broadline and narrowline EPR spectra indicating the coexistence of two phases wherein the radical can undergo either slow motions (the slow phase) or fast motions (the fast phase). The NMR experiments were capable of distinguishing motional activity as a function of proton position along the block. Both the EPR and NMR results indicated that main-chain segmental motion at the center of the DMS blocks exceeded that at the ends and propagated outward along the block as the temperature increased. The temperature dependence of the ratios of (a) the number of radicals in the fast phase to the number in the slow phase and (b) the protons in the rubbery phase to those in the rigid phase agreed qualitatively with this model. Both the EPR and NMR results showed that the primary effect of the perdeuterocyclohexane plasticizer was to enhance the main-chain segmental motions located mainly in the DMS blocks. Finally, the feasibility of extending these EPR and NMR techniques to the study of glass transition phenomena in epoxy resins was established.

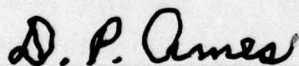
PREFACE

This report is an account of the work performed by the McDonnell Douglas Research Laboratories on the Study of Glass Transition in Cross-linked Polymers using Nuclear and Electron Magnetic Resonance for the Naval Air Systems Command, Contract No. N00019-76-C-0565, from 6 September 1976 to 6 December 1977. The work was performed in the Radiation Sciences Department, managed by Dr. T. J. Menne. The principal investigators were Dr. I. M. Brown and Dr. A. C. Lind. The project monitor was Mr. M. A. Domen, Naval Air Systems Command, Washington, D.C.

This technical report has been reviewed and is approved.

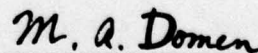


T. J. Menne
Chief Scientist, Radiation Sciences
McDonnell Douglas Research Laboratories



D. P. Ames
Staff Vice President
McDonnell Douglas Research Laboratories

ACCESSION for	
NTIS	Reference Section <input checked="" type="checkbox"/>
DDC	Buff Section <input type="checkbox"/>
UNANNOUNCED	<input type="checkbox"/>
JUS TION I V	
BY	
DISTRIBUTION/AVAILABILITY CODES	
Dis	SPECIAL
A	



M. A. Domen
Project Monitor
Naval Air Systems Command

SUMMARY

Electron paramagnetic resonance (EPR) and proton nuclear magnetic resonance (NMR) have been used to investigate the main-chain segmental motions associated with the glass transitions in the alternating block copolymers of bisphenol-A polycarbonate (BPAC) and dimethylsiloxane (DMS) and to determine the effects of a plasticizer on molecular motion in these copolymers. This investigation also included a feasibility study of applying these same cw and pulsed magnetic resonance techniques to other crosslinked organic polymers such as epoxy resins.

The stable nitroxide radical 4-hydroxy-2,2,6,6-tetramethylpiperidinoxy (TANOL) was used as an EPR spin probe of its static and dynamic environment in the block copolymers. Above 220 K, the EPR spectra of 50 wt% DMS/BPAC samples consisted of a superposition of two spectra, a broadline spectrum and a narrowline spectrum. Detailed studies showed that there are two radical phases wherein the TANOL molecules are undergoing either slow molecular motions (the slow phase with the broadline spectrum) or fast motions (the fast phase with the narrowline spectrum). As the temperature increased, the correlation times for the motions in both phases decreased, and α , the ratio of the number of radicals in the fast phase to the number in the slow phase, increased such that $\ln \alpha \propto -\Delta H/RT$, where $\Delta H = 20.5$ kJ/mole. The variation of α with temperature was interpreted to mean that there is a distribution of segmental motional activity along the DMS blocks. The fact that there were two and only two radical phases implied that the radical is bound in the slow phase and 'free' in the fast phase so that when the host environment undergoes segmental motions, the radical makes a discontinuous jump into the fast phase. Hence, as the region of segmental motional activity grows outward from the centers of the DMS blocks with increasing temperature, the number of radicals in the fast phase (and hence α) also increases.

The radical correlation times in the slow phase, τ_{cs} , and fast phase, τ_{cf} , for copolymer samples with 50 wt% DMS/BPAC ($\overline{DP}_{DMS} = 20$, $\overline{DP}_{BPAC} = 6$) decreased with increasing temperature and were given by $\tau_{cs} = 2.56 \times 10^{-10} \exp(10.5 \text{ kJ mole}^{-1}/RT)$ s between 230 K and 293 K, and $\tau_{cf} = 5.25 \times 10^{-12} \exp(9.3 \text{ kJ mole}^{-1}/RT)$ s between 250 K and 300 K. From the NMR relaxation data between 170 K and 250 K, the correlation time τ_c for main-chain segmental

motion of the DMS blocks in the same copolymer samples was found to be $\tau_c = 4.19 \times 10^{-18} \exp(40.3 \text{ kJ mole}^{-1}/RT) \text{ s}$.

Lineshape analysis of partially spin-lattice relaxed NMR spectra was used to distinguish motional activity as a function of position in the DMS block. This revealed that main-chain segmental motion at the centers of the DMS blocks was greater than at the ends, and the motion at the centers increased as the length of the DMS blocks was increased. As the temperature was increased from below the glass transition, extensive main-chain segmental motion occurred in a small region at the centers of the DMS blocks; restricted motion occurred outside this region. As the temperature was increased further, this region grew from the centers to the ends of the DMS blocks and into the BPAC domains. The temperature dependence of β , the ratio of the number of protons in the rubbery phase to those in the rigid phase, was measured and found to be consistent with this interpretation.

Both EPR and NMR effects were observed upon addition of perdeuterocyclohexane, a selective plasticizer for DMS. The most significant change in the TANOL EPR spectra was an increase in α such that α was linearly proportional to plasticizer content up to 50 wt% amounts of plasticizer. The NMR linewidths of both the aromatic and methyl proton resonances decreased on addition of the plasticizer and indicated that the motions of the DMS blocks and some of the BPAC blocks had been increased.

Preliminary EPR and NMR experiments demonstrated the applicability of using these techniques to study glass transition phenomena in epoxy resins and other organic polymer systems.

TABLE OF CONTENTS

	<u>Page</u>
1 INTRODUCTION	1
2 BLOCK COPOLYMERS	2
2.1 Sample Description and Preparation	2
2.1.1 Sample Description	2
2.1.2 Sample Preparation for EPR Studies	3
2.1.3 Sample Preparation for NMR Studies	4
2.2 EPR Studies	5
2.2.1 Temperature Dependence of Lineshapes	5
2.2.2 Relaxation Times	7
2.2.3 Effect of Molecular Oxygen	11
2.2.4 Effect of Radical Concentration	12
2.2.5 Equilibrium Between Fast and Slow Phases	13
2.2.6 Interpretation of EPR Results	17
2.2.7 Effect of Varying Composition	19
2.2.8 Computer Simulations and Motional Correlation Times	19
2.3 NMR Studies	27
2.3.1 Pulsed NMR Spectrometer	27
2.3.2 Conventional T_1 Measurements	28
2.3.3 Conventional T_2 Measurements	29
2.3.4 Multiple-Pulse Spectra	35
2.3.5 Multiple-Pulse Partially Relaxed Spectra	37
2.3.6 Multiple-Pulse $T_{1\rho}$ Measurements	41
2.3.7 Broadline Partially-Relaxed Spectra	47
3 PLASTICIZER EFFECTS IN BLOCK COPOLYMERS	55
3.1 EPR Studies	55
3.2 NMR Studies	61
4 EPOXY RESINS	
4.1 EPR Studies	65
4.2 NMR Studies	68
5 CONCLUSIONS	70
5.1 Block Copolymers	70
5.2 Plasticizer Paramagnetic Resonance	71
5.3 Epoxy Resins	72
5.4 General	72

*NOT
Preceding Page BLANK - FILMED*

TABLE OF CONTENTS (Continued)

	<u>Page</u>
REFERENCES	74
DISTRIBUTION LIST	76

LIST OF ILLUSTRATIONS

<u>Figure</u>	<u>Page</u>
1 Microstructure of alternating block copolymers	2
2 Copolymer chemical structure	3
3 The spin-probes used	4
4 EPR spectra observed at different temperatures	6
5 The temperature dependence of the order parameter and EPR extrema	7
6 The dependence of EPR lineshapes on applied microwave power . .	8
7 The pulse sequence used to detect the two-pulse electron spin echo	9
8 The EPR absorption spectrum and two-pulse echo height spectrum .	10
9 Peak-to-peak height of the high field line in the fast phase versus exposure time in air	12
10 The temperature dependence of the EPR linewidth of the low field line in the fast phase	13
11 EPR spectra observed at 234 and 331 K	14
12 A typical derivative TANOL spectrum and its integrated form . .	15
13 Temperature dependence of α	16
14 The EPR spectrum of TANOLD and the best-fit computer simulation.	21
15 The EPR spectrum of TANOL and the best-fit computer simulation .	22
16 An illustration of the definition of Δ_ℓ , Δ_h and A_z	23
17 Temperature dependence of Δ_ℓ and Δ_h	24
18 A plot of τ_{cs} versus (temperature) ⁻¹	25
19 A plot of τ_{cf} versus (temperature) ⁻¹	27
20 Temperature dependence of T_1	29
21 Free induction decay signal	31
22 Temperature dependence of T_2	32
23 Temperature dependence of β and T_2	34
24 Multiple-pulse spectra	36
25 Partially spin-lattice relaxed multiple-pulse spectra	38
26 Spin-lattice relaxation, T_1	39
27 Partially spin-lattice relaxed multiple-pulse spectra	40
28 Partially spin-lattice relaxed spectra in the rotating frame . .	43

LIST OF ILLUSTRATIONS (Continued)

<u>Figure</u>	<u>Page</u>
29 Rotating frame spin-lattice relaxation, $T_{1\rho}$	44
30 Temperature dependence of $T_{1\rho}$	45
31 Temperature dependence of τ_c	46
32 Partially spin-lattice relaxed broadline spectra	48
33 Partially spin-lattice relaxed broadline spectra	49
34 Partially spin-lattice relaxed broadline spectra	50
35 Partially spin-lattice relaxed broadline spectra	51
36 Partially spin-lattice relaxed broadline spectra	51
37 Partially spin-lattice relaxed broadline spectra	52
38 Partially spin-lattice relaxed broadline spectra	52
39 EPR spectra observed in a copolymer sample before and after the addition of the perdeuterocyclohexane plasticizer	56
40 Peak-to-peak height of the high field line in fast phase after the addition of the perdeuterocyclohexane plasticizer	57
41 A plot of α versus plasticizer content	58
42 An illustration of λ , the peak height ratio	59
43 A plot of λ versus plasticizer content	60
44 Partially spin-lattice relaxed spectra for plasticized copolymer	62
45 EPR spectra of TANOL in epoxy resin matrix at different times into cure	66
46 EPR spectra of TANOL in epoxy resin matrix at different temperatures	67
47 Spin-lattice relaxation in moist epoxy	69

LIST OF TABLES

<u>Table</u>		<u>Page</u>
1	CHARACTERISTICS OF COPOLYMERS STUDIED	3
2	DMS MOTION INFERRED FROM PARTIALLY RELAXED BROADLINE SPECTRA . .	54

1. INTRODUCTION

In this report, we describe the results of our study of the main-chain segmental motions associated with the glass transitions in the random alternating block copolymers of bisphenol-A polycarbonate (BPAC) and dimethylsiloxane (DMS) using pulsed nuclear magnetic resonance (NMR) and pulsed and cw electron paramagnetic resonance (EPR) techniques. This study is an attempt to better characterize the main-chain segmental motions in the region of the glass transition temperature and identify at a molecular level how the segmental motions are affected by the degree of crosslinking and the presence of a plasticizer. In addition, we have evaluated the feasibility of applying these techniques to other crosslinked organic polymers, e.g., epoxy resins.

Over the past few years, EPR spin-probes and spin-labels have been used to investigate molecular motional effects in biological¹ and synthetic polymers.² In this technique, a stable nitroxide free radical is covalently bound at known specific sites in the polymer (spin-label) or dissolved in the polymer as a guest molecule (spin-probe). In either case, the radical acts as a probe of its dynamic environment in the polymer. The nitroxide radicals are particularly good candidates as EPR probes because (1) they are chemically stable and (2) the EPR spectrum is fairly readily analyzable in terms of an electron spin 1/2 coupled to a single nitrogen nuclear spin 1. We have used the spin-probe technique to investigate the main-chain segmental motions of the block copolymers in this contract.

In solid polymers, proton NMR spectra are broadened by dipolar interactions so that usually only a single line is observed and the chemical shift data are unavailable. Recently, multiple-pulse techniques have been devised whereby this dipolar broadening is substantially reduced and the chemically-shifted lines associated with the nuclei in different molecular groups can be resolved.³ The relaxation times for each type of proton can then be measured, and hence the molecular motional effects at each proton can be determined independently. We have used conventional proton NMR methods to measure the relaxation times of the bulk protons in the block copolymers and multiple-pulse methods to distinguish the motion of protons in different molecular groups.

2. BLOCK COPOLYMERS

2.1 Sample Description and Preparation

2.1.1 Sample Description

In the alternating block copolymers, the BPAC blocks are thought to associate into rigid domains which act as physical crosslinks for the more mobile DMS blocks.⁴ The model shown in Figure 1 illustrates such domain formation in the microstructure. The crosslink density depends on the composition and block lengths, and, as a result, these copolymers range in type from rigid solids to rubbery solids⁵ at room temperature.

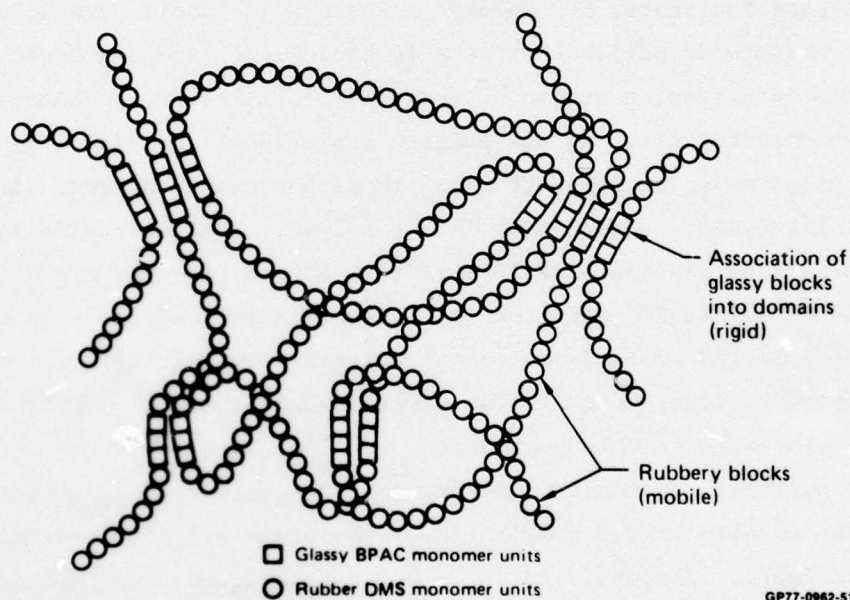


Figure 1 Microstructure of alternating block copolymers.

These copolymers show a two-phase behavior in that the mechanical properties have two major relaxations which have been attributed to two glass transition temperatures.⁴ Thus, in copolymer samples with a DMS/BPAC ratio of 50 wt% ($\overline{DP}_{DMS} = 20$, $\overline{DP}_{BPAC} = 6$), the relaxation occurring at 170 K has been associated with the onset of main-chain segmental motions in the DMS blocks, whereas the relaxation at 345 K has been associated with the onset of the seg-

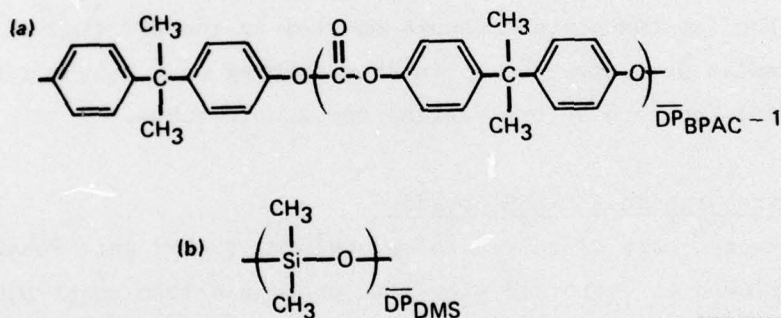
mental motions in the BPAC blocks. The corresponding glass transition temperatures in the DMS and BPAC homopolymers are 150 K and 423 K.

Table 1 lists the compositions, block lengths, and molecular weights of the copolymers investigated.⁶ Figure 2 shows the chemical structure of the blocks.

TABLE 1 CHARACTERISTICS OF COPOLYMERS STUDIED

DMS (wt%)	BPAC (wt%)	Number average degree of polymerization of DMS blocks, \overline{DP}_{DMS}	Number average degree of polymerization of BPAC blocks, \overline{DP}_{BPAC}	Number average molecular weight \overline{M}_N
25	75	20	17.7	—
50	50	20	6.0	—
65	35	20	3.3	60 000
65	35	100	15.9	51 000

GP77-0962-28

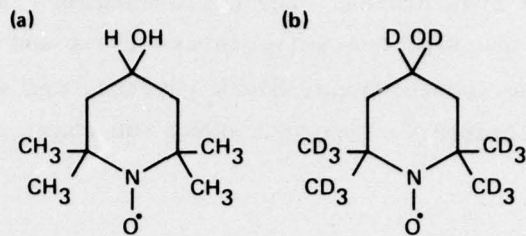


GP77-0962-30

Figure 2 Chemical structure of (a) bisphenol-A polycarbonate (BPAC) and (b) polydimethylsiloxane (DMS) blocks.

2.1.2 Sample Preparation for EPR Studies

In the EPR experiments, we used the stable nitroxide radical 4-hydroxy-2,2,6,6-tetramethylpiperidinoxy [TANOL, Figure 3(a)] as a spin probe in the block copolymers. The perdeuterated analog of this radical [TANOLD, see Figure 3(b)] was also used in selected experiments to aid in the evaluation of the spin-Hamiltonian parameters used in the lineshape simulations.



GP77-0962-22

Figure 3 The spin-probes used.

(a) 4-hydroxy-2,2,6,6-tetramethylpiperidinoxyl (TANOL)

(b) the perdeuterated analog of (a) (TANOLD)

Known weights of TANOL (~ 10 mg) were dissolved in 10 mL amounts of methylene chloride. Known volumes of these solutions were added to solutions of the block copolymer⁶ in methylene chloride using micropipettes (500 μ L and 100 μ L). Thin transparent films were obtained when these solutions evaporated slowly over a 48 h period. Trapped solvent was removed from the films by heating in a vacuum oven for 24 h at $\sim 50^\circ\text{C}$. The films were cut into thin strips and compression molded into 3.2 mm o.d., 10 mm long cylindrical samples at $\sim 130^\circ\text{C}$. The samples were kept in 5 mm o.d. NMR tubes which were inserted into the low-temperature dewars mounted in the EPR cavity. The oxygen-free samples were prepared by further pumping on a vacuum line to 10 mPa ($\sim 10^{-5}$ Torr) for 24 h before sealing the sample tubes.

2.1.3 Sample Preparation for NMR Studies

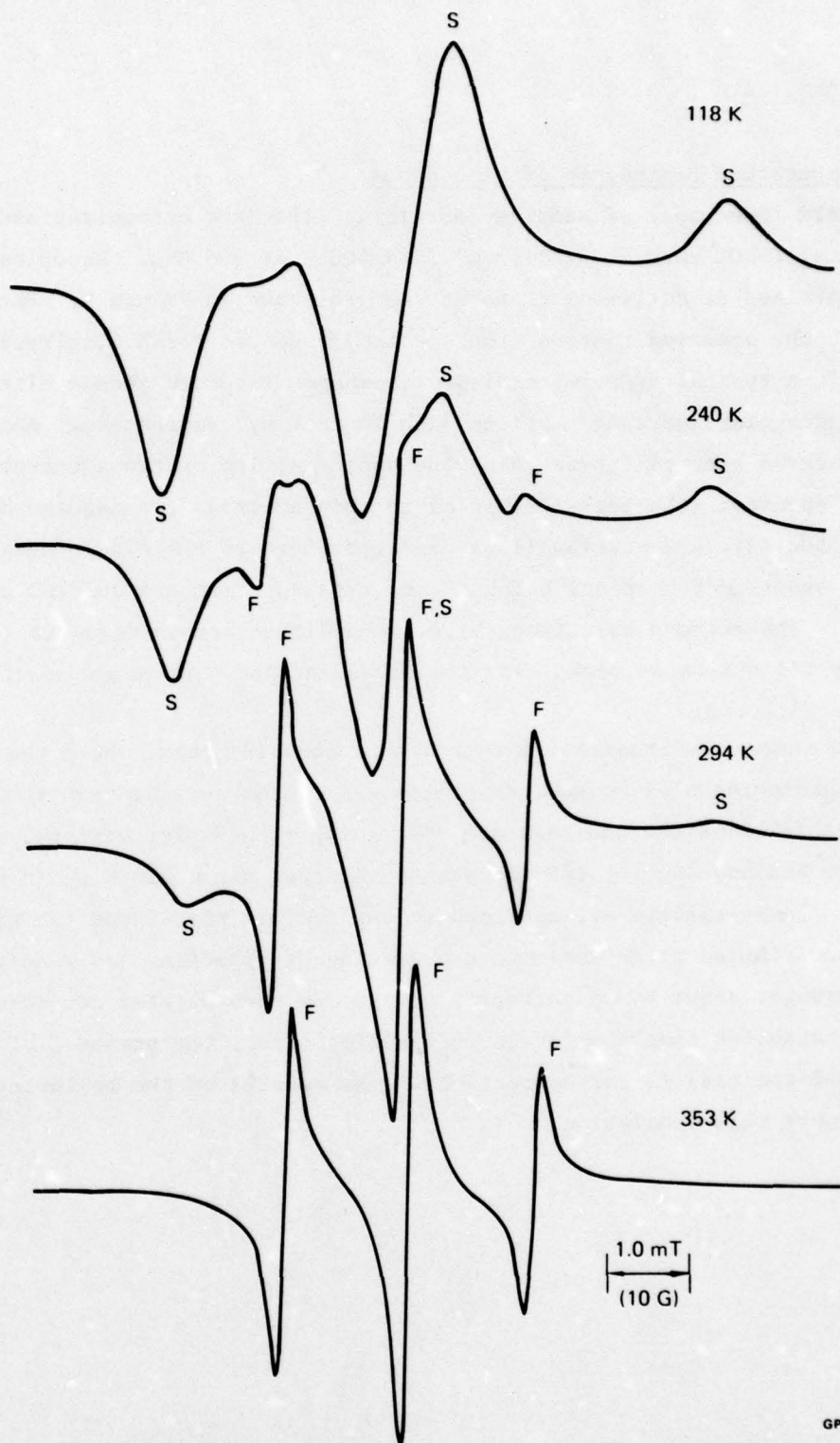
The copolymers⁶ were dissolved in chloroform, poured into Petri dishes, covered, and allowed to evaporate slowly to produce a film about 0.05 mm thick. The large surface-to-volume ratio of these films facilitated removal of volatile solvents and low-molecular-weight impurities in a subsequent 24 h heating to 120°C in a vacuum oven. The films were compression molded into cylinders 3.2 mm in diameter and 6 mm long. The molded samples were placed in 5 mm NMR tubes, vacuum pumped for 24 h at 90°C to remove oxygen, backfilled with helium at 36 kPa (270 Torr), and sealed. The oxygen was removed because it is a paramagnetic impurity which would adversely affect the nuclear spin-lattice relaxation time measurements. The helium was used to provide a good thermal contact between the sample and the NMR tube so that the sample temperature could be adjusted quickly and accurately.

2.2 EPR Studies

2.2.1 Temperature Dependence of Lineshapes

The EPR lineshapes of samples containing different concentrations of the free radical TANOL were studied from 77 to 400 K at 9.5 GHz. Examples of the spectra obtained at different temperatures are shown in Figure 4. Between 77 and 220 K, the observed spectra (the spectrum taken at 118 K displayed in Figure 4 is a typical example) exhibit lineshapes expected from a nitroxide radical undergoing increased motions with increasing temperature. Above 220 K, the observed spectra appear to be the superposition of two spectra: (1) a broadline spectrum (the peaks belonging to this spectrum are denoted by S in Figure 4) and (2) three narrow lines centered close to the middle peak of the broadline spectrum (the peaks belonging to this spectrum are denoted by F in Figure 4). The extrema splittings (i.e., the difference in magnetic field values for the outermost peaks) for the broadline and narrowline spectra are plotted in Figure 5.

We attribute the broadline spectrum to a slow (S) phase where the radicals are undergoing slow molecular motions and the narrowline spectrum to a fast (F) phase where the radicals are undergoing much faster motions. An alternative explanation for the lineshapes observed above 220 K would be the following. These spectra are assigned to one radical phase, and the narrow lines are attributed to an incomplete averaging of hyperfine and g-anisotropy, possibly brought about by anisotropic motion. We have exerted considerable effort to establish that the former explanation (i.e., the presence of two superimposed spectra) is the correct one. The results of the following experiments support this conclusion.



GP77 0962 17

Figure 4 EPR spectra observed at different temperatures for a sample of the block copolymer with 50 wt% DMS/BPAC ($DP_{BPAC} = 6$ and $DP_{DMS} = 20$) containing the stable free radical TANOL. The derivative peaks associated with the slow phase and fast phase are denoted by S and F, respectively.

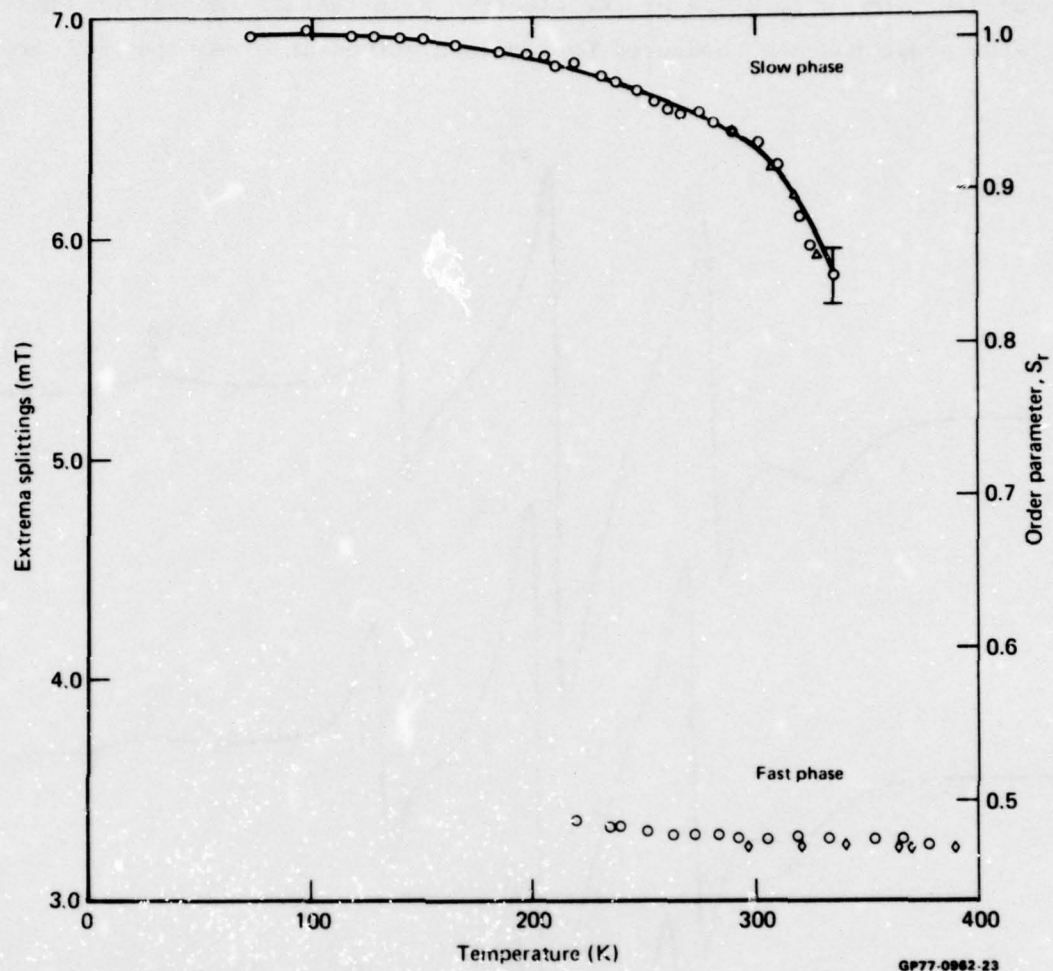
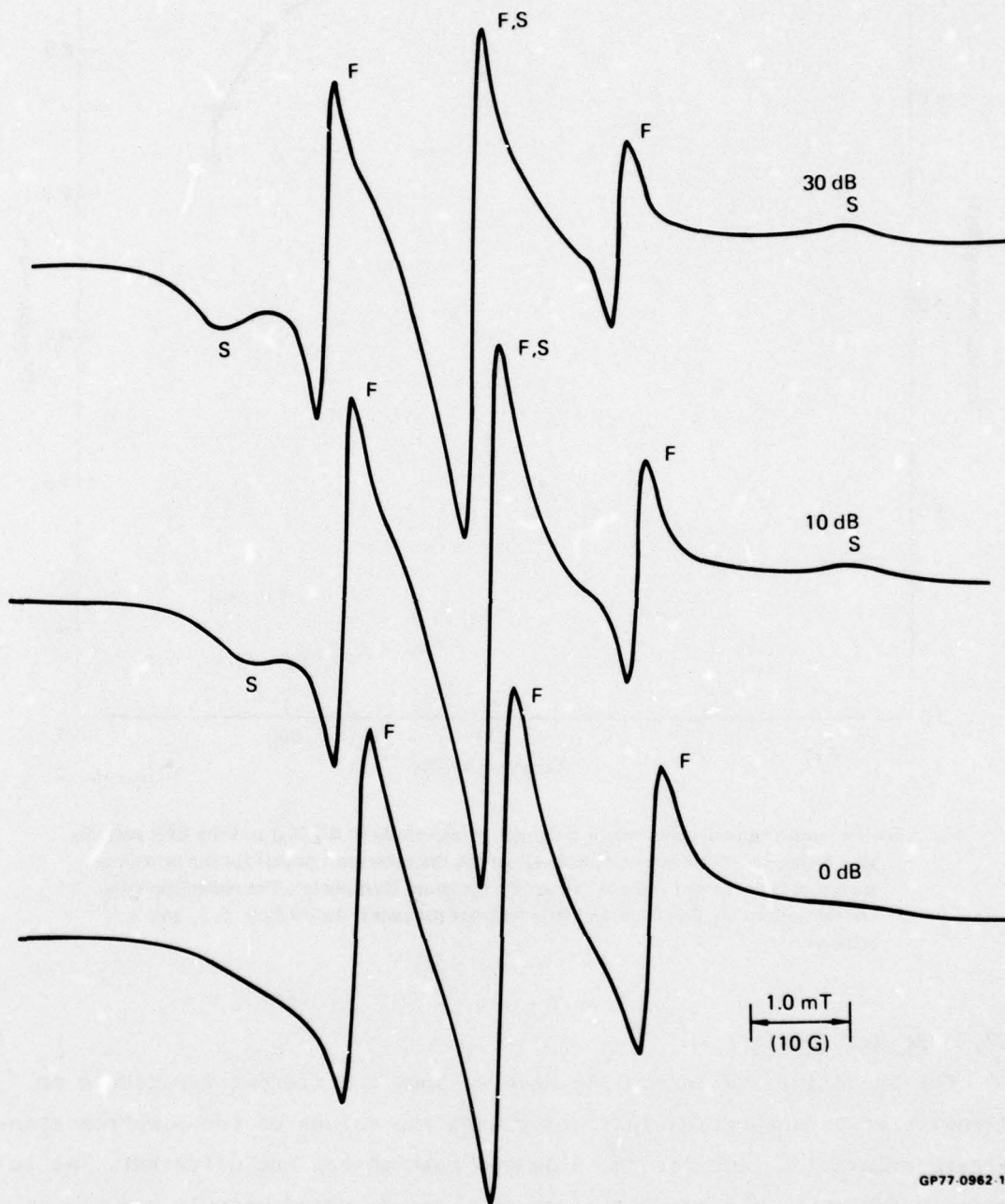


Figure 5 The temperature dependence of the order parameter $S_r (= A'_z/A_z)$ and the EPR extrema (the difference in the magnetic field values for the outermost peaks) for the broadline spectrum (slow phase) and the narrowline spectrum (fast phase). The radical/polymer concentrations are 0.5, 0.09, and 0.04 wt% for the points denoted by \circ , Δ , and \diamond , respectively.

2.2.2 Relaxation Times

The broadline and narrowline spectra show a different dependence on microwave power saturation indicating that the values of the electron spin-lattice relaxation time for the slow and fast phases are different. As is shown in Figure 6, the broadline spectrum can be progressively reduced in amplitude with increasing microwave power with no reduction in the amplitude of the narrowline spectrum until at a power increase of 30 dB the broadline spectrum can be reduced to almost zero intensity. The actual temperature

dependence from 77 to 294 K of the electron spin-lattice relaxation time for the slow phase has been measured by a pulsed method in a related MDRL program.



GP77-0962-16

Figure 6 The dependence of the EPR lineshapes on applied microwave power. Spectra obtained with 30, 10, and 0 dB settings of the microwave attenuator to the microwave cavity containing the polymer samples are shown. The peaks associated with the slow phase and fast phase are denoted by S and F, respectively.

Pulsed experiments involving the generation of electron spin echoes⁷ show that the phase memory time (viz., the time that characterizes the two-pulse electron spin echo envelope decay) is much longer for the slow phase than for the fast phase. This is exhibited in the following way. If, as is shown in Figure 7, two microwave pulses of width P are applied at $t = 0$ and $t = \tau$, the electron spin echo appears at $t = 2\tau$. As τ is increased, the echo height decreases, and the overall echo envelope decay is characterized by the phase memory time T_M which can be defined as the time for the echo amplitude to attenuate to $1/e$ of its value at $\tau = 0$. Spectra can be obtained by recording the echo height versus magnetic field using a boxcar integrator with the boxcar gate set at $t = 2\tau$ and a gate width less than the echo width.⁸

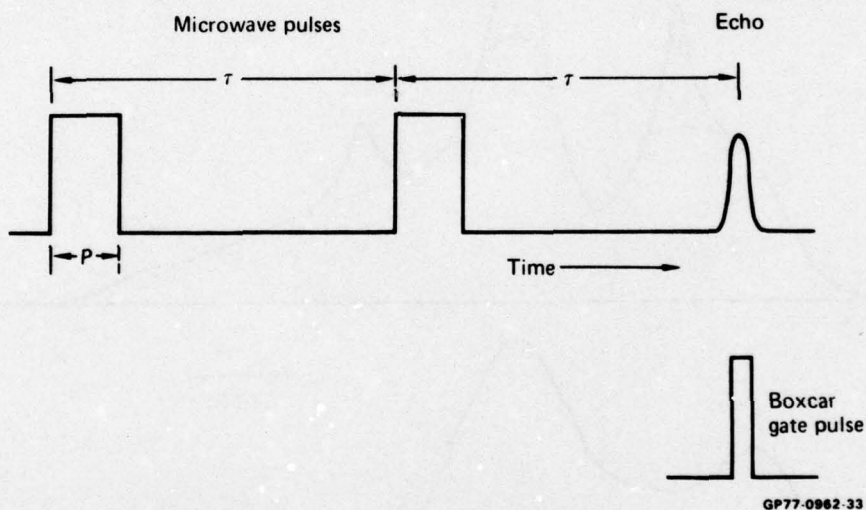


Figure 7 The pulse sequence used to observe the two-pulse electron spin echo.

If a system contains two free radicals with widely different T_M values T_{M1} and T_{M2} , where $T_{M1} \gg T_{M2}$, we have found that it is possible to record an echo height spectrum of only the species with the T_{M1} value by choosing τ such that $T_{M1} \gtrsim \tau \gg T_{M2}$. Thus, in the contractual period, we have developed this form of electron spin echo spectroscopy into a form of time domain spectroscopy where it is possible to select and record one spectrum from a superposition of two EPR spectra with different relaxation times.

We have applied this technique to the block copolymers, and Figure 8 shows the results. Figure 8(a) is the EPR absorption showing the slow phase superimposed on the fast phase lines. These absorption spectra were recorded

in the manner described in Section 2.2.5. Figure 8(b) shows the echo height spectrum obtained with the pulse sequence shown in Figure 7 with $P = 20$ ns, $\tau = 800$ ns. Although it is not exactly the shape of the broadline absorption in Figure 8(a), it closely approximates it. There is no indication of the narrow lines in this spectrum, presumably because the value of T_M for these lines is $T_{M2} \ll 800$ ns. We have thus separated and selectively recorded the broadline spectrum only.

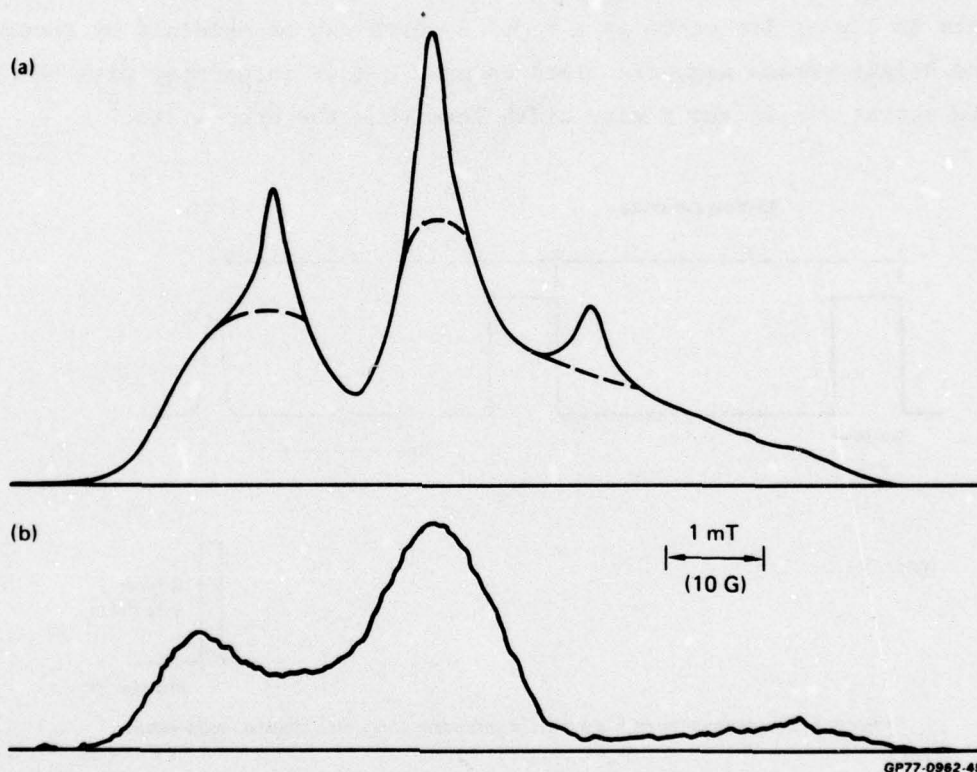


Figure 8 (a) The EPR absorption spectrum resulting from an integration of the EPR derivatives spectrum of TANOL in the block copolymer with 50 wt% DMS/BPAC ($\overline{DP}_{BPAC} = 6$, $\overline{DP}_{DMS} = 20$) recorded at 294 K. The dashed lines are estimates of the broadline lineshapes.
 (b) The two-pulse echo height versus magnetic field for the same sample as used to obtain (a) with $P = 20$ ns, $\tau = 800$ ns.

Furthermore, using a single $\pi/2$ pulse, it has been possible to detect the free-induction decay from each of the three narrow lines with a time characterizing this decay of $T_2 \lesssim 30$ ns. The free-induction decay signals from the

broad lines were not observed because they are determined by a value of $T_2 \ll 50$ ns. They are, in fact, given by a time $\leq 1/\gamma H_1$, where H_1 is the amplitude of the microwave magnetic fields, so that in our experiments with $H_1 = 7$ G, we can expect them to have a $T_2 \leq 8$ ns.

Thus, using a two-pulse sequence, the echo height spectrum will respond only to the broadline (slow phase) lineshape. On the other hand, using a single pulse, the free-induction decay signal responds only to the narrowline spectrum. The above relaxation experiments indicate that the broadline spectrum is inhomogeneously broadened, whereas the narrow lines are homogeneously broadened (or nearly so). Thus, the broadline and narrowline spectra have a completely different character.

2.2.3 Effect of Molecular Oxygen

It was observed that the EPR linewidths of the narrowline spectrum are sensitive to the presence of molecular oxygen, whereas the broad lines are unchanged. Thus, at 294 K, both the low- and high-field lines in the narrowline spectrum had linewidths of 0.24 ± 0.01 mT measured with the sample exposed to air, but 0.18 ± 0.01 mT when the sample was in vacuum. This line broadening is caused either by Heisenberg exchange or electron-electron dipolar interactions between the unpaired spin on the nitroxide spin-probe and the paramagnetic molecular oxygen which is sorbed into the solid polymer.

On exposure of evacuated samples to air, the line broadening is also accompanied by a decrease in intensity of the narrow lines. We investigated this effect by measuring the intensity of the high-field narrow line at different times following exposure of an evacuated sample to air. The results are plotted in Figure 9. The time dependence of the peak height is due to the time taken for the oxygen to diffuse into the solid polymer and suggests an EPR method of determining the diffusion coefficient for oxygen into the solid block copolymers.

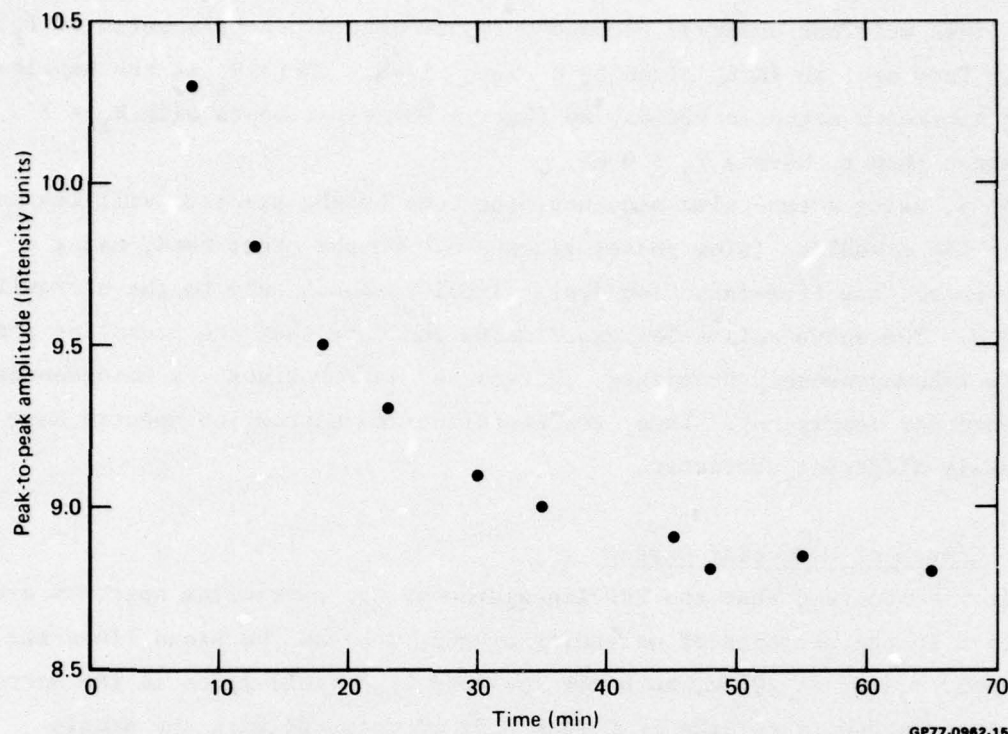


Figure 9 Peak-to-peak height of the high field line in the fast phase versus exposure time of the sample to air. The sample which had a 50 wt% DMS/BPAC ratio and block lengths $\overline{DP}_{DMS} = 20$, $\overline{DP}_{BPAC} = 6$ contained TANOL.

2.2.4 Effect of Radical Concentration

The temperature dependences of the lineshapes were measured with radical concentrations of 0.5, 0.09, 0.04, and 0.017 wt%. As is shown in Figures 5 and 10, the extrema splittings are independent of radical concentration, whereas the linewidths of the narrow lines depend on radical concentration for radical/polymer ratios $\gtrsim 0.5$ wt%.

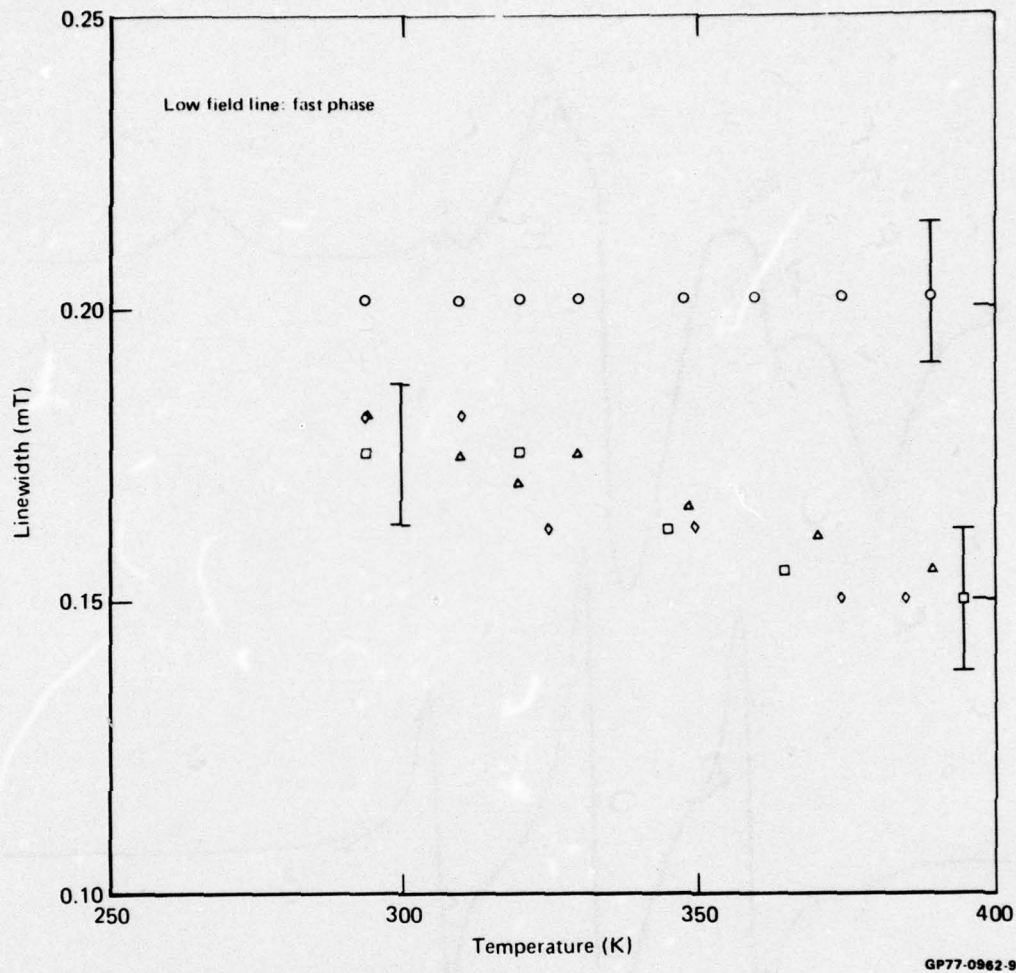
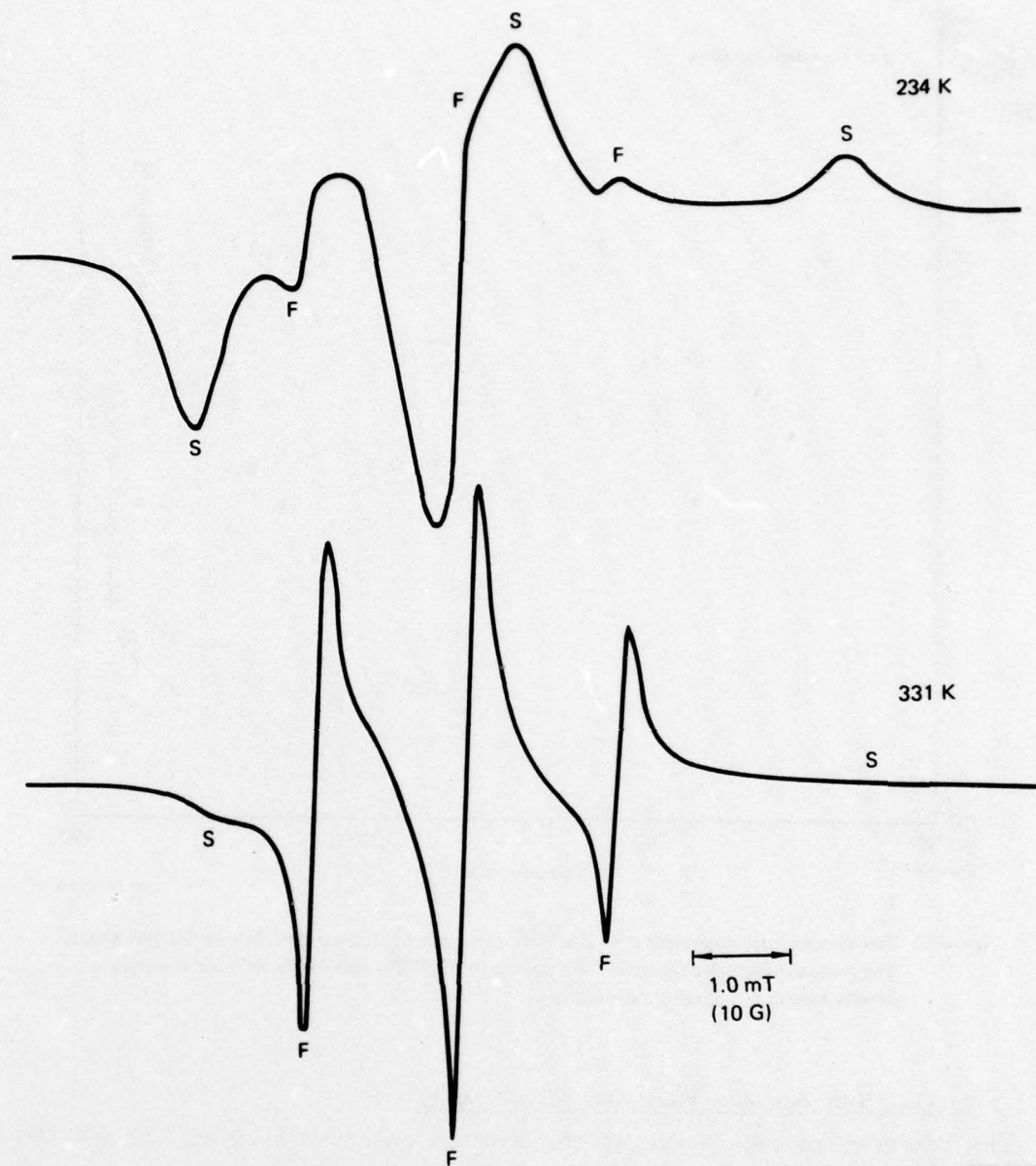


Figure 10 The temperature dependence of the EPR linewidth of the low field line in the fast phase. The radical/polymer concentrations are 0.5, 0.09, 0.04, and 0.015 wt% for the points denoted by \circ , Δ , \diamond , and \square , respectively.

2.2.5 Equilibrium Between Fast and Slow Phases

The temperature dependence of the spectra observed between 220 and 400 K suggests that there is an equilibrium between the number of radicals in the fast phase and the number of radicals in the slow phase. The peak heights in the first derivative spectra indicate that the number of radicals in the fast phase increases at the expense of the number of radicals in the slow phase, but the relative numbers in each phase are reproducible on cycling the temperature. For example, Figure 11 shows that at 234 K most of the radicals are in the slow phase with few in the fast phase, whereas at 331 K the opposite holds.



GP77-0962-12

Figure 11 EPR spectra observed at 234 and 331 K for a sample of the block copolymer with 50 wt% DMS/BPAC ($\overline{DP}_{BPAC} = 6$ and $\overline{DP}_{DMS} = 20$) containing the stable free radical TANOL. The derivative peaks associated with the slow phase and fast phase are designated S and F, respectively.

We define

$$\alpha = \frac{\text{the number of radicals in the fast phase}}{\text{the number of radicals in the slow phase}}$$

We have measured the temperature dependence of α between 215 and 369 K from a double integration of the first derivative spectra. This was accomplished by digitizing and integrating the first derivative spectra using a multichannel signal averager (Nicolet 1070). Figure 12 is a typical example.

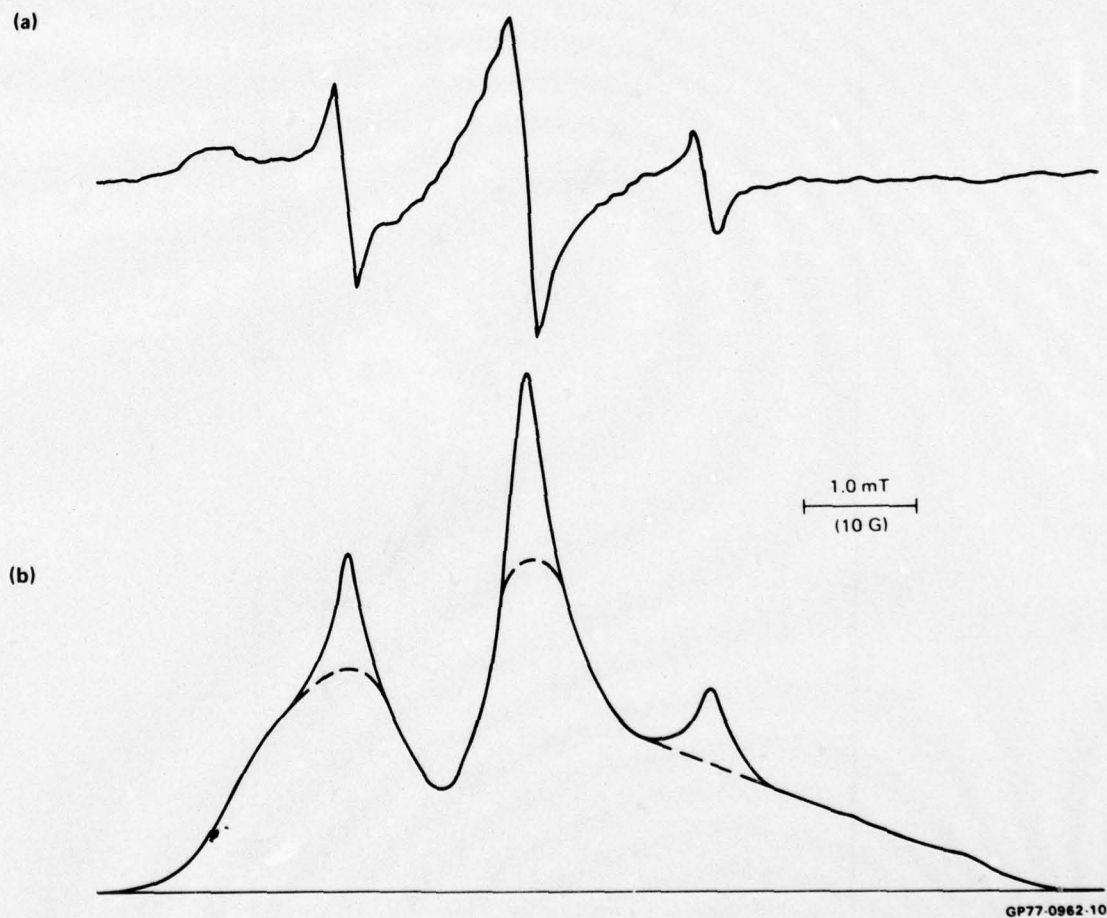


Figure 12 (a) A typical derivative EPR spectrum of TANOL in the block copolymer with 50 wt% DMS/BPAC ($\overline{DP}_{BPAC} = 6$, $\overline{DP}_{DMS} = 20$).
(b) The EPR absorption spectrum resulting from an integration of (a). The dashed lines are estimates of the broadline lineshapes.

The second integral was then obtained by evaluating the areas under each spectrum in Figure 12(b), using a calculator (Hewlett Packard 9810A) and a digitizer (Hewlett Packard 9864) after disentangling the lineshapes in the overlap regions. The error bars in Figure 13 are set by the accuracy of the spectral overlap determination, i.e., how the dashed lines are drawn in Figure 12(b).

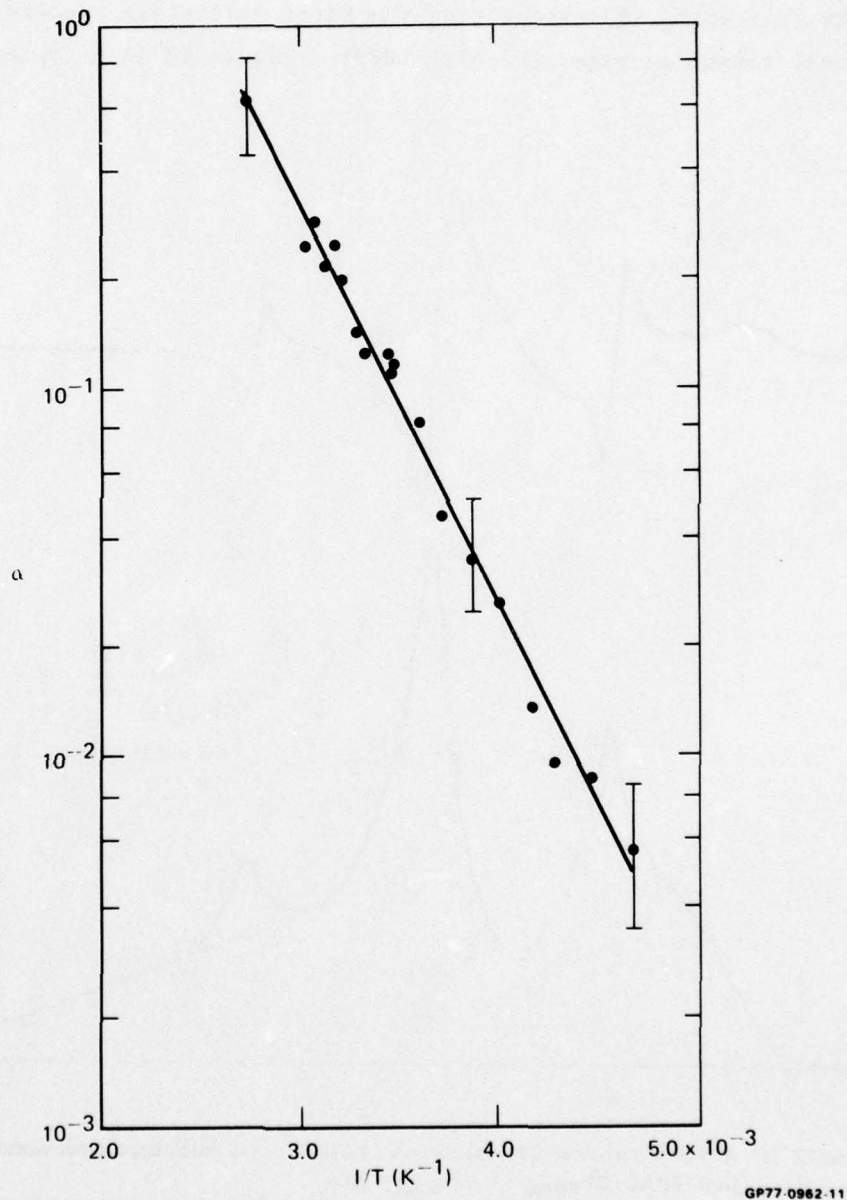


Figure 13 Temperature dependence of α for 50 wt% DMS/BPAC ($\overline{DP}_{BPAC} = 6$, $\overline{DP}_{DMS} = 20$).

The low-field and high-field lines of the broadline spectrum are fairly well determined. Estimates of the overlap of the central lines primarily establish the error bars.

The temperature dependence of α shown in Figure 13 indicates that $\ln \alpha$ is linearly proportional to $1/T$ with a slope that defines an enthalpy ΔH given by

$$\begin{aligned}\Delta H &= R \times \text{slope} \\ &= 20.5 \pm 3.5 \text{ kJ/mole,}\end{aligned}$$

where R is the universal gas constant.

2.2.6 Interpretation of EPR Results

All the above results involving the behavior of the relaxation times and the dependences of the spectra on molecular oxygen, radical concentration, and microwave pulse sequences are consistent with the interpretation that above 220 K there are two radical phases present. These are phases in the sense that the radical can be present in one of two different environments. As is indicated from the shapes of the spectra and the results in Figures 5 and 10, the motional frequencies of the radicals in both phases increase with increasing temperatures, but at any given temperature, the motions are much faster in one phase than in the other.

We assume, as previous work² indicates, that the correlation time for the radical motions decreases with decreasing values of the correlation time for the segmental motions of the adjacent main chains. Hence, we assign the fast phase to radicals located in rubbery DMS block environments, i.e., blocks which are undergoing main-chain segmental motions and hence are above their glass transition temperature. The slow phase is attributed to radicals located in domains of associated BPAC blocks and in regions of DMS blocks whose segmental motions are restricted by the proximity of the rigid BPAC domains. This model therefore incorporates the idea of distributions (in frequency and/or amplitude) of segmental motional activity along the DMS chains and hence is consistent with the NMR results described in Section 2.3.

However, the idea of distributions of segmental motions resulting from restrictions imposed by the rigid associated BPAC blocks raises the question: why are there only two spectra observed? At any temperature above the lower glass transition temperature, because of the distribution in segmental

motional activity, one would expect the superposition of a distribution of spectra, each characterized by a correlation time, which can range in values from the slow to the fast motional extremes. However, the observed spectra would appear to indicate only two situations of fast and slow motions with no intermediate cases. This puzzling feature has led us to conclude that the TANOL spin-probe is bound to certain sites in the polymer when it is in the slow phase; one possibility is hydrogen bonding between the OH group on the nitroxide and the oxygen in the DMS block.

When the correlation time for segmental motion of this DMS block reaches a certain value, there is sufficient thermal energy to detach the TANOL from its bound site. The radical will then make a discontinuous transition from the slow to the fast phase. Thus, in the bound state, the TANOL can still undergo localized motions, but these will have much longer correlation times than the end-over-end tumbling motions possible when it is free.

At temperatures just above 220 K, only the less restricted DMS monomer units at the center of the DMS blocks will undergo enough segmental motional activity to allow the spin probes located in these regions to be free and in the fast phase. As this segmental motion grows out from the center of the DMS blocks with increasing temperature, more radicals will be free and in the fast phase. This model will then account for the equilibrium between the fast and the slow radical phases.

The exact interpretation of the enthalpy ΔH depends on how the TANOL radicals can get from the slow to the fast phase. This, in turn, depends on the exact type of molecular motion the radical undergoes. There are two extreme situations. If the radical is undergoing fast translational motions when it is free, on increasing the temperature, the radicals can diffuse from the rigid regions into the rubbery regions; the value of ΔH is then determined by (a) the difference between the heat of solution of the radical in the rubbery region and the heat of solution of the radical in the rigid regions, and also (b) the binding energy of the radical-polymer bond. On the other hand, if the radical undergoes rotational diffusion only at a fixed location when it is free, then the radical can go from the slow to the fast phase when the boundary defining the region of segmental motional activity recedes past it. The value of ΔH is determined by (1) the enthalpy involved in the process of the rigid DMS blocks becoming rubbery and (2) the binding energy of the radical-polymer bond.

We cannot be certain which of these interpretations is correct, but it seems that the latter is more probable since we expect the translational diffusion rates out of the rigid regions to be slow.

The apparent-phase effect proposed by Resing⁹ explains some of the NMR results where the observed lineshape was a superposition of a narrow line on a broad line. These lines were attributed to a wide distribution of correlation times rather than to two phases. However, we discount the possibility that a wide distribution of correlation times will explain our observations of two superimposed spectra. Even without detailed computer simulations, we would expect that the summation of spectra over the required range of correlation times (10^{-8} to 10^{-10} s) would result in a center peak with a much higher intensity relative to the outer lines than is observed and shown in Figure 4.

2.2.7 Effect of Varying Composition

A measurement of α was made on a copolymer sample with 65 wt% DMS/BPAC ($\overline{DP}_{\text{DMS}} = 20$, $\overline{DP}_{\text{BPAC}} = 3.3$) at 293 K by the method outlined in Section 2.2.5. The value of $\alpha = 0.36$ was obtained and should be compared with the value measured in the 50 wt% DMS/BPAC ($\overline{DP}_{\text{DMS}} = 20$, $\overline{DP}_{\text{BPAC}} = 6$) sample ($\alpha = 0.12$ in Figure 13).

If α depended only on the composition, a value of $\alpha = 0.22$ should have been measured. The excess value of α suggests that at 293 K larger regions of the DMS blocks are undergoing main-chain segmental motions in the 65 wt% DMS sample than in the 50 wt% sample. The increased mobility of the DMS blocks in the 65 wt% sample could arise because not all the BPAC blocks are in domains.¹⁰ The tendency for this effect to occur would be expected to increase with decreasing BPAC block length.

2.2.8 Computer Simulations and Motional Correlation Times

An effort was made to computer simulate the EPR spectra of the nitroxide radicals we have observed in the block copolymer samples. Two programs have been used: one to simulate the spectra of rigid, randomly oriented nitroxide radicals and the other to simulate the spectra of radicals undergoing molecular tumbling.¹¹

First values of the parameters characterizing the EPR spectra of the nitroxide radical in a rigid block copolymer medium must be determined. The values of these parameters are then substituted into the program which simu-

lates the effects of molecular motion. The molecular motional correlation times τ_c (the inverse is 2π times the motional frequency) can be obtained in principle by comparing the observed spectra with the computer-generated spectra employing τ_c as a variable parameter.

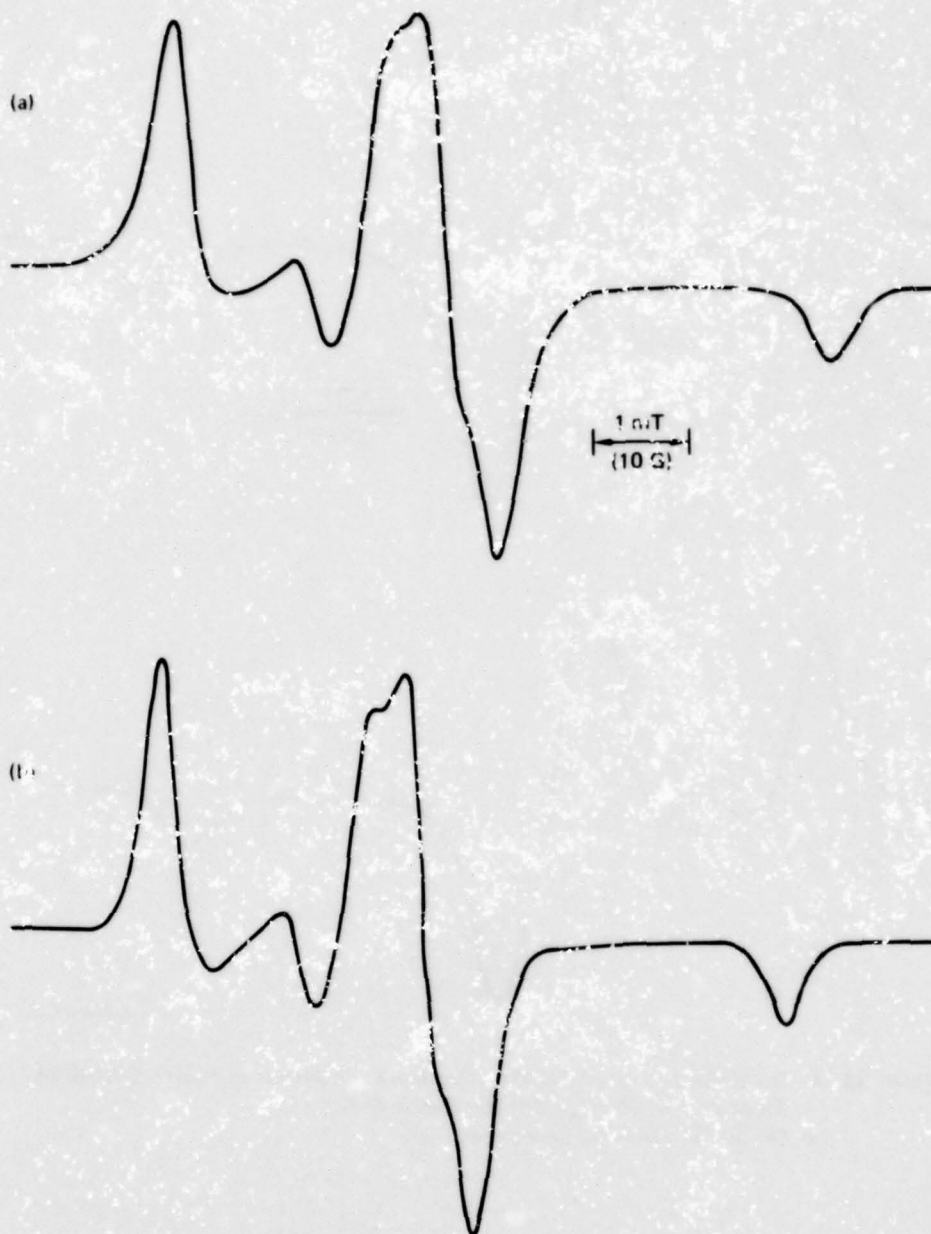
The rigid spectrum is generated by summing the correctly weighted contributions from radicals at all orientations. Seven variable parameters are involved in a fit of the simulated spectrum to the observed spectrum. These parameters are (g_x, g_y, g_z) , (A_x, A_y, A_z) , the principal values of the g tensor and nitrogen hyperfine coupling tensor, respectively, and T_2 , the electron spin-spin relaxation time which is a measure of the broadening of each contribution to the overall lineshape.

Although reasonable fits could be obtained for the rigid spectrum of the nitroxide radical TANOL taken at 77 K, a more precise determination of the seven parameters could be obtained by first simulating the spectrum observed from TANOLD, the perdeuterated analog of TANOL. The observed lines in this spectrum were narrower because the proton broadening was reduced and there is indication of the g and A anisotropy in the structure of the observed spectrum shown in Figure 14(a). The best fit to this spectrum is shown in Figure 14(b) and was generated with the following parameters' values:

$$\begin{array}{lll} g_x = 2.0100, & g_y = 2.0063, & g_z = 2.0027, \\ A_x = 0.65 \text{ mT}, & A_y = 0.65 \text{ mT}, & A_z = 3.45 \text{ mT}, \\ T_2 = 2.5 \times 10^{-8} \text{ s}. & & \end{array}$$

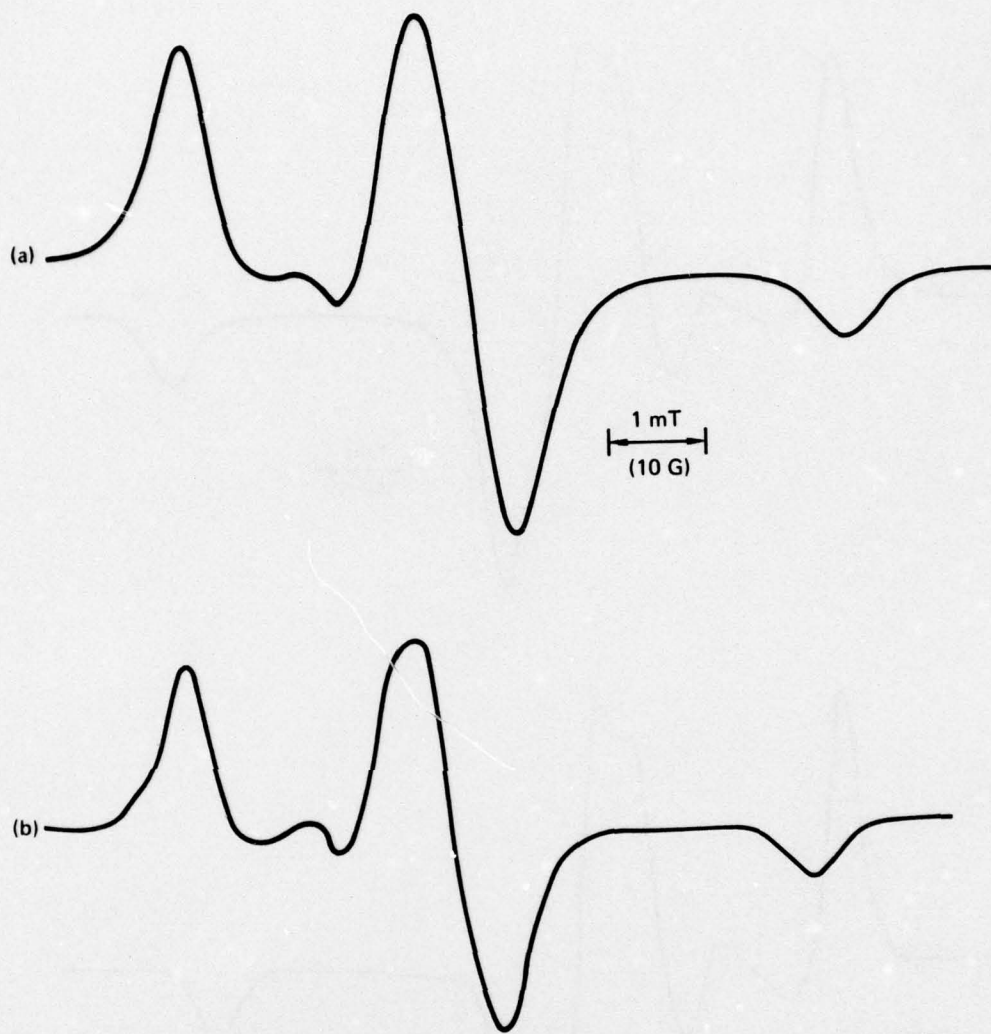
A computer simulation of the rigid TANOL spectrum was then obtained by assuming that the values of all the parameters except the broadening parameter T_2 were the same as for TANOLD. Thus, Figure 15(b) is the best-fit to the observed TANOL spectrum obtained at 77 K and shown in Figure 15(a). This best-fit is given by the parameters

$$\begin{array}{lll} g_x = 2.0100, & g_y = 2.0063, & g_z = 2.0027, \\ A_x = 0.65 \text{ mT}, & A_y = 0.65 \text{ mT}, & A_z = 3.45 \text{ mT}, \\ T_2 = 1.6 \times 10^{-8} \text{ s}. & & \end{array}$$



GP77 0962-47

Figure 14 (a) The EPR spectrum of TANOLD (the perdeuterated analog of TANOL) in the block copolymers of 50 wt% DMS/BPAC ($\overline{DP}_{BPAC} = 6$ and $\overline{DP}_{DMS} = 20$) observed at 77 K. (b) The best-fit computer simulation of the observed spectrum in (a).



GP77-0962-46

Figure 15 (a) The EPR spectrum of TANOL in the block copolymers of 50 wt% DMS/BPAC ($\overline{DP}_{BPAC} = 6$, $\overline{DP}_{DMS} = 20$) observed at 77 K.
 (b) The best-fit computer simulation of (a).

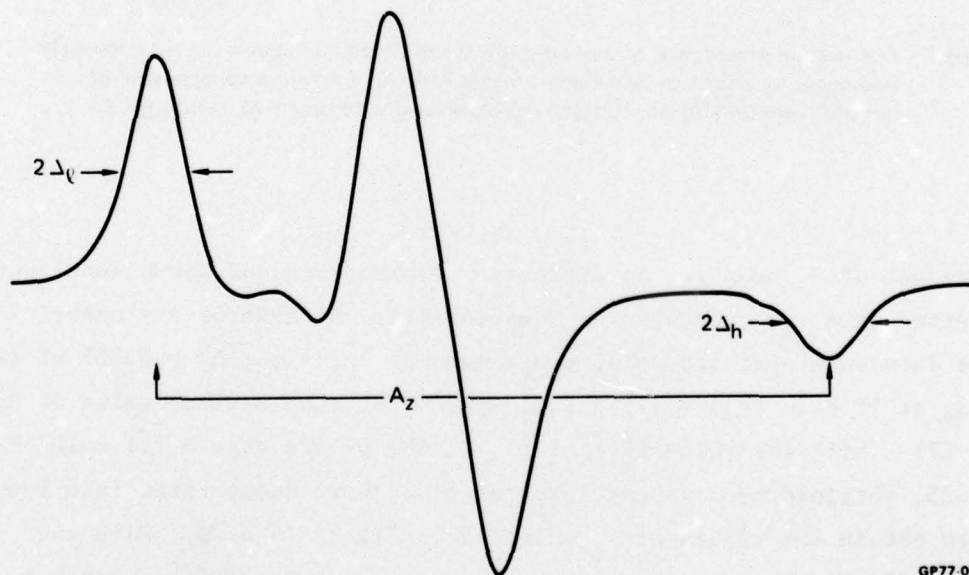
The computer simulations of the spectra of the TANOL spin-probe undergoing slow molecular motions showed a feature that did not agree with the behavior of the experimental spectra. As is illustrated in Figure 16, Δ_h and Δ_l are defined as the half-widths at half-height of the high-field and low-field lines in the broadline spectrum, respectively. These widths were measured as a function of temperature, and the results are plotted in Figure 17. Both widths show a minimum occurring at approximately 190 K. On the

other hand, our computer simulations and Freed's¹² theoretical work indicate that Δ_h and Δ_ℓ should increase monotonically with decreasing τ_c values. This discrepancy was serious enough that an exact analysis of the spectra and an evaluation of the temperature dependence of τ_c from detailed computer simulations was not attempted. Instead, we have used a more simplified analytical approach outlined by Freed¹² to obtain approximate values of τ_{cs} , the correlation time for the motions of the radical in the slow phase.

In this treatment, τ_{cs} is given by

$$\tau_{cs} = a(1 - S_r)^b, \quad (1)$$

where S_r is the order parameter defined as A_z'/A_z , and A_z' , A_z are the extrema splittings in the presence of motion and in the rigid lattice case, respectively; a and b are parameters that depend on Δ_s^r and Δ_h^r , the values of Δ_ℓ and Δ_h in the rigid lattice. The values of a and b are listed in Reference 12 for different values of δ , where $\delta = 2\Delta_\ell^r/1.59$.



GP77-0962-44

Figure 16 An illustration of the definition of Δ_ℓ , Δ_h and A_z .

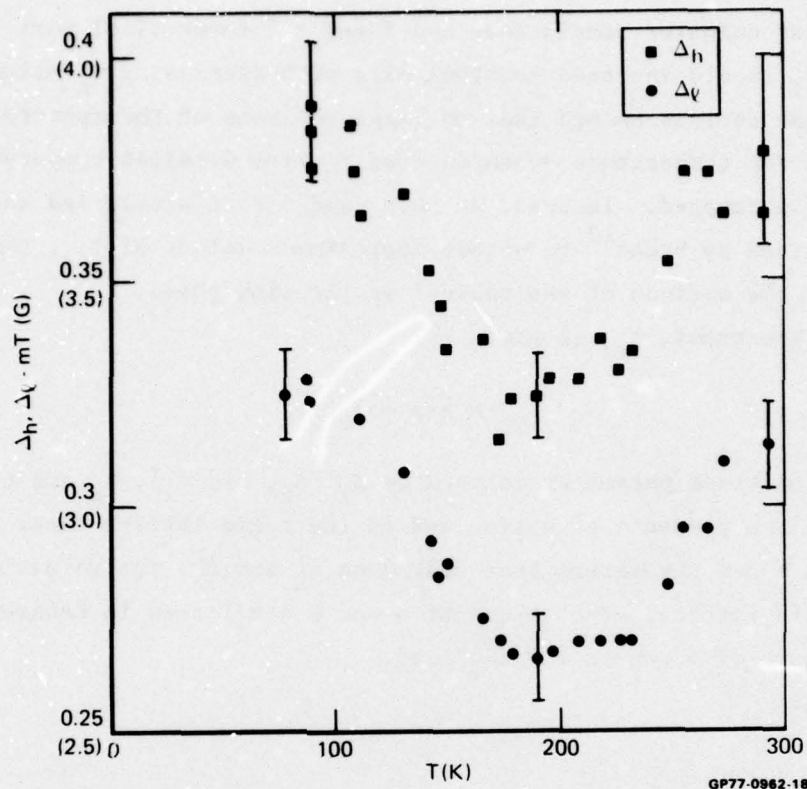


Figure 17 Temperature dependences of the half-width at half-height for extrema (Δ_{ℓ} is for low-field extremum, Δ_h is for high-field extremum) for TANOL in the block copolymer of BPAC and DMS with DMS/BPAC = 50 wt% and block lengths $\overline{DP}_{DMS} = 20$, $\overline{DP}_{BPAC} = 6$.

The values of S_r measured at different temperatures and shown in Figure 5 were converted into τ_{cs} values using Equation (1). Because of the uncertainty in Δ_{ℓ}^r , the data were analyzed using two values of Δ_{ℓ}^r ; viz., $\Delta_{\ell}^r = 0.325$ mT (the value of Δ_{ℓ} at 77 K in Figure 17) and $\Delta_{\ell}^r = 0.265$ mT (the minimum value of Δ_{ℓ} in Figure 17). With the value $\Delta_{\ell}^r = 0.265$ mT, the values of $a = 7.1 \times 10^{-10}$ s and $b = 1.25$, obtained by a linear interpolation, were substituted into Equation (1) to obtain the values of τ_{cs} plotted in Figure 18 as \bullet . With the value $\Delta_{\ell}^r = 0.325$ mT, the corresponding values of $a = 5.9 \times 10^{-10}$ s and $b = 1.33$ gave the values of τ_{cs} plotted in Figure 18 as \blacksquare . The difference in the values of Δ_{ℓ}^r chosen made little difference in the calculated values of τ_{cs} .

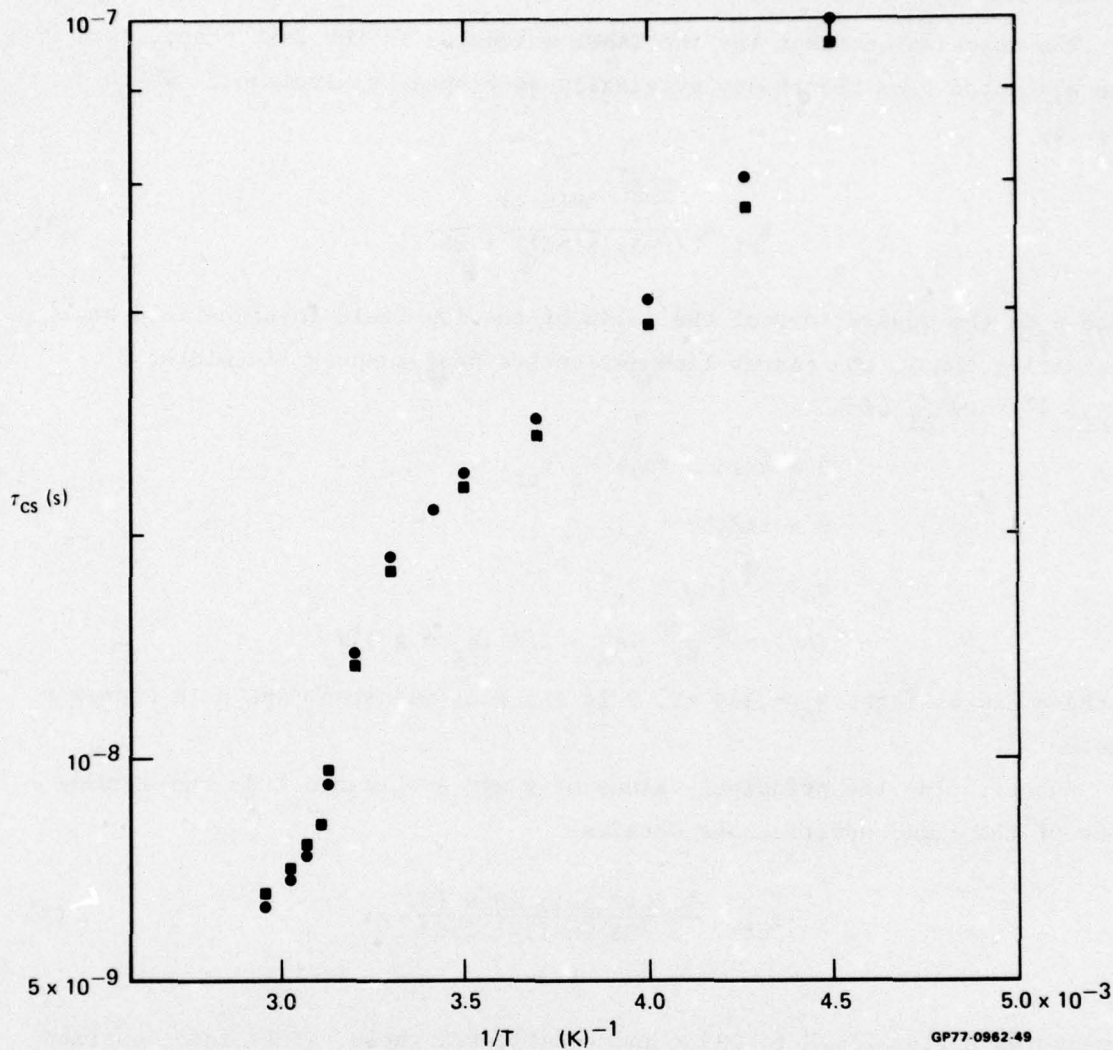


Figure 18 A plot of τ_{CS} , the correlation time for the slow phase, versus (temperature)⁻¹. The values denoted by ● and ■ were obtained by assuming $\Delta\psi = 0.265$ and 0.325 mT respectively.

We suspect that at the high-temperature end of the temperature range shown in Figure 18, the values of S_r , and hence of τ_{CS} , will be lowered by the spectral overlap with the narrowline spectrum. Below ~ 294 K, however, the values of S_r , and hence τ_{CS} , are less affected by spectral overlap since the intensity of the narrowline spectrum is reduced with decreasing temperature.

Assuming that τ_{CS} is of the form

$$\tau_{CS} = \tau_{CS}^0 \exp \Delta E/RT, \quad (2)$$

the best data fit below 293 K in Figure 18 is $\Delta E = 10.5 \pm 1.5 \text{ kJ}\cdot\text{mole}^{-1}$.

The correlation times for the TANOL molecules in the fast phase, τ_{cf} , were evaluated from the theory originally developed by Kivelson,¹³ which is given by

$$\tau_{cf} = \frac{\frac{\sqrt{3}}{2} \Delta H(n-1)}{(n-1)(B'-C') + 2B'}, \quad (3)$$

where n is the square root of the ratio of the low-field to high-field peak intensities, ΔH is the center-line derivative peak-to-peak linewidth, $B' = B/\tau_{cf}$, $C' = C/\tau_{cf}$ with

$$B = 4/15 b (\Delta\gamma) H_0 \tau_{cf},$$

$$C = 1/8 b^2 \tau_{cf},$$

$$b = \frac{4\pi}{3} (A_z - A_x),$$

$$(\Delta\gamma) = \frac{2\pi \beta h}{h} [g_z - 1/2 (g_x + g_y)].$$

In these expressions, $H_0 = 340 \text{ mT}$, β is the Bohr magneton, and h is Planck's constant.

Substituting the principal values of g and A obtained from the simulations of the rigid spectra, one obtains

$$\tau_{cf} = \frac{1.524 (n-1) \Delta H \times 10^9}{2.785 (n-1) + 2.88} \text{ s}. \quad (4)$$

We measured n from 234 K to 293 K and substituted these values into Equation (4) to obtain the temperature dependence of τ_{cf} . It was not possible to evaluate the width of the center line because of the overlap with the broad line. We therefore used the widths of the low-field line for ΔH . This should be a good approximation since $-B \sim C$.

The $\ln \tau_{cf}$ versus $1/T$ dependence shown in Figure 19 would indicate that τ_{cf} is given by

$$\tau_{cf} = \tau_{cf}^0 \exp \Delta E/RT, \quad (5)$$

with $\Delta E = 9.3 \text{ kJ/mole}$. It is interesting to note that at 293 K $\tau_{cf} = 2.4 \times 10^{-10} \text{ s}$, whereas $\tau_{cs} = 2 \times 10^{-8} \text{ s}$.

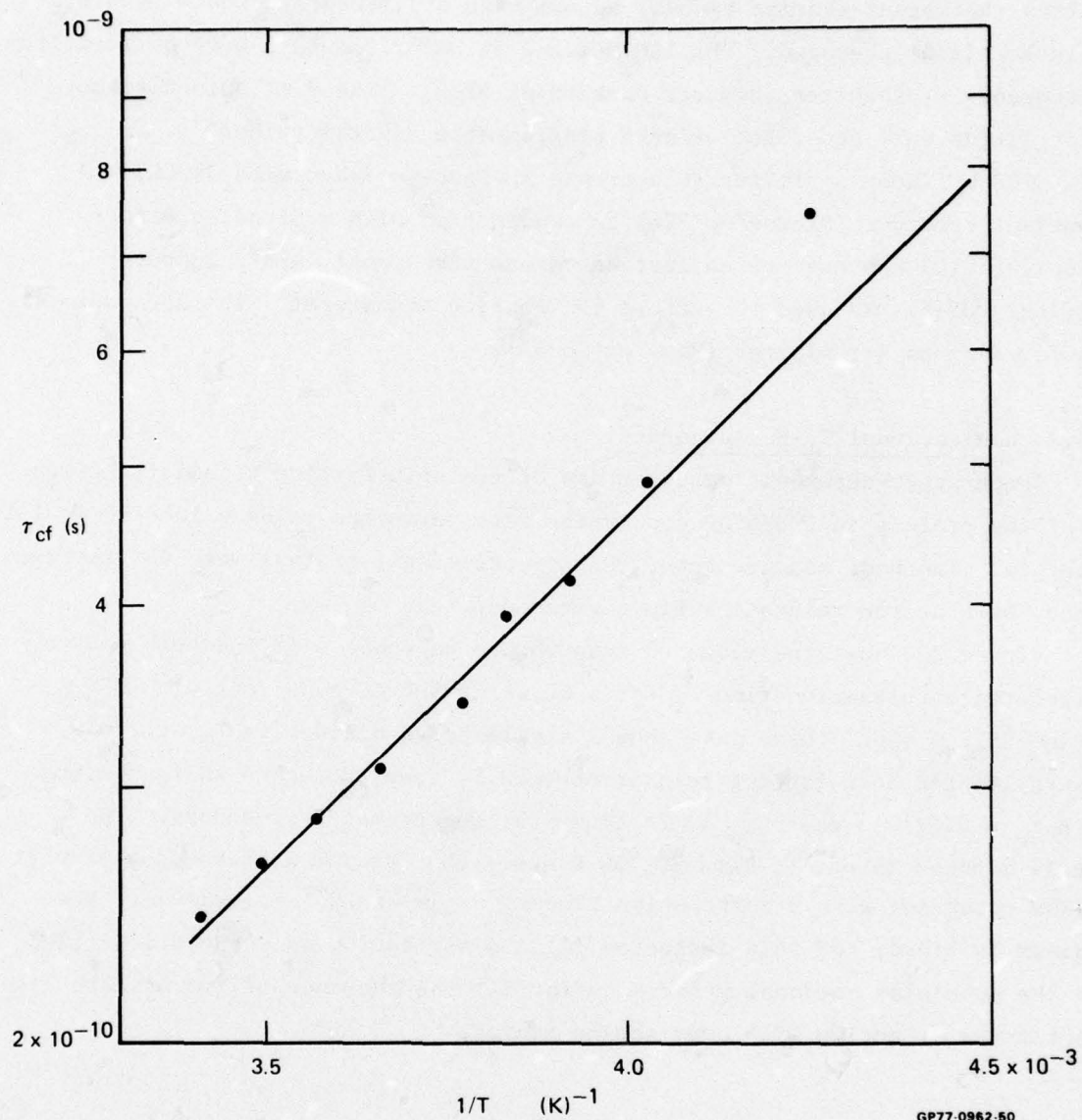


Figure 19 A plot of τ_{cf} , the correlation time for the motion in the fast phase as determined from the ratio of the heights of the low and high field lines, versus $(\text{temperature})^{-1}$.

2.3 NMR Studies

2.3.1 Pulsed NMR Spectrometer

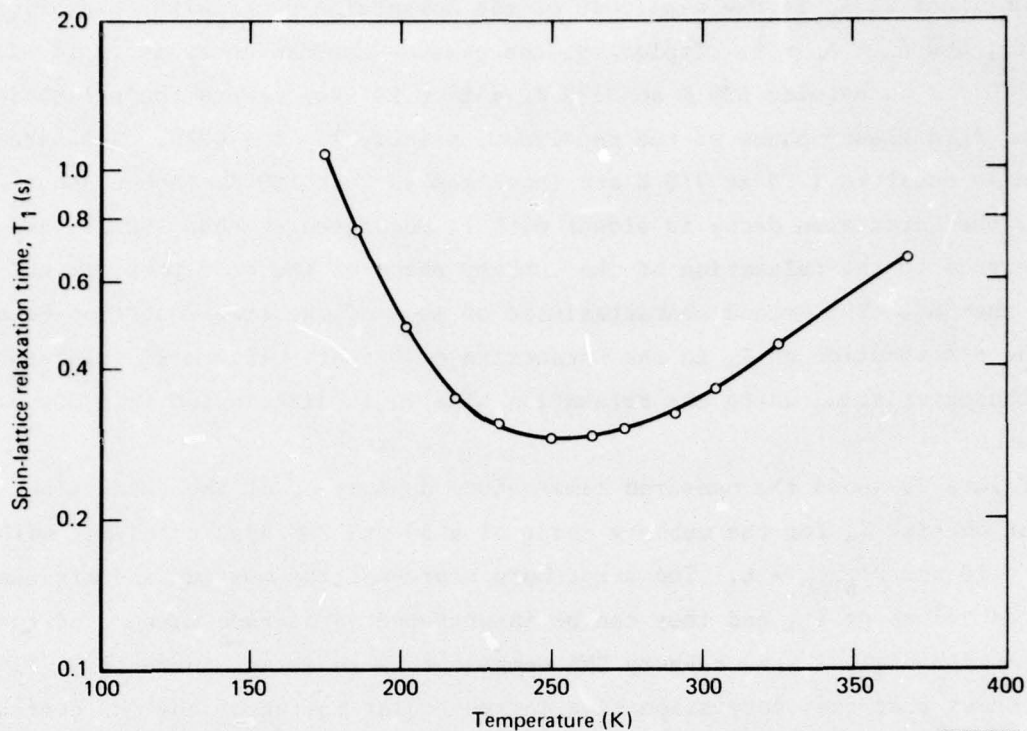
All proton NMR measurements were obtained with a single coil spectrometer operating at 100 MHz. An external fluorine lock sample at 94 MHz was used to

control the magnet (Varian V-4014) to minimize drift so that weak signals could be signal-averaged. The 100 MHz and 94 MHz rf signals were derived from a frequency synthesizer (Hewlett Packard HP 5100). The 8 mT pulsed rf magnetic fields were generated using a programmable digital pulser¹⁴ and a 100 W linear amplifier (Electronic Navigation Industries 3100L). A transient recorder (Biomation 826) in conjunction with a signal-averager (Nicolet 1070) was used to collect and store the signal, and a computer (Digital PDP-8) was used to perform the Fourier transforms. The data were displayed on an X-Y plotter (Moseley 7000A).

2.3.2 Conventional T_1 Measurements

Temperature-dependent measurements of the spin-lattice relaxation times T_1 of the protons in DMS/BPAC copolymers were performed using a 180° - 90° pulse sequence. In these measurements, the non-equivalent protons were not resolved; hence, bulk proton relaxation times were measured.

Figure 20 shows the measured temperature dependence of the bulk proton spin-lattice relaxation time T_1 for a 50 wt% DMS/BPAC copolymer with $\overline{DP}_{\text{DMS}} = 20$ and $\overline{DP}_{\text{BPAC}} = 6$. These data show a single broad minimum in T_1 at 250 K. Generally, the spin-lattice relaxation time T_1 goes through a sharp minimum when $\tau_c = 0.62/\omega_0$, where ω_0 is 2π times the spectrometer frequency. The single minimum in our T_1 data at 250 K shows that at 250 K there is molecular motion occurring with a correlation time τ_c of about 10^{-9} s. However, the minimum is broad, and this indicates (1) a distribution of correlation times for the molecular motional process and/or (2) the presence of two or more distinct types of motion with overlapping minima.



GP77-0962-3

Figure 20 Temperature dependence of the bulk spin-lattice relaxation time T_1 in a 50 wt% DMS/BPAC copolymer with $\overline{DP}_{DMS} = 20$ and $\overline{DP}_{BPAC} = 6$.

2.3.3 Conventional T_2 Measurements

Temperature-dependent measurements of the spin-spin relaxation times T_2 of the protons in DMS/BPAC copolymers were performed by observing the free-induction decay signal following a single 90° rf pulse. The homogeneity of the magnetic field was good enough to allow this technique to be used.

Figure 21 shows the free-induction decay signal of a 50 wt% DMS/BPAC copolymer with $\overline{DP}_{DMS} = 20$ and $\overline{DP}_{BPAC} = 6$. The first characteristic of this decay signal, which is common to all free-induction decays, is the distinct two-component decay which can be represented by

$$S(t) = A_G \exp[-(t/T_{2G})^n] + A_L \exp(-t/T_2),$$

where $S(t)$ is the normalized free-induction decay signal, A_G is the amplitude of the pseudo-Gaussian decay with relaxation time T_{2G} , n is a parameter

between 1 and 2, A_L is the amplitude of the Lorentzian decay with relaxation time T_2 , and $A_G + A_L = 1$. Typically, the pseudo-Gaussian decay is rapid with $T_{2G} = 20 \pm 2 \mu\text{s}$ between 130 K and 370 K, and it is assigned to the relaxation of the rigid glassy phase of the copolymer, principally the BPAC. The parameter n is equal to 1.25 at 370 K and increases to 2 at 130 K. Above about 170 K, the Lorentzian decay is slower with T_2 much greater than 100 μs , and it is assigned to the relaxation of the rubbery phase of the copolymer, principally the DMS. The second characteristic of many of the free-induction decays was the distribution of T_2 in the Lorentzian component. Figure 21 illustrates this characteristic, where the relaxation time T_2 is distributed from 300 μs to 410 μs .

Figure 22 shows the measured temperature dependence of the spin-spin relaxation time T_2 for the rubbery phase of a 50 wt% DMS/BPAC copolymer with $\overline{DP}_{\text{DMS}} = 20$ and $\overline{DP}_{\text{BPAC}} = 6$. The error bars represent the maximum and minimum measured values of T_2 , and they can be interpreted as a crude measure of the distribution of T_2 in the rubbery DMS component. The abrupt increase in T_2 at 170 K shows that the correlation time for molecular motion of the DMS decreases with temperature, having a value of approximately 10 μs at 170 K, since the correlation time τ_c at a rapid transition in T_2 is approximately equal to the value of T_2 at the low-temperature side of the transition.¹⁵ The rapid increase in T_2 above 170 K for the copolymer is small compared to the observed increase in T_2 for the DMS homopolymer,¹⁶ which increases to over 1 s. Here, the BPAC domains restrict the DMS motion, and this is demonstrated by the more modest increase in T_2 with increasing temperature.

The transition in T_2 at 170 K is assigned to the glass transition temperature T_g of the major portion of the DMS component of the copolymer; the T_g of the uncrosslinked homopolymer is about 150 K. The assignment of 170 K as T_g is supported by torsion pendulum results which show a loss peak at 170 K assigned to the glass transition.⁴ The larger value of T_g and more modest increase in T_2 above the transition, compared with those for the homopolymer, are attributed to the effects of the physical crosslinks provided by the BPAC domains.

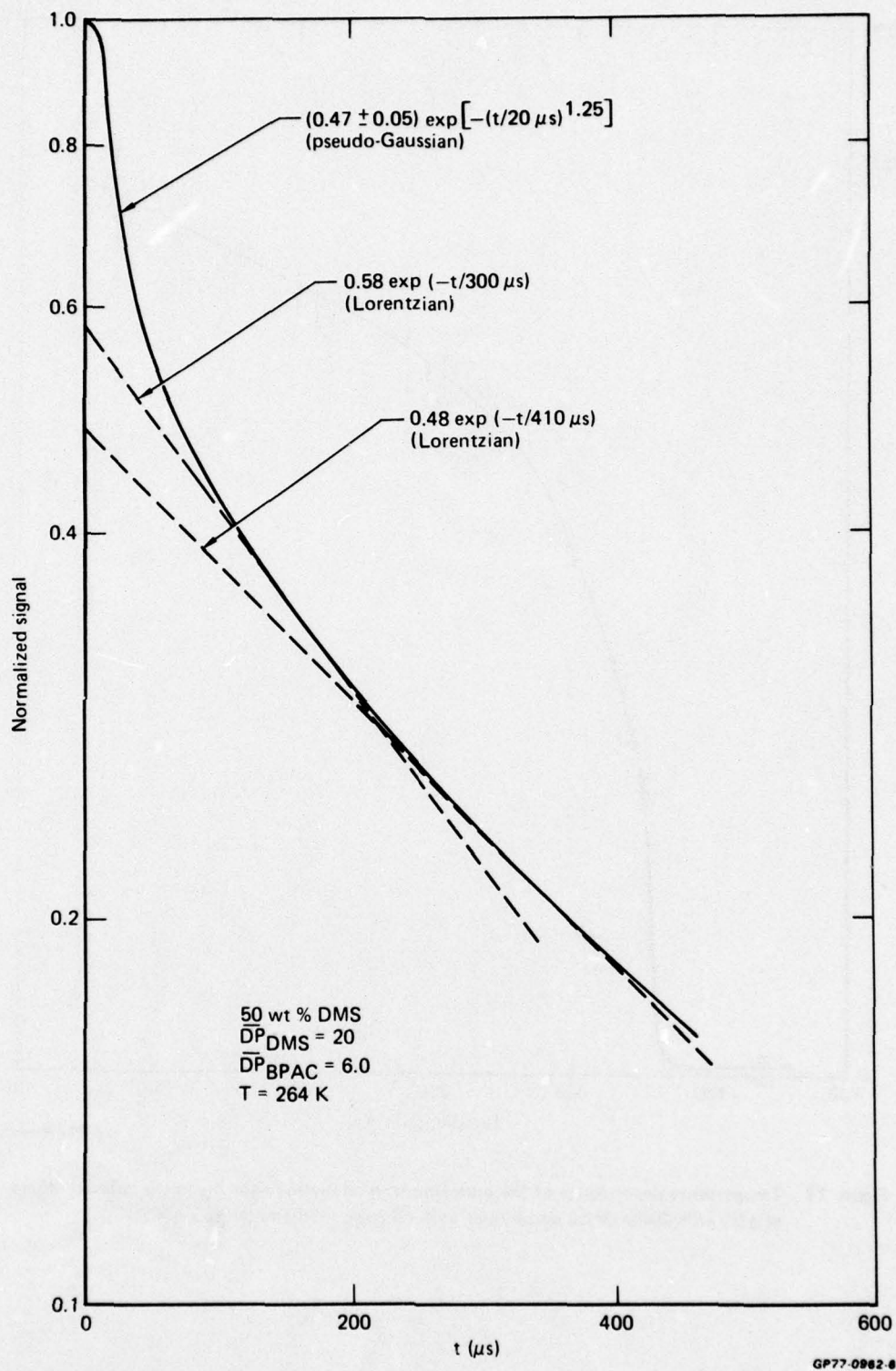


Figure 21 Free-induction decay signal of a DMS/BPAC copolymer showing the pseudo-Gaussian decay and the distribution of the Lorentzian decay.

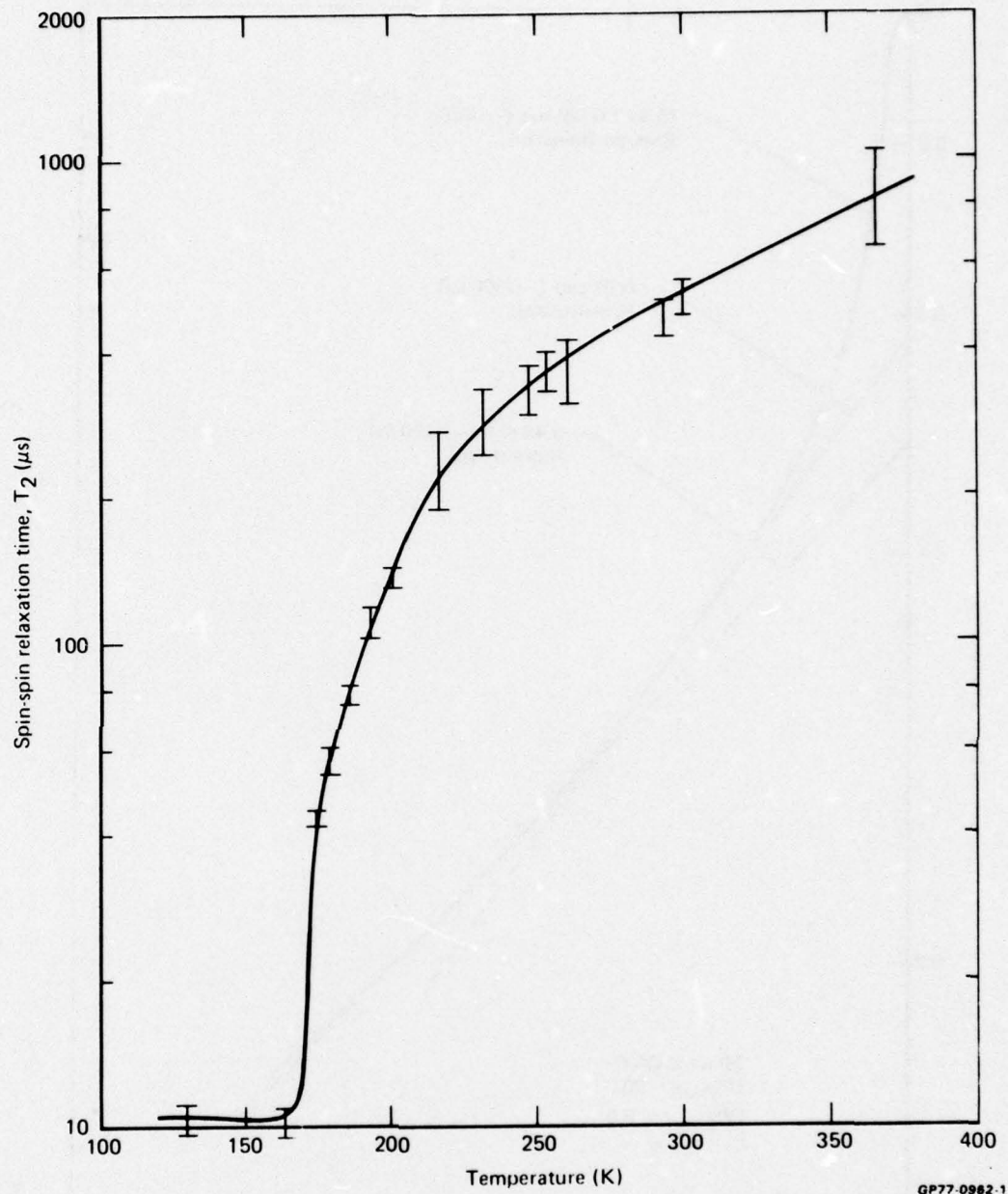


Figure 22 Temperature dependence of the bulk spin-spin relaxation time T_2 in the rubbery phase of a 50 wt% DMS/BPAC copolymer with $\bar{DP}_{\text{DMS}} = 20$ and $\bar{DP}_{\text{BPAC}} = 6$.

The free-induction decay signals were used to determine the ratio of the number of protons in the rubbery phase to those in the rigid phase. This is simply the ratio of the amplitudes of the two components in the free-induction decay and is denoted by $\beta = A_L/A_G$. This is plotted along with T_2 as a function of inverse temperature in Figure 23. The rapid increase in β at $T \approx 170$ K corresponds to the bulk of the DMS becoming rubbery at the glass transition temperature T_g . If all of the DMS were rubbery and all of the BPAC were rigid, then β would be equal to 1.47 (the ratio of the number of protons in the DMS component to those in the BPAC component). Fortuitously, β is equal to 1.5 at room temperature, but it ranges from 0.7 just above the bulk glass transition temperature to 2.3 at 370 K. We interpret this increase in β with temperature as evidence that a portion of the copolymer has a broad distribution of glass transition temperatures. Section 2.3.7 identifies this distribution, at least in part, along the length of the DMS blocks.

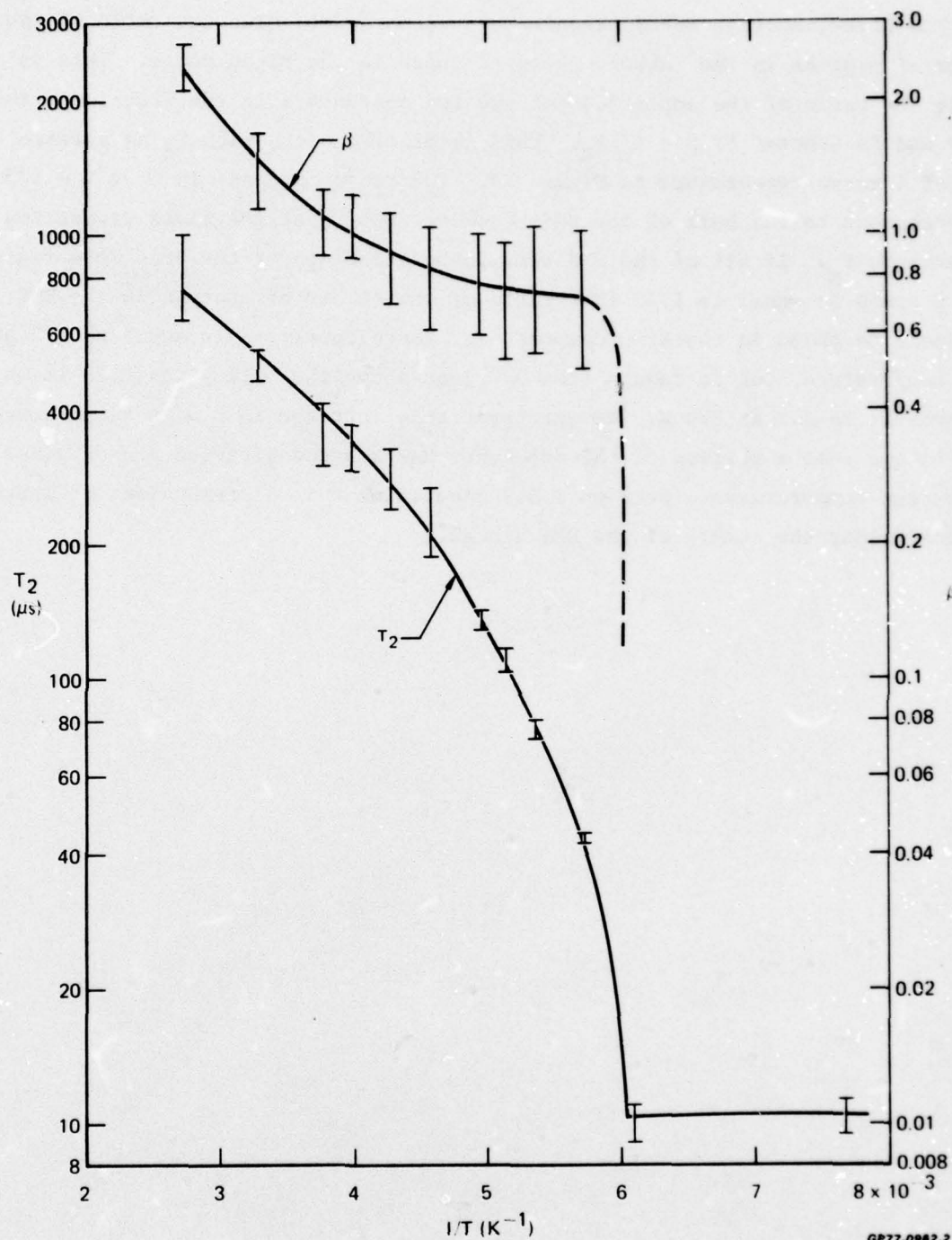
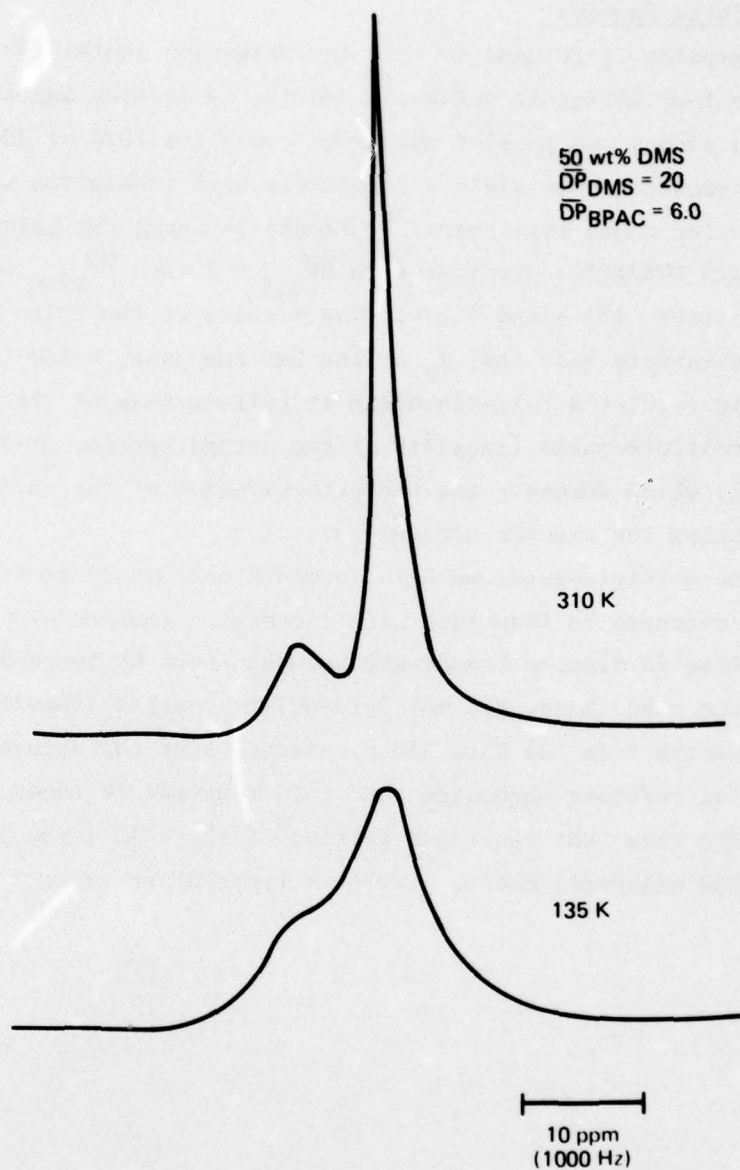


Figure 23 The ratio β of the protons in the rubbery phase to those in the rigid phase and the spin-spin relaxation time T_2 of the protons in the rubbery phase of a 50 wt% DMS/BPAC copolymer with $\overline{DP}_{\text{DMS}} = 20$ and $\overline{DP}_{\text{BPAC}} = 6$.

2.3.4 Multiple-Pulse Spectra

The multiple-pulse cycle used in this investigation contained eight 0.7 μ s rf pulses with four different phases,¹⁷ and the cycle time was 48 μ s. The nuclear induction signal was sampled once each cycle for 1024 or 2048 cycles and was Fourier transformed to yield a relatively high resolution spectrum suitable for studying these copolymers.¹⁸ Figure 24 shows two multiple-pulse spectra of a 50 wt% DMS/EPAC copolymer with $\overline{DP}_{\text{DMS}} = 20$ and $\overline{DP}_{\text{BPAC}} = 6$ at two different temperatures, 135 K and 310 K. The results of the spin-spin relaxation time T_2 measurements show that T_2 of the DMS component below 170 K is 10 μ s, and this would predict a half-linewidth at half-maximum of $(2\pi T_2)^{-1} = 16\ 000$ Hz. The multiple-pulse linewidth of the methyl protons at 135 K is only about 350 Hz, which demonstrates the effectiveness of the multiple-pulse technique in reducing the dipolar broadening.

At 310 K, the multiple-pulse methyl linewidth narrows to about 75 Hz. Apparently, this decrease in linewidth with increasing temperature is caused by further reduction in dipolar broadening brought about by increased molecular motion. On the other hand, the multiple-pulse aromatic linewidth did not decrease significantly from 135 K to 310 K. Recall that the spin-spin relaxation time T_{2G} also remained unchanged over this temperature range. These results support the view that the major portion of the BPAC component is not undergoing extended segmental motion over this temperature range.



GP77-0962-4

Figure 24 Multiple-pulse spectra of a DMS/BPAC copolymer at 310 and 135 K. The resonance line on the left is produced by the aromatic protons, and the line on the right is produced by the methyl protons.

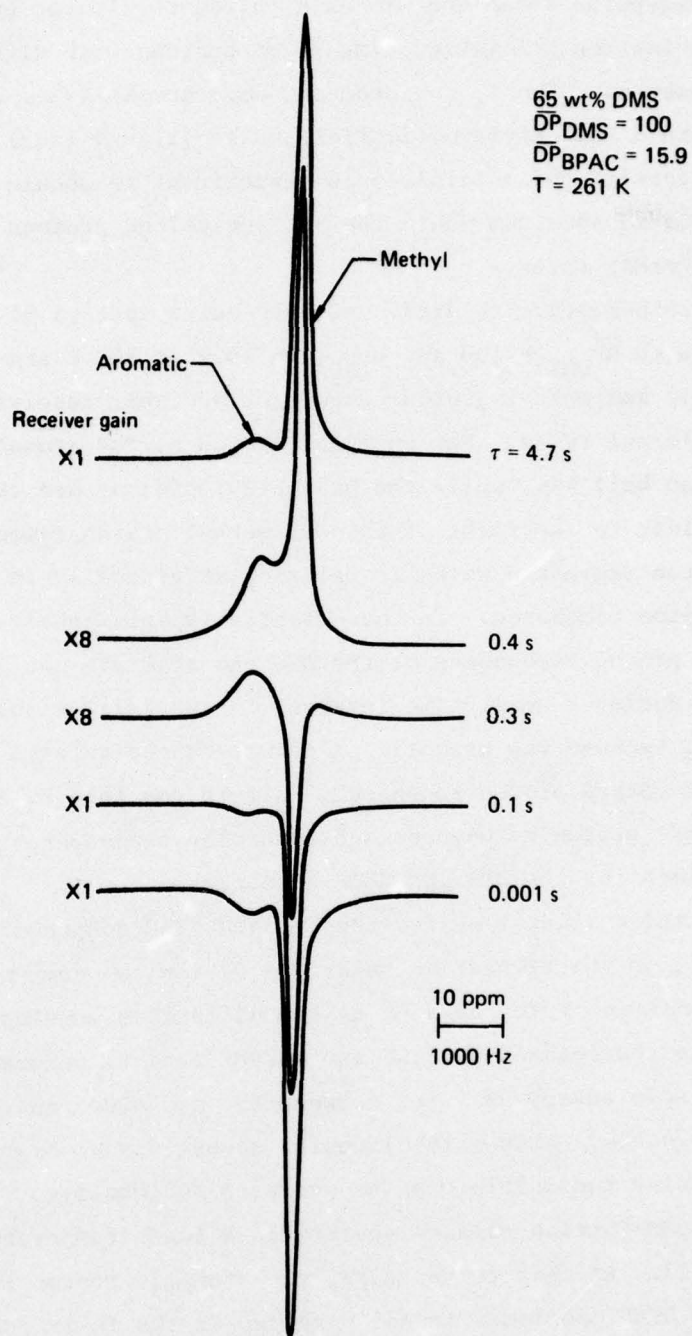
2.3.5 Multiple-Pulse Partially Relaxed Spectra

The multiple-pulse technique was used to reduce dipolar broadening and permit the spin-lattice relaxation time T_1 of protons with different chemical shifts to be measured. The T_1 measurements were accomplished by inverting the proton spins with a 180° rf magnetic field pulse (1.4 μ s long), waiting a time τ , and then performing the multiple-pulse experiment to obtain a partially spin-lattice relaxed spectrum where the non-equivalent protons can be seen relaxing at different rates.

Partially spin-lattice relaxed, multiple-pulse spectra of a 65 wt% DMS/BPAC copolymer with $\overline{DP}_{\text{DMS}} = 100$ and $\overline{DP}_{\text{BPAC}} = 15.9$ at 261 K are shown in Figure 25. The aromatic and methyl proton resonances are well resolved and are seen to relax at different rates. For example, at 0.3 s, the aromatic protons have relaxed more than half way, while the DMS methyl protons are still inverted; the slight shoulder to the right of the DMS methyl proton resonance is the BPAC methyl proton resonance which is relaxing at virtually the same rate as the aromatic proton resonance. In these partially spin-lattice relaxed spectra, the methyl proton resonances of the DMS and BPAC are not generally resolved except during a small time interval in the relaxation, e.g., at $\tau = 0.3$ s. However, because the aromatic proton resonance relaxes at the same rate as the BPAC methyl proton resonance,¹⁹ it is possible to correct for the overlapping methyl proton resonances and determine the separate proton spin-lattice relaxations for the DMS and BPAC components.

The spin-lattice relaxation for the DMS and BPAC components is shown in Figure 26. Early in the relaxation, near $\tau = 0$, the two components relax at significantly different rates as seen by the difference in slopes of the two curves. Later in the relaxation, the two curves tend to become parallel. This is because spin energy diffuses between the two components and causes them to relax together. This spin diffusion occurs via dipolar coupling during the time τ while the multiple-pulse cycle is inoperative.

Partially spin-lattice relaxed spectra at a lower temperature, 90 K, is shown in Figure 27. At this temperature, the aromatic proton resonance in this low, 35 wt% BPAC copolymer is not resolved in the fully relaxed spectrum. However, the aromatic proton resonance is resolved in some of the partially relaxed spectra. These spectra show that at 90 K the DMS protons relax faster than the BPAC protons; at 261 K, the reverse is true. While T_1 data for the homopolymers of DMS¹⁶ and BPAC²⁰ suggest that this might happen, these experiments have demonstrated for the first time that this occurs in the copolymer.



GP77-0962-53

Figure 25 Partially spin-lattice relaxed multiple-pulse proton NMR spectra of DMS/BPAC block copolymer. τ is the time between the spin-inverting pulse and the multiple-pulse sequence.

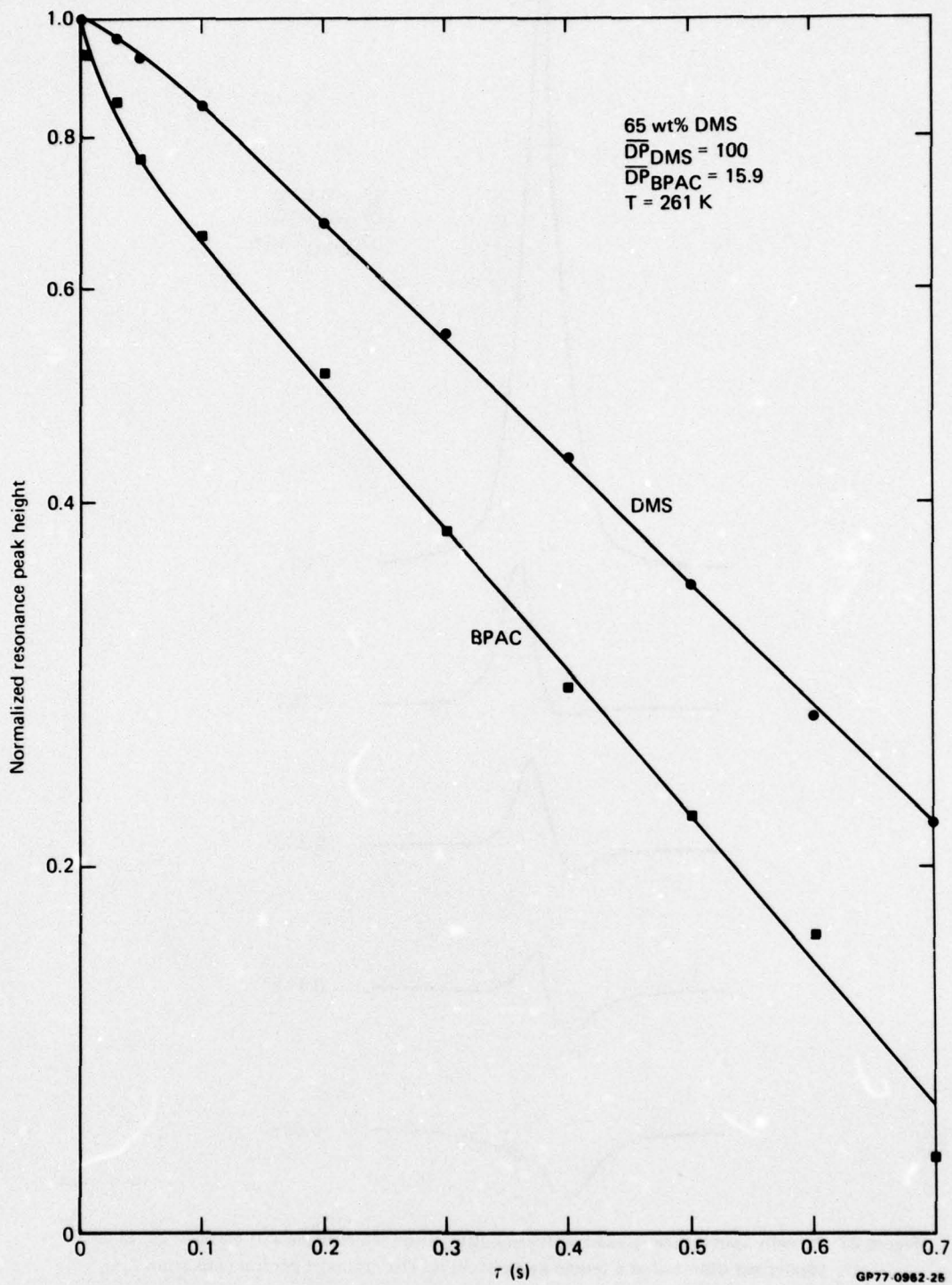


Figure 26 Spin-lattice relaxation of the two components of DMS/BPAC as determined from the multiple-pulse spectra. τ is the time between the spin-inverting pulse and the sampling of the spectra.

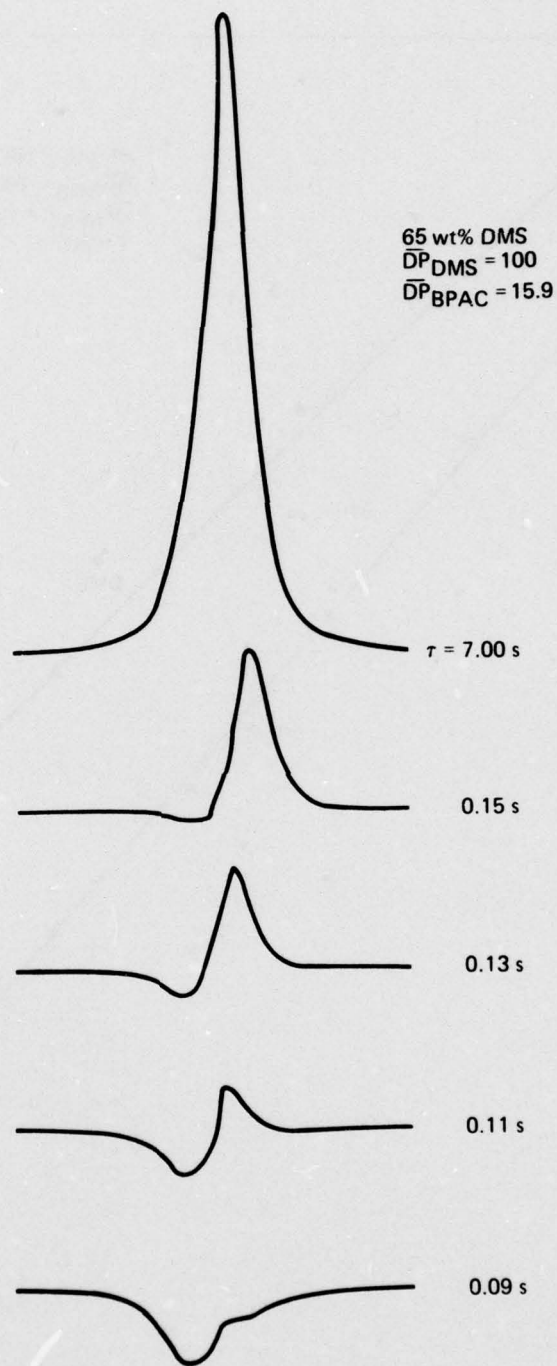


Figure 27 Partially spin-lattice relaxed multiple-pulse proton NMR spectra of DMS/BPAC block copolymer obtained at a temperature of 90 K. The aromatic proton peak is on the left, and the methyl proton peak is on the right. τ is the time between the spin-inverting pulse and the multiple-pulse sequence. These spectra show that at 90 K the DMS protons relax faster than the BPAC protons.

2.3.6 Multiple-Pulse $T_{1\rho}$ Measurements

The $T_{1\rho}$ measurements were also accomplished by applying preconditioning pulses prior to initiating the multiple-pulse experiment. In this case, a 90° rf pulse (0.7 μ s long) was applied to the sample to rotate the proton spins perpendicular to the large, static magnetic field H_0 . Immediately after this 90° rf pulse, a spin-locking rf field H_1 was applied to the sample. The phase of the spin-locking field was adjusted to produce a rotating magnetic field which remained parallel to the proton spins as they precessed about H_0 . In this rotating frame, the spin-locking field H_1 appears as a static magnetic field to the protons. The field H_1 was left on for a time τ_L during which the proton spins relaxed to the lattice under the influence of the field H_1 . Immediately after turning off the H_1 field, the multiple-pulse cycle was initiated. The resulting spectrum was a partially spin-lattice relaxed spectrum in the rotating frame.

Partially spin-lattice relaxed, multiple-pulse spectra in the rotating frame of a 50 wt% DMS/BPAC copolymer with $\overline{DP}_{\text{DMS}} = 20$ and $\overline{DP}_{\text{BPAC}} = 6$ at 298 K are shown in Figure 28. A spin-locking field H_1 of 2.94 mT was used. For a spin-locking time τ_L of 0.1 ms, practically all of the proton spins remained aligned parallel to the rotating magnetic field H_1 ; few relaxed to the lattice. When τ_L was increased to 20.1 ms, Figure 28 shows that about half of the methyl protons have relaxed and more than half of the aromatic protons have relaxed. The heights of these resonance peaks are plotted as a function of τ_L in Figure 29. This figure shows that the spin-lattice relaxations of the DMS and BPAC protons in the rotating frame are not coupled together as they were in the spin-lattice relaxation in the laboratory frame (compare with Figure 26). In the rotating frame, both relaxations are independent exponential decays. This is because the time required for spin diffusion to couple the two components is greater than the time required for each of them to relax to the lattice. The spin-lattice relaxation times $T_{1\rho}$ for the DMS and BPAC protons at 298 K are 31 ms and 16 ms, respectively.

In an effort to determine the correlation time τ_c for segmental motion of the DMS component, a series of partially spin-lattice relaxed, multiple-pulse spectra in the rotating frame were obtained as a function of temperature for three different DMS/BPAC copolymers. The results of these measurements are shown in Figure 30. The minima in $T_{1\rho}$ for the DMS protons in all three

copolymers occur at 180 ± 3 K. Similar to T_1 , $T_{1\rho}$ also goes through a minimum when the correlation time τ_c for molecular motion is equal to ω_1^{-1} , where ω_1 is the angular frequency of precession of the protons about the spin-locking field H_1 . Since H_1 is 2.94 mT, τ_c for DMS at a temperature of 180 K is 1.3×10^{-6} s.

To be certain that these results were not affected by spin diffusion to or from the BPAC protons, we performed auxiliary experiments in our MDRL studies on a DMS/BPFC block copolymer. Again, the DMS proton $T_{1\rho}$ minimum occurred at 180 K. Since it is unlikely that the BPFC and BPAC would have the same correlation times for molecular motion at 180 K, we conclude that these $T_{1\rho}$ experiments have measured the main-chain segmental motion of DMS and not BPAC.

The correlation times for DMS motion determined from the T_1 minimum, the T_2 transition, and the $T_{1\rho}$ minimum are plotted as a function of inverse temperature in Figure 31. The three points fall on a straight line whose slope yields an activation energy for DMS molecular motion of 40.3 kJ/mole. This is to be compared with an activation energy of 50.5 kJ/mole determined for this copolymer by measuring the dielectric loss at the glass transition.²¹ If only our T_2 and $T_{1\rho}$ data are used, since the T_1 minimum was so broad, we obtain an activation energy of 51.9 kJ/mole, which is in better agreement with the dielectric loss results. Finally, the value of τ_c determined from the dielectric loss data²¹ at $T = 170$ K was 9×10^{-6} s which compares favorably with the value of 10^{-5} s determined from the T_2 transition.

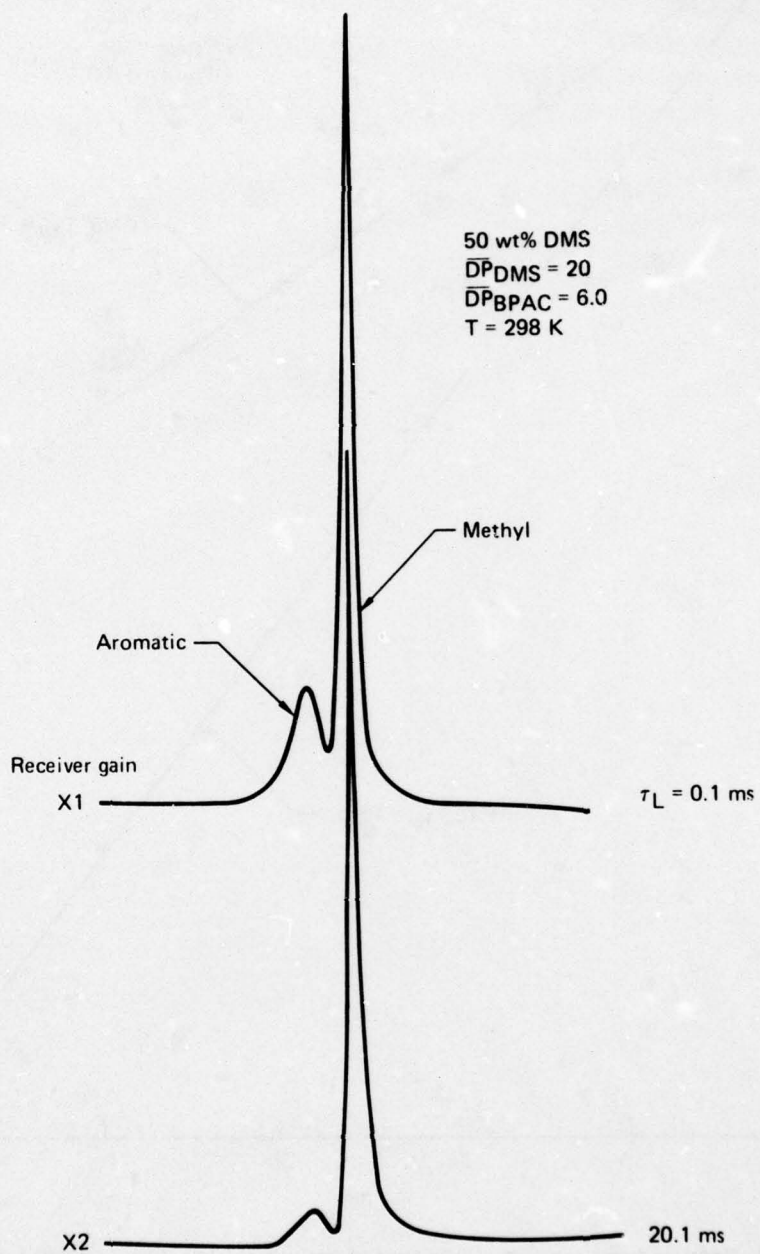


Figure 28 Partially spin-lattice relaxed DMS/BPAC multiple-pulse spectra in rotating frame. τ_L is the duration of spin locking prior to observing the spectra.

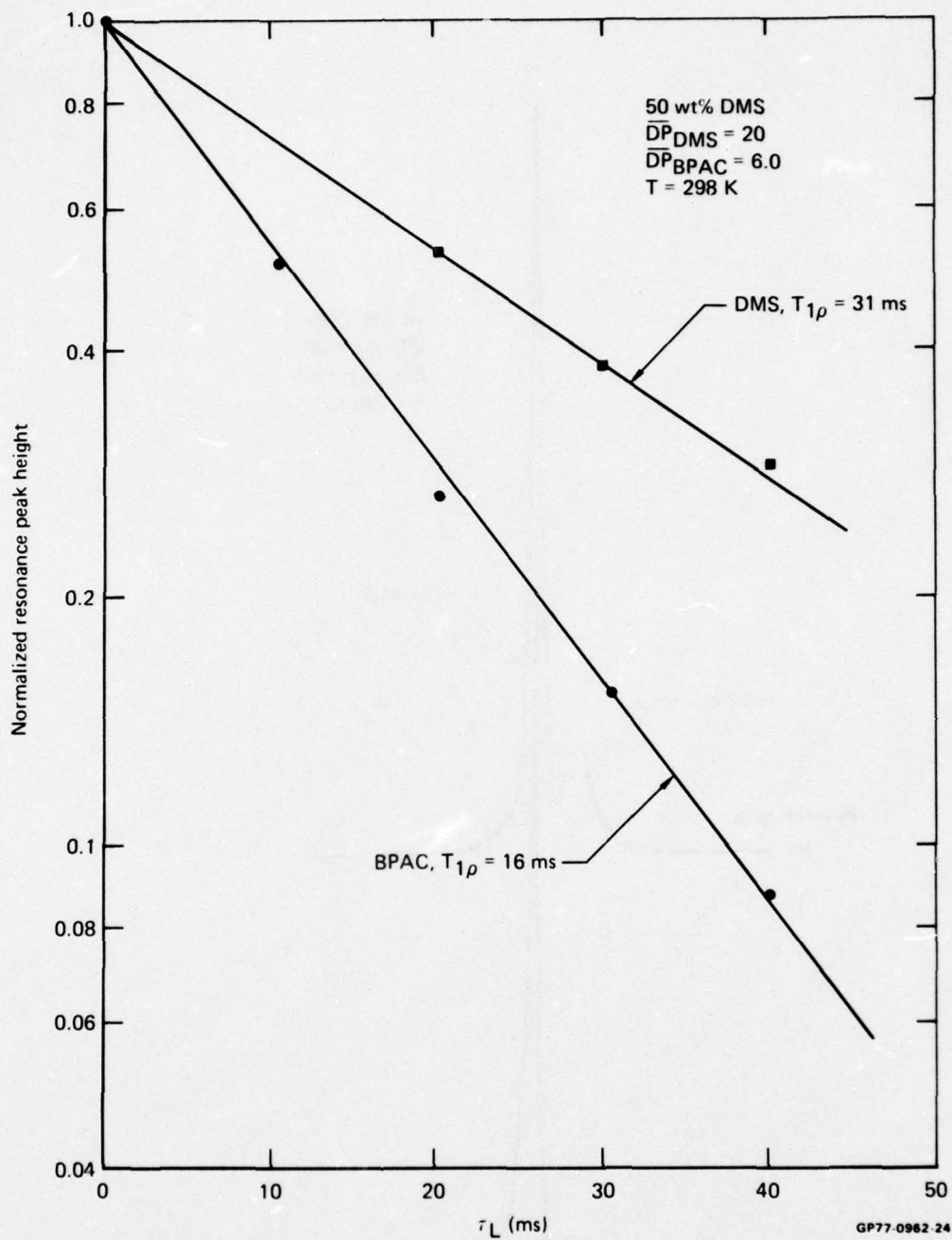


Figure 29 Rotating frame spin-lattice relaxation of the two components of DMS/BPAC determined from multiple-pulse spectra. τ_L is the duration of spin locking prior to observing the spectra.

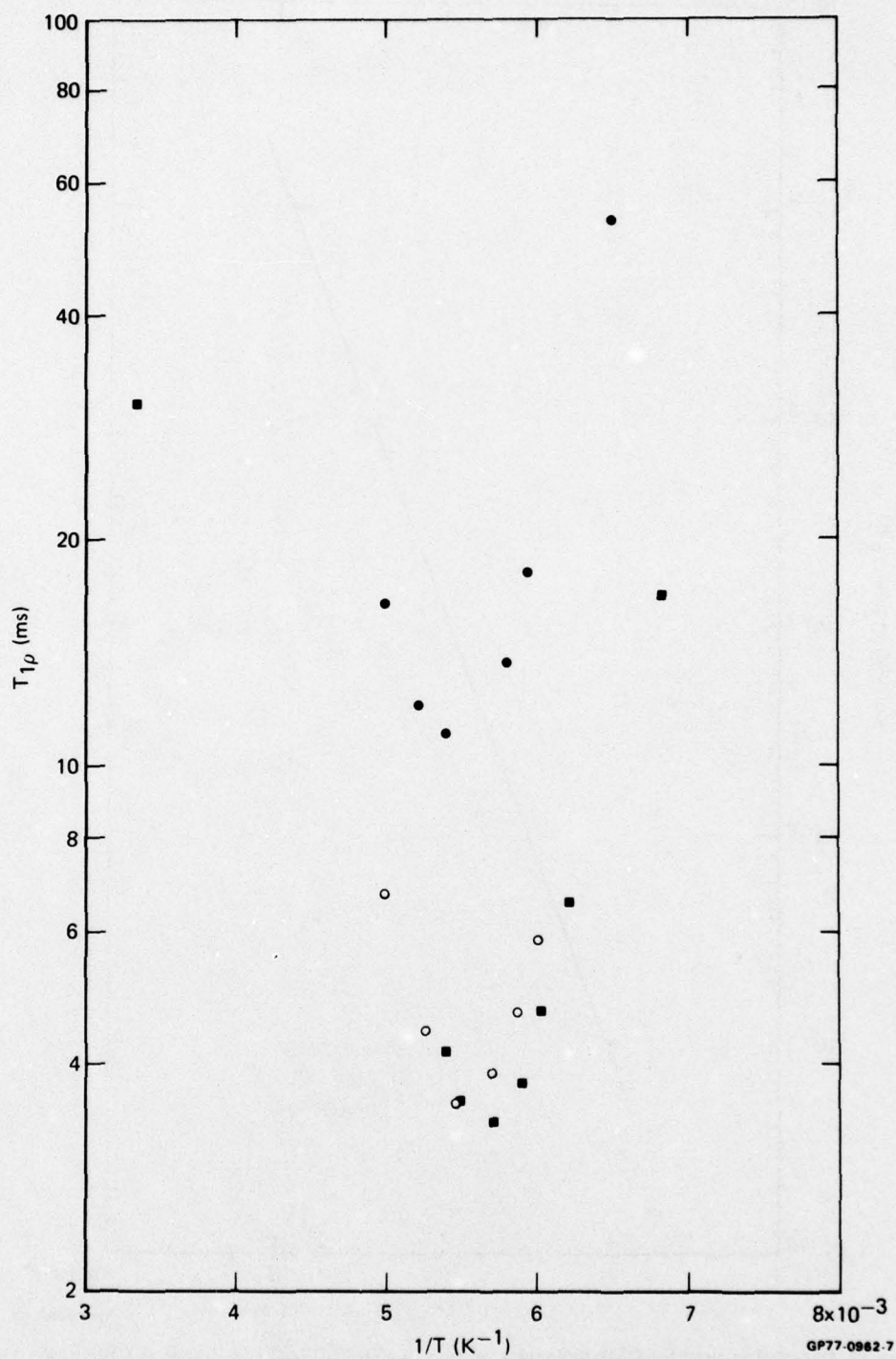


Figure 30 Temperature dependence of the spin-lattice relaxation time in the rotating frame for DMS/BPAC copolymers with 65 wt% DMS, $\overline{DP}_{DMS} = 20$ (○); 65 wt% DMS, $\overline{DP}_{DMS} = 100$ (●); and 50 wt% DMS, $\overline{DP}_{DMS} = 20$ (■).

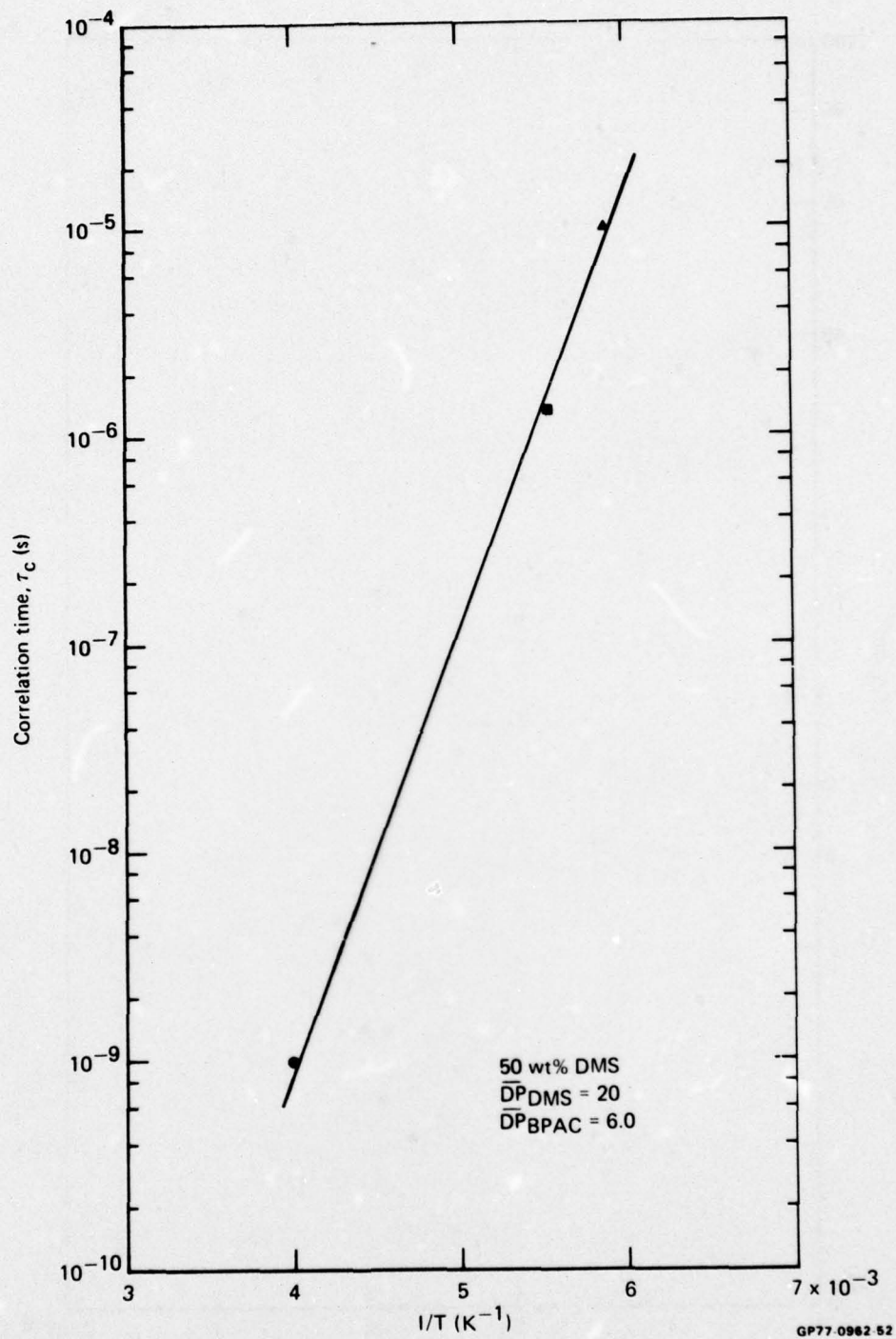


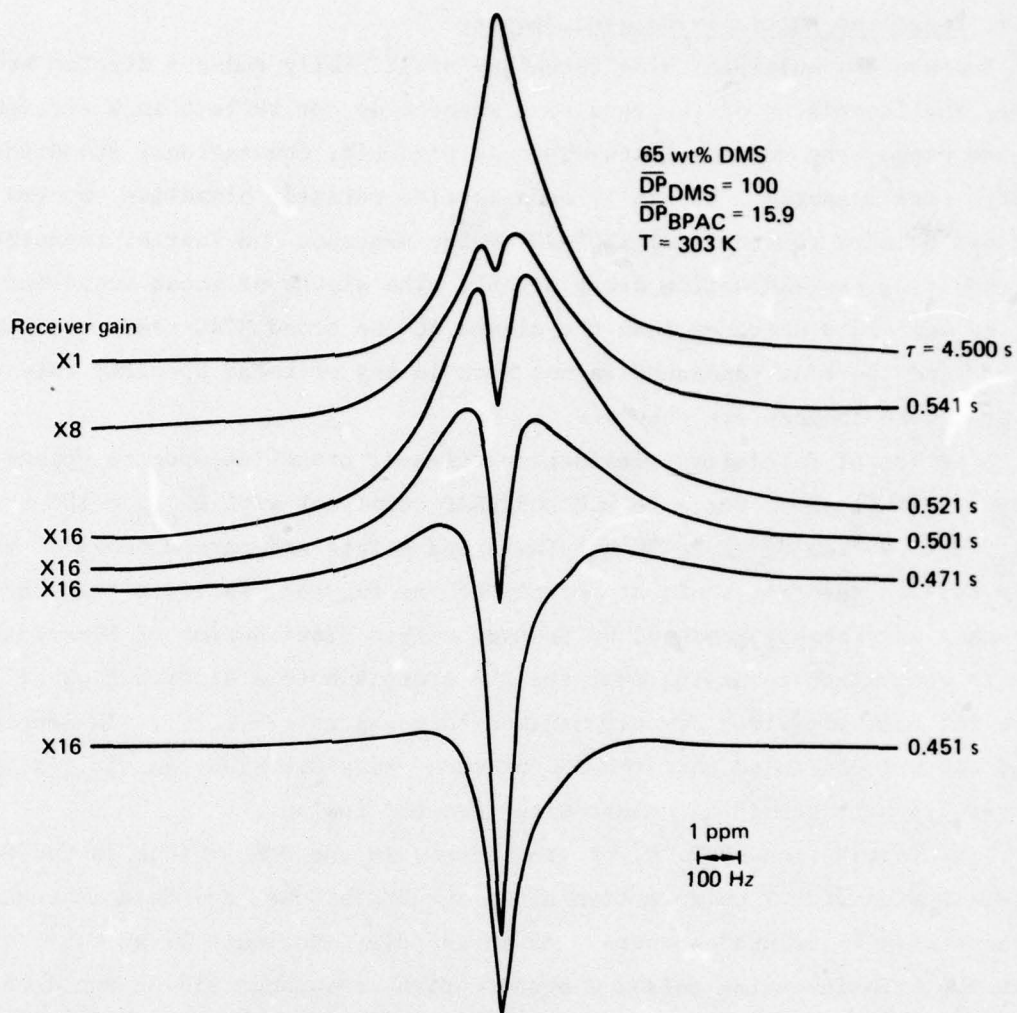
Figure 31 Correlation time for DMS molecular motion in a DMS/BPAC copolymer as a function of inverse temperature as determined from T_1 minimum (●), $T_{1\rho}$ minimum (■), and T_2 transition (▲). The slope of the line connecting the points yields an activation energy of $40.3 \text{ kJ}\cdot\text{mole}^{-1}$.

2.3.7 Broadline Partially-Relaxed Spectra

Because the multiple-pulse technique artificially reduces dipolar broadening, the linewidths of the resulting spectra do not reflect in a straightforward manner the natural linewidth. As a result, conventional broadline spectra were measured. Partially spin-lattice relaxed, broadline spectra were obtained using a conventional 180° - 90° pulse sequence and Fourier transforming the resulting free-induction decay signal. The widths of these broadline spectra were much narrower than the widths of the broad BPAC resonance linewidths, and the BPAC resonance is not seen in any of these spectra; only the DMS proton resonances are observed.

A series of partially spin-lattice relaxed, broadline spectra appear in Figures 32 through 35 for a 65 wt% DMS/BPAC copolymer with $\overline{DP}_{DMS} = 100$ and $\overline{DP}_{BPAC} = 15.9$ from 303 K to 90 K. The broad skirts and narrow peaks of the fully relaxed spectra, shown at the top of the figures, indicate that the resonance is probably produced by protons with a distribution of linewidths. This is equivalent to saying that the DMS protons have a distribution of T_2 's, since the half linewidth at half maximum is equal to $(2\pi T_2)^{-1}$. In Section 2.3.3, it was concluded that the DMS protons had a distribution of T_2 's, so the results here are in agreement with that conclusion.

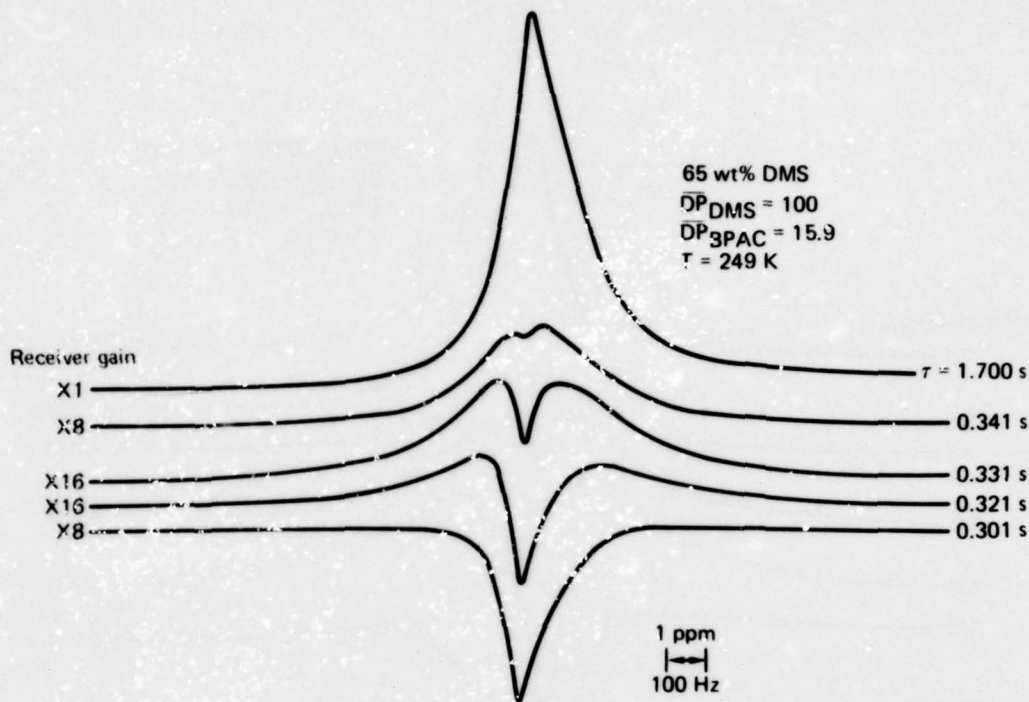
The distribution of T_2 's, or linewidths, in the DMS protons is caused by a distribution of molecular motion along the DMS blocks, and this is revealed in the partially relaxed spectra. As an example, in Figure 32 at 0.541 s after the spin inverting pulse, a broad upright resonance line coincident with a narrow inverted line is seen. The protons producing the upright resonance are relaxing faster than the protons producing the inverted resonance. The multiple-pulse spectra have shown that at this temperature, 303 K, the protons in the BPAC blocks relax to the lattice faster than protons in the DMS blocks, causing the DMS protons to relax more rapidly via their spin diffusion coupling to the BPAC protons. It follows that the DMS protons at the ends of the DMS blocks (closest to the BPAC protons) will relax faster than the DMS protons in the centers of the DMS blocks. Thus, in the spectrum at $\tau = 0.541$ s, we can assign the more rapidly relaxing protons (upright resonance) to those near the ends of the DMS blocks and the more slowly relaxing protons (inverted resonance) to those near the centers of the DMS blocks. Since molecular motion is known to narrow dipolar-broadened resonance and the narrow resonance is assigned to the protons at the centers of the DMS blocks, it is concluded that the centers of the DMS blocks are in greater motion than their ends.



GP77-0962-41

Figure 32 Partially spin-lattice relaxed DMS/BPAC broadline spectra. τ is the time between the spin-inverting pulse and the sampling of the spectra.

The spectra at different times in the relaxation reveal molecular motion at different distances from the ends of the DMS blocks.¹⁹ As an example, the spectrum for $\tau = 0.451 \text{ s}$ shows a broad line emerging above the baseline; this broad line is caused by the protons close to the ends of the DMS blocks adjacent to the rigid BPAC domains. The broader this line, the more restricted is the motion at the ends of the DMS blocks. Likewise, the spectrum for $\tau = 0.541 \text{ s}$ shows the narrow inverted line just before it becomes upright and is no longer observable; this narrow line is caused by the protons closest to the

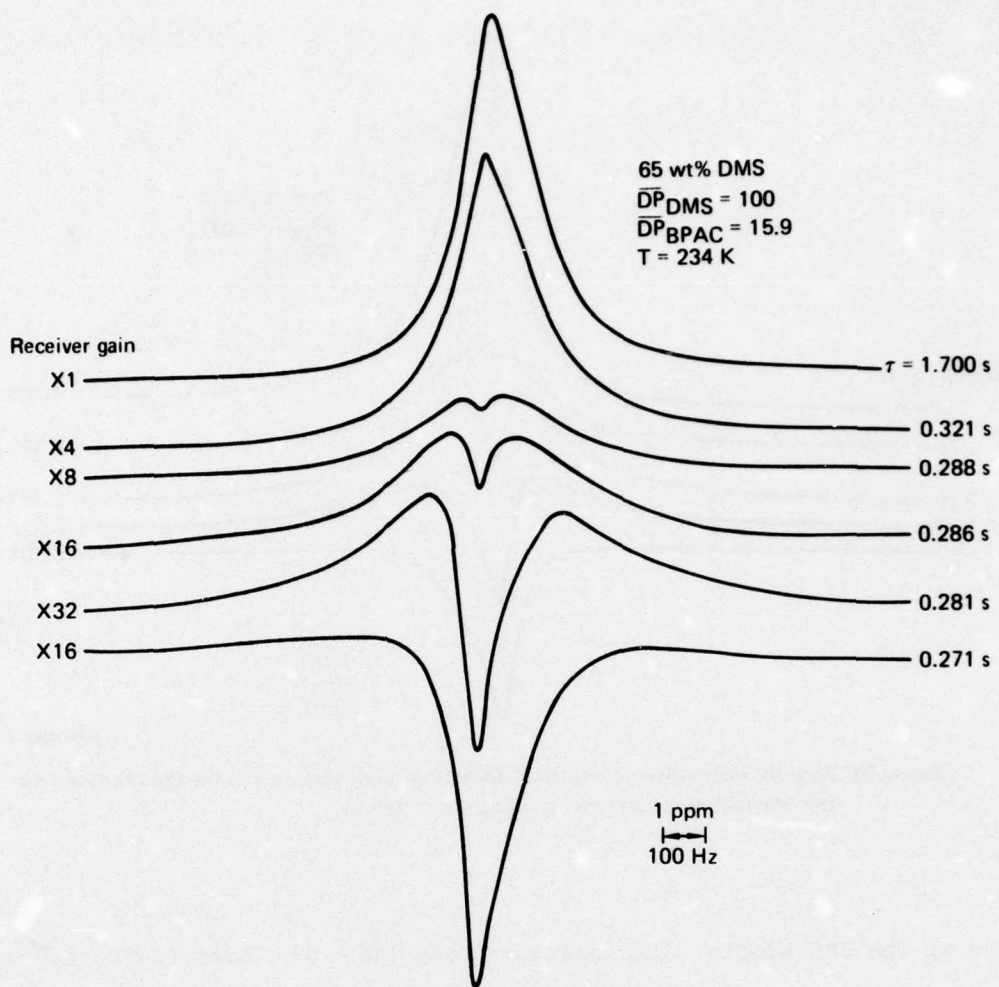


GP77-0962-42

Figure 33 Partially spin-lattice relaxed DMS/BPAC broadline spectra. τ is the time between the spin-inverting pulse and the sampling of the spectra.

centers of the DMS blocks. The narrower this line, the less restricted is the motion at the centers of the DMS blocks.

The spectra in the other figures for this copolymer at lower temperatures show that the broad resonance produced by protons at the ends of the DMS blocks becomes broader as the temperature is lowered. This means the molecular motion at the ends of the DMS blocks is reduced as the temperature is lowered. The narrow inverted resonance also broadens with decreasing temperature but to a lesser degree. This means the motion at the centers of the DMS blocks is not reduced as much as that at the ends as the temperature is lowered. At 219 K, an interesting result is seen; the narrow inverted resonance becomes upright. This happens because at 219 K the DMS protons relax to the lattice faster than the BPAC protons. This reversal in the relative rates of spin-lattice relaxation for the DMS and BPAC protons at low temperatures was demonstrated in the multiple-pulse T_1 experiments, e.g., see Figure 27.



GP77-0962-40

Figure 34 Partially spin-lattice relaxed DMS/BPAC broadline spectra. τ is the time between the spin-inverting pulse and the sampling of the spectra.

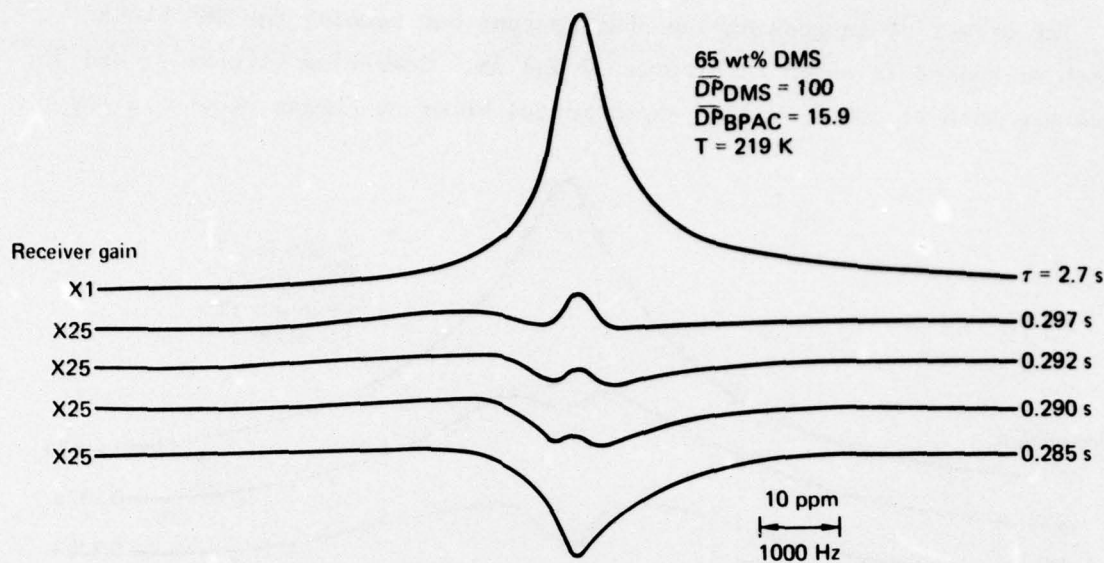


Figure 35 Partially spin-lattice relaxed DMS/BPAC broadline spectra. τ is the time between the spin-inverting pulse and the sampling of the spectra.

The effect of reducing the block lengths of the copolymer but keeping the composition the same is shown in Figure 36. These spectra are for 303 K and should be compared with the 303 K spectra shown in Figure 32. The spectra for the samples with shorter block lengths have increased linewidths for the protons at the centers of the DMS blocks, but the linewidths of the protons at the ends of the DMS blocks are unchanged; hence, only the molecular motion at the centers of the DMS blocks is reduced by decreasing the block lengths.

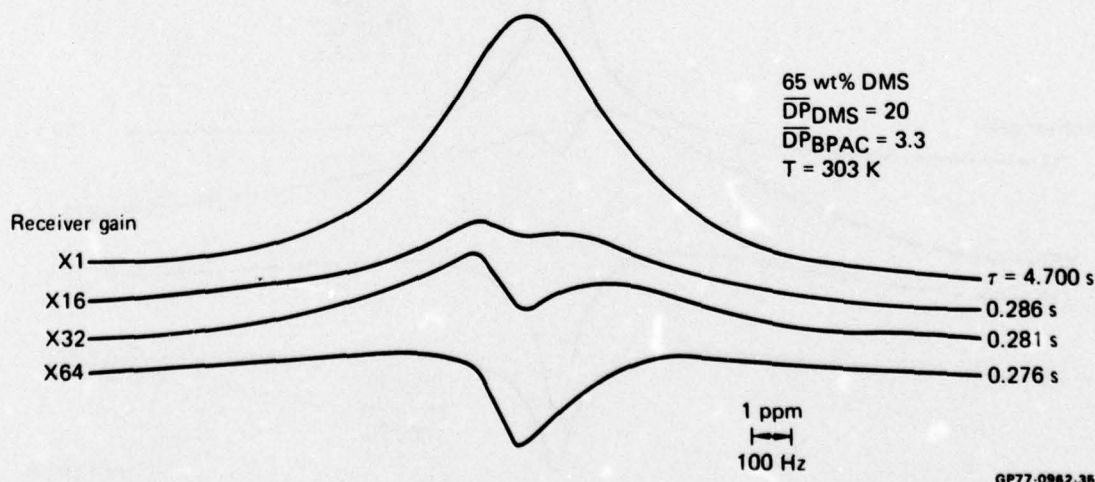


Figure 36 Partially spin-lattice relaxed DMS/BPAC broadline spectra. τ is the time between the spin-inverting pulse and the sampling of the spectra.

The effect of increasing the BPAC content but keeping the DMS block length unchanged is shown in Figures 37 and 38. Comparing Figures 37 and 36, which are both at 303 K, within experimental error no change occurs in the

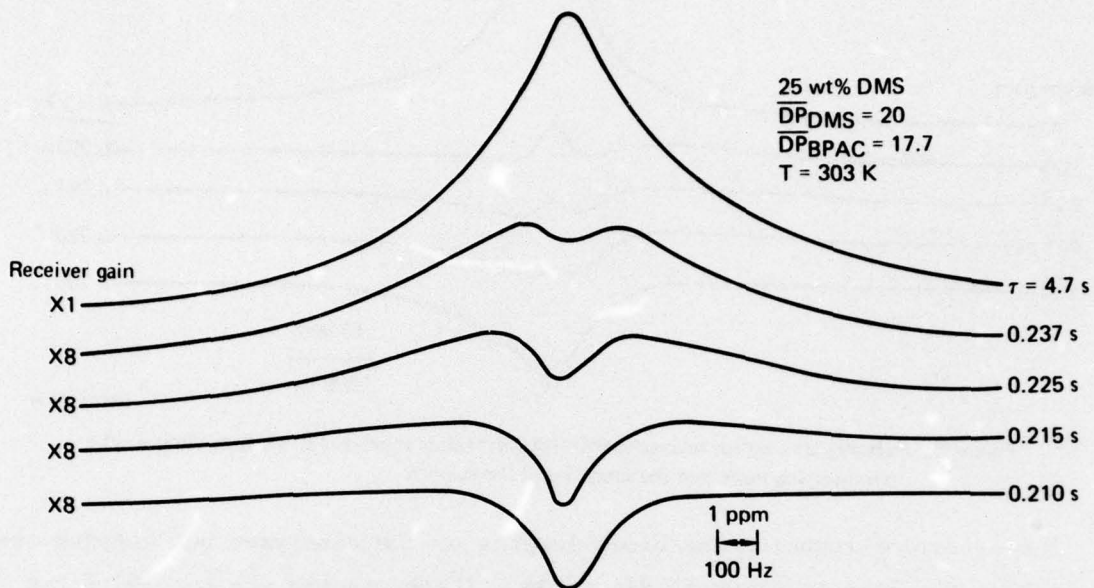


Figure 37 Partially spin-lattice relaxed DMS/BPAC broadline spectra. τ is the time between the spin-inverting pulse and the sampling of the spectra.

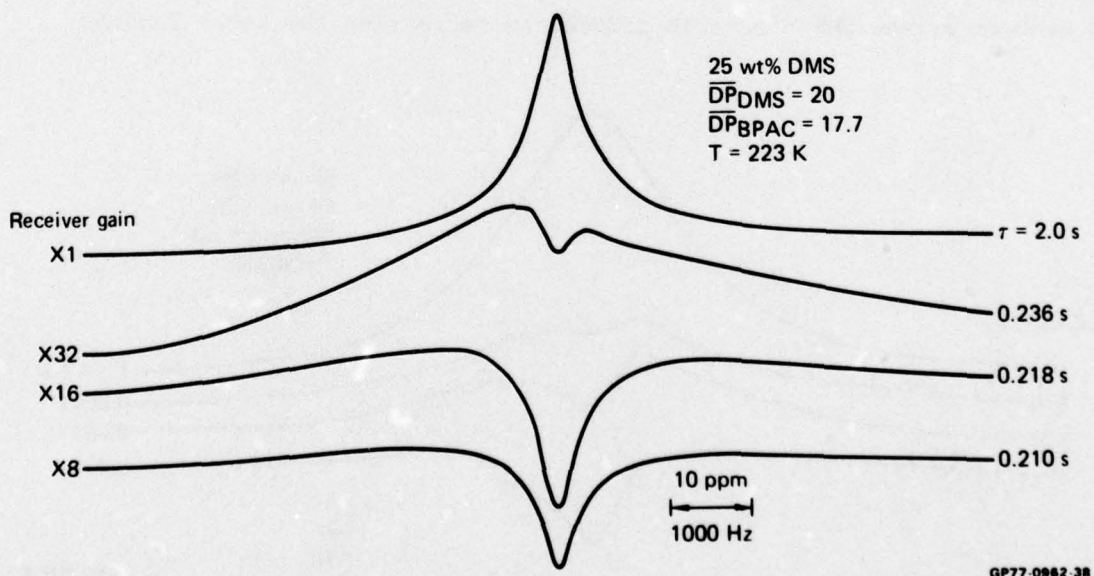


Figure 38 Partially spin-lattice relaxed DMS/BPAC broadline spectra. τ is the time between the spin-inverting pulse and the sampling of the spectra.

resonance width of the protons at the centers of the DMS blocks, but the resonance width of the protons at the ends of the DMS blocks increases as the composition is changed from 65 wt% DMS to 25 wt% DMS and the DMS block length is kept at $\overline{DP}_{DMS} = 20$. The ends of the DMS blocks are probably more rigid in the 25 wt% copolymer because the BPAC domains are larger than in the 65 wt% copolymer.

Thus, for the compositions and block lengths studied, the motion at the centers of the DMS blocks is not a function of composition but is only a function of DMS block length. The motion at the ends of the DMS blocks as a function of composition and block length cannot be simply described from these results.

It is not obvious whether the effects of the increased molecular motion at the centers of the DMS blocks are caused by a decrease in the correlation time for molecular motion τ_c , an increase in extent of motion, or a combination of these two. If it is assumed that above 170 K the correlation time τ_c is less than the low-temperature value of the spin-spin relaxation time T_{2LT} ($= 10^{-5}$ s), then the NMR linewidth is primarily governed by the extent of the motion and not by the correlation time for the motion. In this case, a model can be used to estimate the spatial restriction to molecular motion.²² If it is further assumed that the radius vectors joining adjacent monomer units move rapidly in all directions but are excluded from a cone of half angle θ_o , then the measured value of T_2 ($= 1/2\pi f_{1/2}$) is given by

$$T_2 = \frac{T_{2LT}}{\sin^2 \theta_o} \cdot \quad (6)$$

Thus, the broad upright and narrow inverted resonance linewidths can be used in this equation to provide an estimate of the freedom of motion at the ends and centers of the DMS blocks, respectively. The smaller the value of θ_o , the less restricted and more isotropic is the molecular motion.

The order parameter S_p , which does not depend upon a particular physical model, can also be used to characterize anisotropic molecular motion. It is the average of the angle-dependent dipolar interaction,

$$S_p = \frac{1}{2} \langle 3 \cos^2 \theta - 1 \rangle \cdot \quad (7)$$

The order parameter is equal to zero for isotropic motion, and it increases toward 1 as the motion becomes more restricted. If the correlation time for molecular motion is less than the low-temperature spin-spin relaxation time T_{2LT} , then

$$S_p = \frac{T_{2LT}}{T_2} \quad (8)$$

These parameters are used to quantitatively characterize the molecular motion at the centers and ends of the DMS blocks as a function of temperature and block length and are listed in Table 2.

TABLE 2 DMS MOTION INFERRED FROM PARTIALLY RELAXED BROADLINE SPECTRA

Sample	Temperature (K)	Linewidth, $f_{1/2}$ (Hz)		Restricted anisotropic molecular motion parameters			
		Broad upright line	Narrow inverted line	Ends of DMS blocks		Centers of DMS blocks	
				θ_o (deg)	S_p	θ_o (deg)	S_p
25 wt % DMS	303	630	75	11	0.04	3.9	0.0047
$\overline{DP}_{DMS} = 20$	248	1770	83	19	0.11	4.1	0.0052
$\overline{DP}_{BPAC} = 17.7$	224	3000	146	26	0.19	5.5	0.0092
65 wt % DMS	303	350	20	8.5	0.022	2.0	0.0012
$\overline{DP}_{DMS} = 100$	249	500	21	10	0.031	2.1	0.0013
$\overline{DP}_{BPAC} = 15.9$	234	540	25	10	0.034	2.3	0.0016
	219	1250*	210**	16	0.079	6.5	0.013

*Inverted because DMS protons relax faster than BPAC protons at this temperature.

**Upright because DMS protons relax faster than BPAC protons at this temperature.

GP77-0962-54

3. PLASTICIZER EFFECTS IN BLOCK COPOLYMERS

3.1 EPR Studies

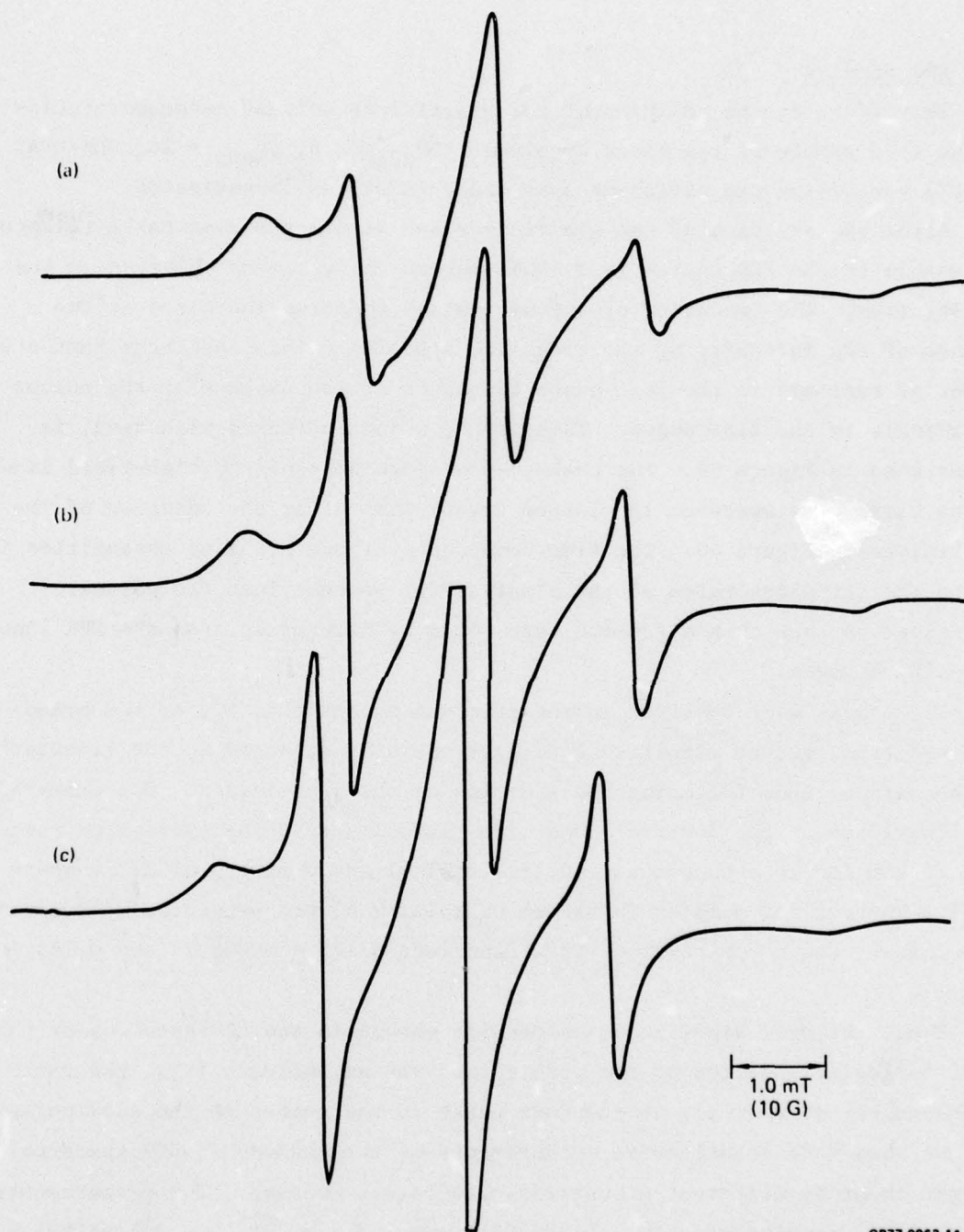
The effect of the addition of the plasticizer solvent perdeuterocyclohexane to a sample of the block copolymer ($\overline{DP}_{BPAC} = 6$, $\overline{DP}_{DMS} = 20$; DMS/BPAC = 50 wt%) containing the nitroxide spin probe TANOL was investigated.

After the addition of the plasticizer and within the time taken to return the sample to the EPR cavity (~ 3 min), marked changes were observed in the EPR spectrum. The intensity of the narrowline spectrum increased at the expense of the intensity of the broadline spectrum. This indicates that the number of radicals in the fast phase increases at the expense of the number of radicals in the slow phase. This trend, which increased with time, is illustrated in Figure 39. The peak-to-peak intensity of the high-field line of the narrowline spectrum is plotted versus time after the addition of the plasticizer in Figure 40. The time dependence of the EPR line intensities is due to the diffusion rates of the plasticizing solvent into the polymer. This suggests that this diffusion rate could be determined from the EPR line intensity changes.

No changes were observed in the extremum splittings, A'_2 , of the broadline spectrum, and no significant changes could be detected in the linewidths of the narrow lines following the addition of the plasticizer. For example, the linewidths of the low-field and high-field lines of the narrowline spectrum of samples in a vacuum were 0.18 ± 0.01 mT and 0.20 ± 0.01 mT, respectively, whereas for samples in vacuum containing 43 wt% perdeuterocyclohexane plasticizer, the corresponding linewidths were 0.175 ± 0.005 mT and 0.185 ± 0.01 mT.

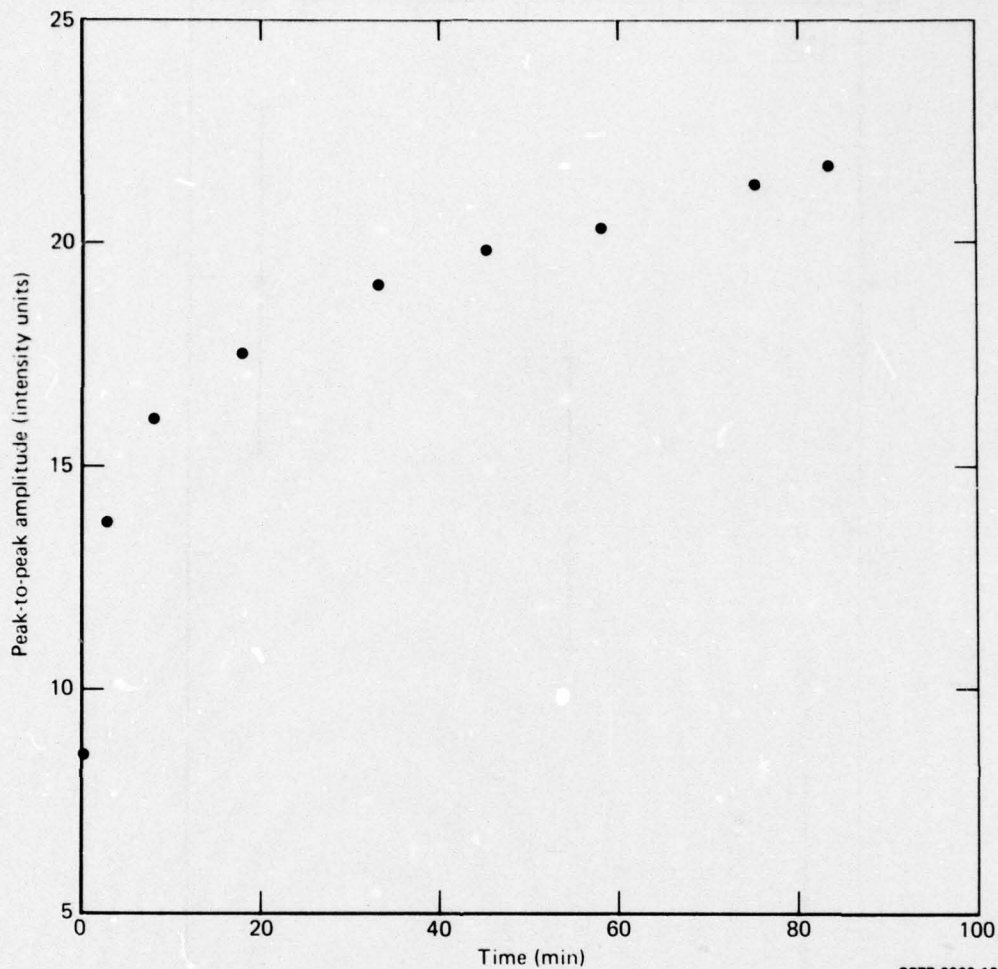
Thus, the only significant observable change in the EPR spectrum of the TANOL following addition of the plasticizer was an increase in α , the ratio of the number of radicals in the fast phase to the number in the slow phase.

We have made quantitative measurements of the changes in EPR spectrum brought about by different amounts of plasticizer content. The measurements were made in samples with 50 wt% DMS/BPAC ($\overline{DP}_{BPAC} = 6$, $\overline{DP}_{DMS} = 20$) at 294 K exposed to air. Figure 41 is a plot of α , the ratio of the areas under the narrowline and broadline absorption spectra as determined by the double integration method of the derivative spectra as described in Section 2.2.5, versus the wt% of plasticizer content. As can be seen from Figure 41,



GP77-0962-14

Figure 39 EPR spectra observed in a block copolymer sample containing TANOL (a) before the addition of the perdeuterocyclohexane plasticizer, (b) 8 min, and (c) 75 min after the addition of the plasticizer. The sample had a 50 wt% BPAC/DMS ratio with $\overline{DP}_{DMS} = 20$ and $\overline{DP}_{BPAC} = 6$.



GP77-0982-13

Figure 40 Peak-to-peak height of the high field line in fast phase versus time after addition of the perdeuterocyclohexane plasticizer to the sample. The sample which had a DMS/BPAC ratio = 50 wt% and block lengths $\bar{DP}_{DMS} = 20$, $\bar{DP}_{BPAC} = 6$ contained TANOL.

for small values of α (below plasticizer contents of 30 wt%), there is an approximate linear relation between α and plasticizer content. Above 30 wt%, the data in Figure 41 would appear to indicate a deviation from linearity. Unfortunately, as α increases, the uncertainty in its value also increases. As is described in Section 2.2.5, this arises because of the uncertainty in estimating the area under the center narrow line because of the spectral overlap with the broadline spectrum.

Since neither the narrowline or broadline spectrum changes shape with increasing plasticizer content, the ratio of the height of the low-field peaks in the narrowline (h_f in Figure 42) and broadline spectrum (h_s in

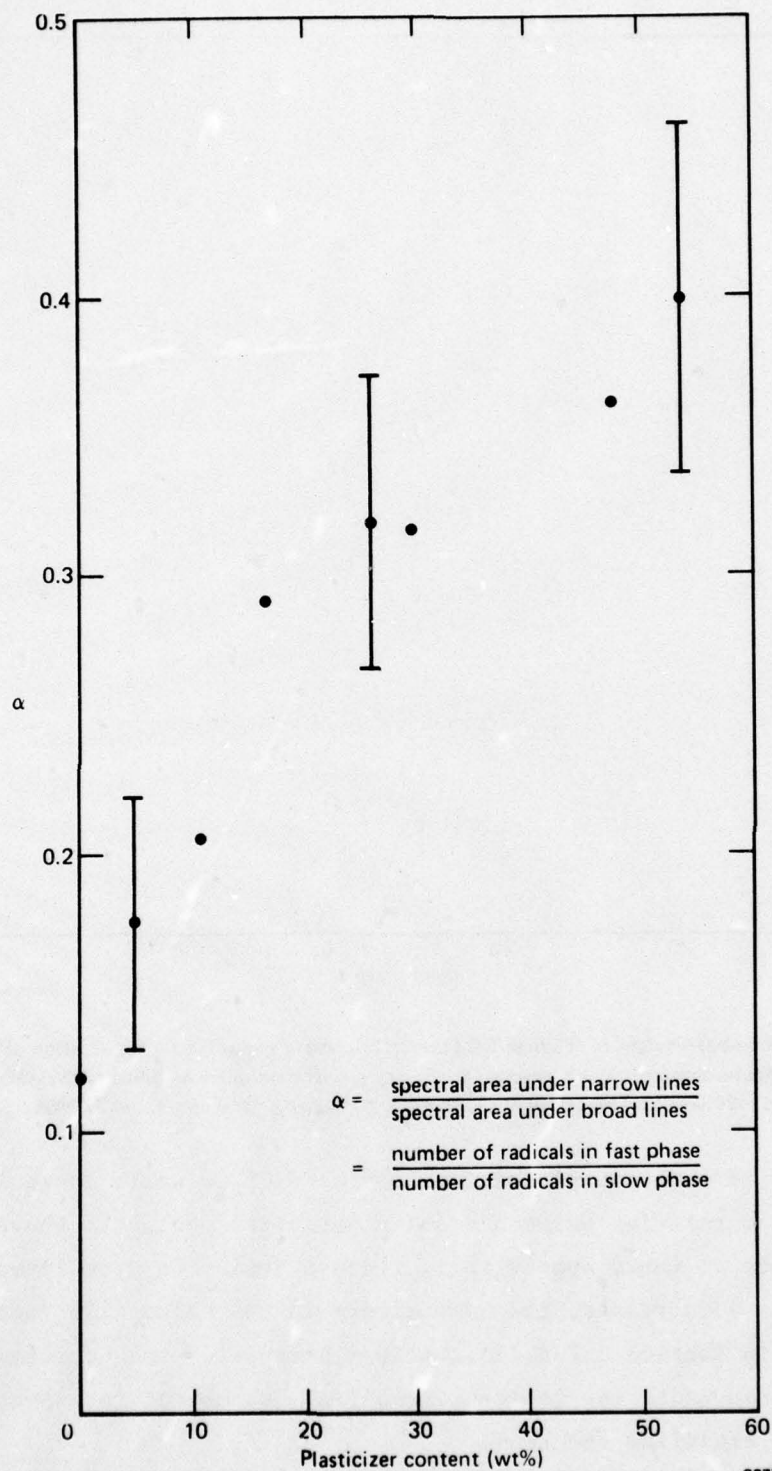
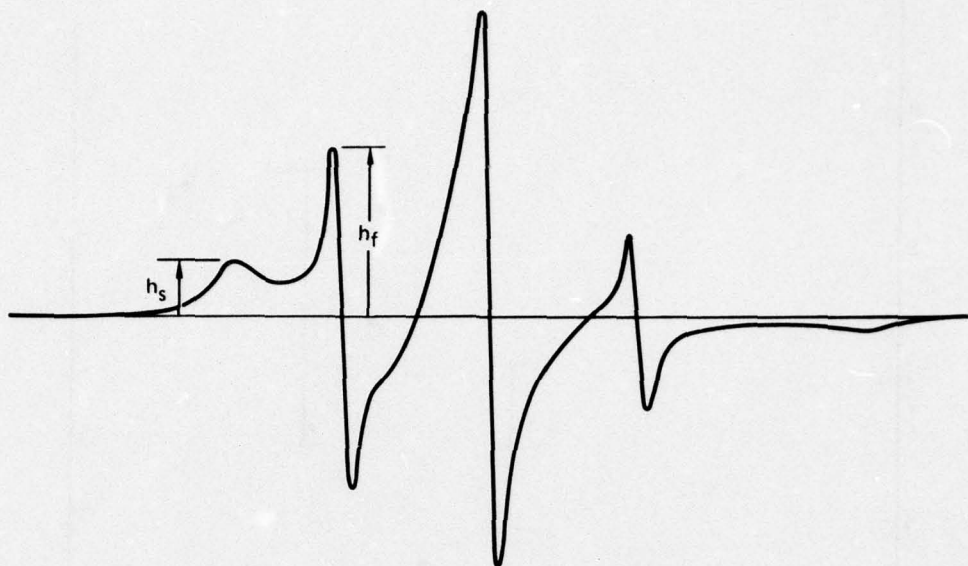


Figure 41 A plot of α versus plasticizer content. The block copolymer sample was 50 wt% DMS/BPAC ($\overline{DP}_{BPAC} = 6$, $\overline{DP}_{DMS} = 20$); the plasticizer was perdeuterocyclohexane.



GP77-0962-43

Figure 42 An illustration of λ , the peak height ratio ($= h_f/h_s$).

Figure 42) should be proportional to α , the ratio of the number of radicals in the fast phase to the number of radicals in the slow phase. We have measured this peak height ratio ($\lambda = h_f/h_s$) versus plasticizer content, and the results are plotted in Figure 43. There is some spectral overlap of the low-field peaks of the broadline and narrowline spectra. This overlap was estimated by assuming a Lorentzian lineshape for the low-field narrow line and calculating its contribution at the magnetic field value corresponding to the low-field peak of the broadline spectrum. This contribution was calculated to be 0.85% of the low-field narrowline intensity. The measured values of λ which were corrected for this overlap are plotted in Figure 43, which shows that λ is linearly proportional to plasticizer content up to values of 50 wt% plasticizer.

The only significant changes observed following the addition of the perdeuterocyclohexane plasticizer, viz., the increase in intensity of the narrowline spectrum and corresponding decrease in intensity of the broadline spectrum, can be rationalized in terms of the model described in Section 2.2.6. The effect of the plasticizer is to restore the segmental motional activity to the DMS blocks which are restricted by the rigid BPAC domains.

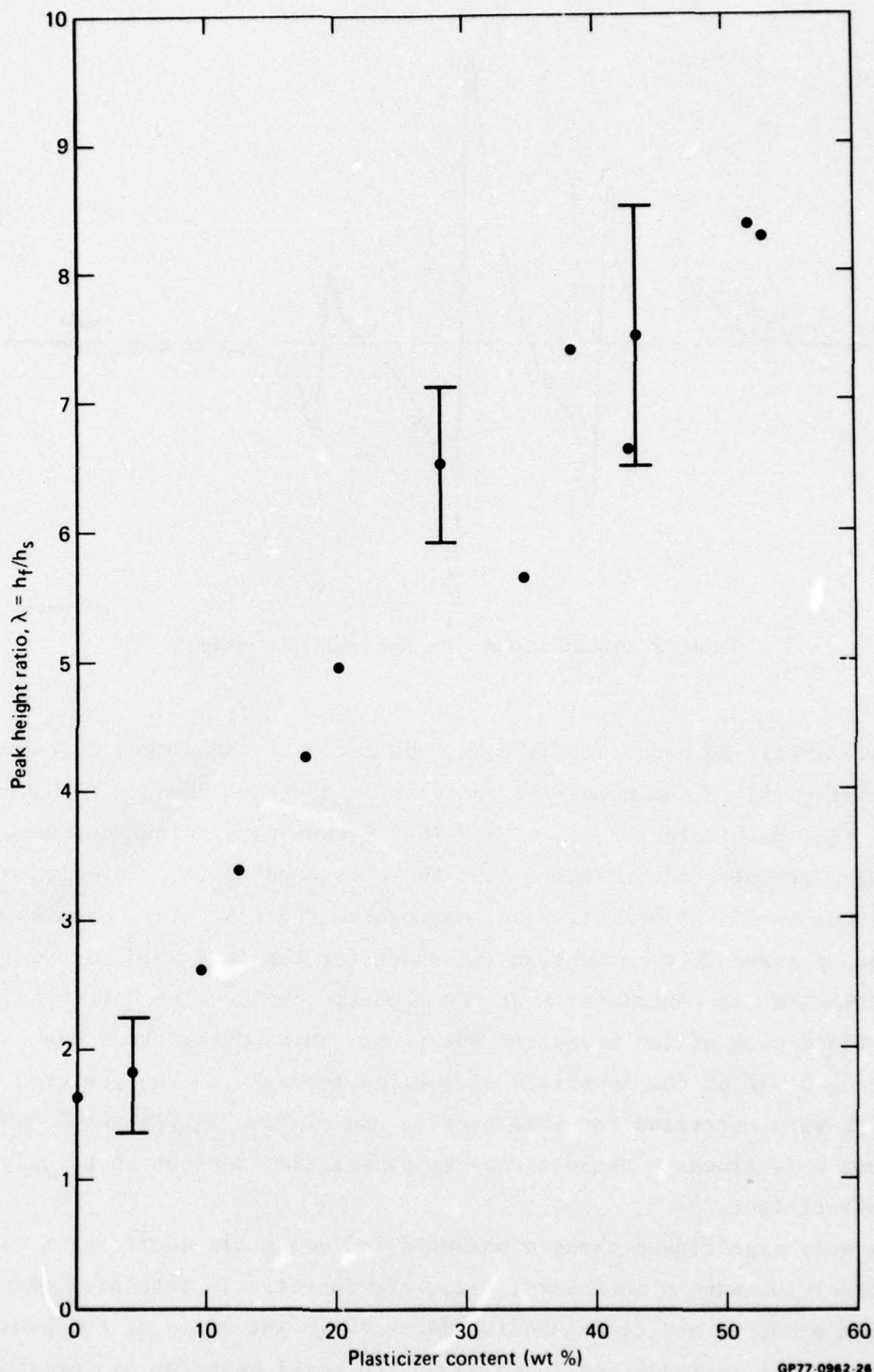


Figure 43 A plot of λ , the ratio of the peak heights of the low-field lines in the narrowline and broadline spectra versus perdeuterocyclohexane plasticizer content.

In so doing, the TANOL radicals bound to these DMS blocks are released and go from the slow phase to the fast phase. The EPR linewidths show that once in the fast phase, the motions of the TANOL radical are affected little by the presence of the plasticizer, i.e., below 50 wt% plasticizer.

It is interesting to compare the EPR plasticizer results with the temperature dependence of the EPR spectra. From Figure 41, the addition of 50 wt% plasticizer increases α from $\alpha = 0.12$ to $\alpha = 0.4$; the corresponding temperatures at which $\alpha = 0.12$ and $\alpha = 0.4$ are seen from Figure 16 to be 293 and 345 K. Thus, the addition of 50 wt% perdeuterocyclohexane produced the same EPR results as though the sample temperature had been raised by 52 K. Alternatively, this may imply that the addition of 50 wt% plasticizer is equivalent to a lowering of the T_g of the central regions of the DMS blocks by 52 K.

3.2 NMR Studies

Perdeuterocyclohexane (C_6D_{12}) was used to plasticize a 50 wt% DMS/BPAC copolymer with $\overline{DP}_{DMS} = 20$ and $\overline{DP}_{BPAC} = 6$. Perdeuterocyclohexane is a good solvent for DMS and a poor solvent for BPAC, and LeGrand²³ has shown that it preferentially plasticizes the DMS component of the copolymer.

Broadline spectra of this copolymer at 303 K in the presence of atmospheric oxygen with plasticizer contents between 50 and 90 wt% resolved an aromatic proton resonance and a methyl proton resonance. This is shown for a 59 wt% plasticized sample in Figure 44 for $\tau = 2.7$ s. The aromatic resonance line appears to be a superposition of a narrow and a broad line. The narrow aromatic line and the methyl line are both about 130 Hz wide, and the broad aromatic line is about 370 Hz wide. In the unplasticized copolymer, the aromatic line is about 7 000 Hz wide, and the methyl line is about 300 Hz wide at room temperature, so the plasticizer had a considerable effect on the linewidth and, hence, molecular motion in both DMS and BPAC components.

The ratio β of the number of protons in the rubbery phase to the number in the rigid phase was determined from the free-induction decay signal, as described in Section 2.3.3. For a 59 wt% plasticized sample, the free-induction decay consisted of two Lorentzian components with amplitudes of 0.275 and 0.725 and relaxation times of 23 μ s and 958 ± 144 μ s, respectively. This yields a β of 2.64, which is greater than the value of $\beta = 1.5$ measured in the unplasticized copolymer. From the known composition, the ratio of the number of protons in the DMS to the number in BPAC is 1.47; therefore, approximately 32% of the BPAC protons contribute to the rubbery signal.

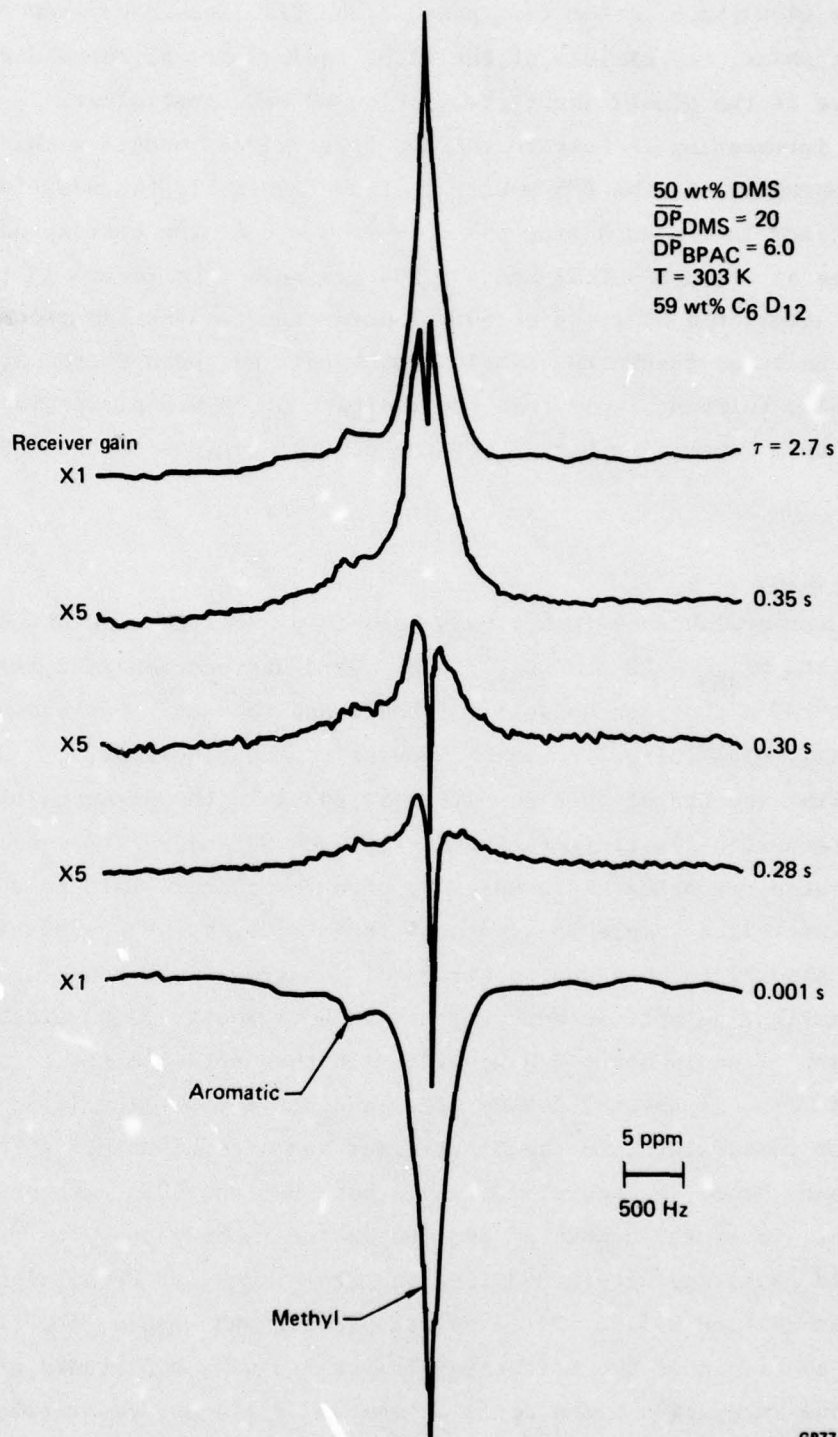


Figure 44 Partially spin-lattice relaxed plasticized DMS/BPAC broadline spectra. τ is the time between the spin-inverting pulse and the sampling of the spectra.

The ratio β was also determined from the ratio of areas beneath the resonance peaks in the broadline spectra. The ratio of the area beneath the aromatic resonance to the area beneath the methyl resonance was 0.15 ± 0.05 . The large uncertainty arises from overlap of the resonances. From the known composition, the ratio of the number of BPAC aromatic protons to total number of DMS and BPAC methyl protons is 0.31. If 32% of the BPAC protons are in a rubbery region as previously determined from the free-induction decay signal, this ratio becomes 0.12 and agrees with the measured ratio of the areas beneath the resonance peaks. Thus, the 59 wt% C_6D_{12} plasticizes about 32% of the BPAC component as well as plasticizing the DMS component.

We attempted to determine why the aromatic resonance contained both broad and narrow lines. Since the width of the narrow aromatic resonance was approximately equal to that of the DMS resonance, these aromatic protons must have mobilities similar to those of the DMS protons. Because of the method used in synthesizing this copolymer,⁵ about 30% of the DMS blocks contain bisphenol-A (BPA) monomers instead of the average BPAC hexamer. Thus, it might be possible that the narrow aromatic resonance results from aromatic protons in the non-associated BPA monomers which move with the DMS. However, only 4.7% of the aromatic protons are located in the BPA monomers; hence, the remaining 27.3% (32% - 4.7%) of the aromatic protons must be located in BPAC blocks which have been plasticized. Since the measured ratio of the areas beneath the narrow and broad aromatic resonances was about 0.41, which was much larger than the expected value of $4.7\%/27.3\% = 0.17$, we conclude that the BPA aromatic protons could not have produced the entire narrow resonance. Thus, aromatic protons in non-associated BPAC blocks must also contribute to this narrow resonance.^{18,23}

The other spectra shown in Figure 44 are partially spin-lattice relaxed, broadline spectra. The narrow inverted resonance peak seen in these spectra at $\tau = 0.28, 0.30, \text{ and } 0.35 \text{ s}$ is attributed to protons with increased molecular motion at the centers of the DMS blocks. This was seen in the nonplasticized copolymers, but the effect is greatly enhanced with the plasticizer. We believe that this enhanced effect is a result of decreased spin diffusion along the DMS blocks caused by the presence of the plasticizer. The bulk average T_1 for the DMS and BPAC protons, as determined from these spectra, was 0.45 s, which, when corrected for the presence of oxygen,¹⁹ would be 0.52 s.

The plasticizer has an effect on the copolymer which is equivalent to an increase in temperature. This equivalence can be obtained from Figure 23 which shows that the value of $\beta = 2.64$ observed in the 59 wt% plasticized copolymer at 303 K is observed in the unplasticized copolymer at the higher temperature of 362 ± 25 K. Also, this equivalence can be obtained from the T_1 data in Figure 20, which show that the $T_1 = 0.52$ s observed in the 59 wt% plasticized copolymer at 303 K (corrected for oxygen effects) was observed in the unplasticized copolymer at 345 K.

4. EPOXY RESINS

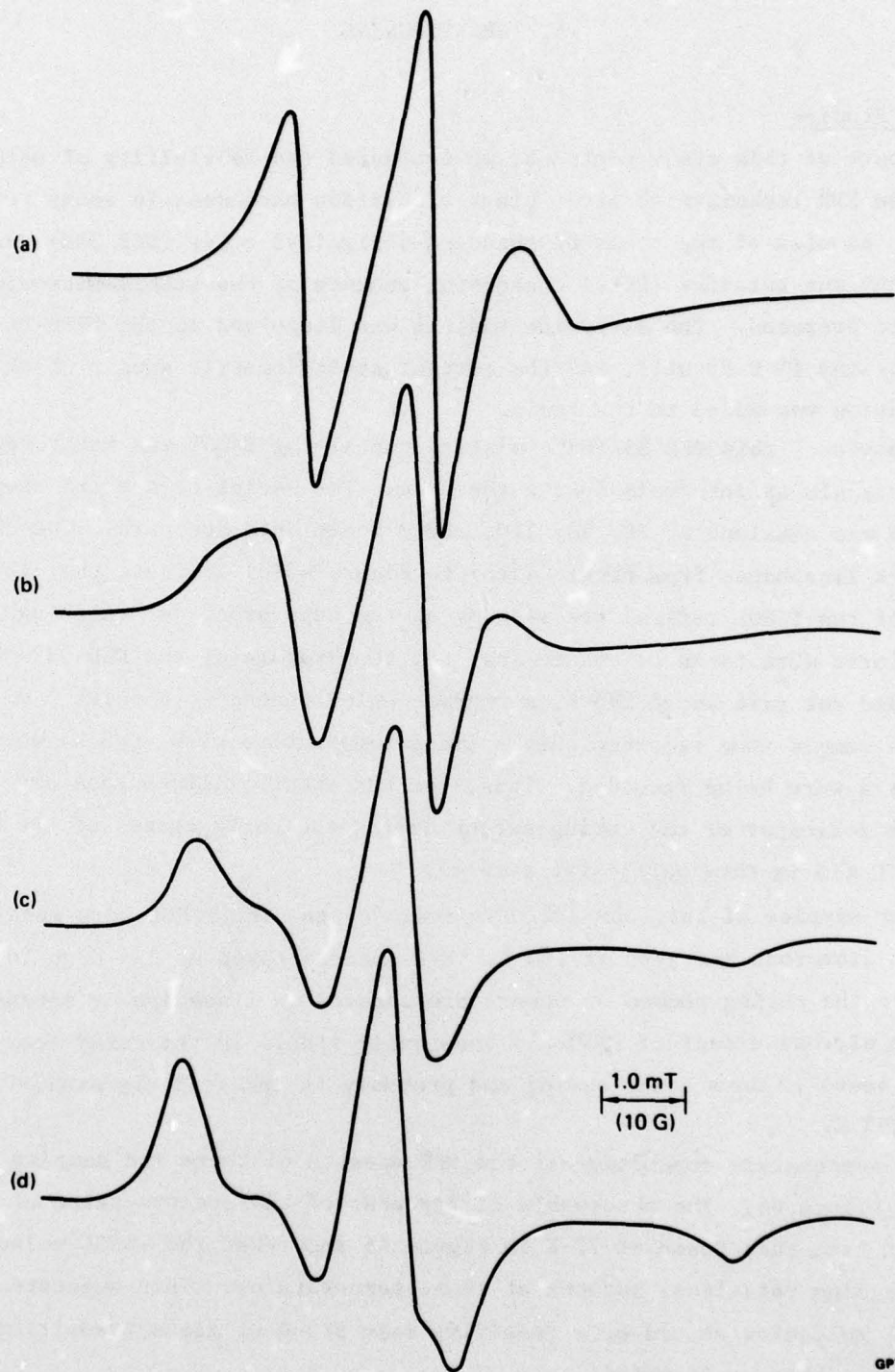
4.1 EPR Studies

As part of this study contract, we evaluated the feasibility of using the spin probe EPR technique to study glass transition phenomena in epoxy resin systems. Samples of the resin bisphenol-A-diglycidyl ether (DER 332) cured with diethylene triamine (DETA) containing amounts of the stable nitroxide TANOL were prepared. The nitroxide radical was dissolved in the DETA to known concentrations (~ 0.09 wt%), and the correct stoichiometric amount of this DETA solution was added to the resin.

A sample of this DER 332/DETA mixture containing TANOL was monitored by the EPR signals at intervals during the cure. The series of spectra shown in Figure 45 was obtained at 30, 60, 120, and 270 min into the cure. The changes in the EPR lineshapes from Figure 45(a) to Figure 45(d) indicate that the motions of the TANOL radical are slowing as the cure proceeds. Although no great efforts were taken to ensure that the temperature of the DER 332/DETA mixture did not rise above 293 K, a thermocouple located at a point 3 mm below the sample tube recorded only a small temperature rise (< 3 K) when the spectra were being recorded. Thus, the EPR spectral lineshapes are a sensitive indicator of the curing extent during the early stages of the cure (up to 270 min in this particular sample).

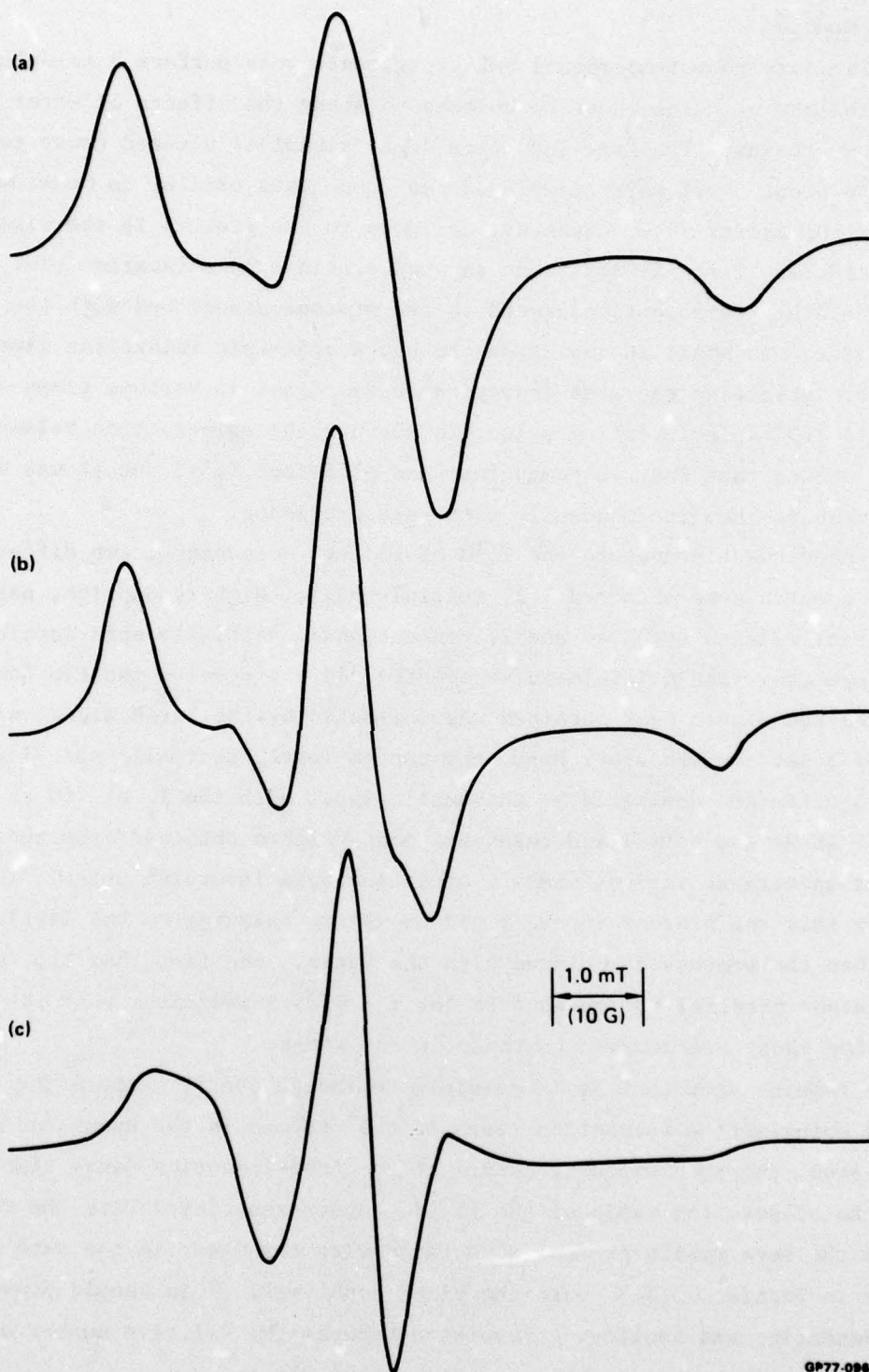
Other samples of this DER 332/DETA resin containing TANOL were molded into 4 mm diam rods and kept at 293 K. EPR spectra taken at 293 K up to 15 days after the curing showed no observable changes in lineshape or intensity. Thus, the nitroxide radical TANOL is chemically stable in the cured epoxy rods up to at least 15 days after curing and probably is indefinitely stable if kept at 293 K.

The temperature dependence of the EPR spectra of these rod samples is shown in Figure 46. The observable differences of the spectra taken at 373 K and 293 K from that taken at 77 K in Figure 46 show that the TANOL molecules are undergoing rotational motions at these temperatures. This suggests that the TANOL molecules should be a sensitive spin probe of glass transition phenomena in this resin matrix.



GP77-0962-20

Figure 45 EPR spectra of the TANOL radical spin probe dissolved in a mixture of bisphenol-A diglycidyl ether (DER 332) and the hardener, diethylene triamine (DETA): (a) 30 min into cure, (b) 60 min into cure, (c) 120 min into cure, (d) 270 min into cure.



GP77-0862-19

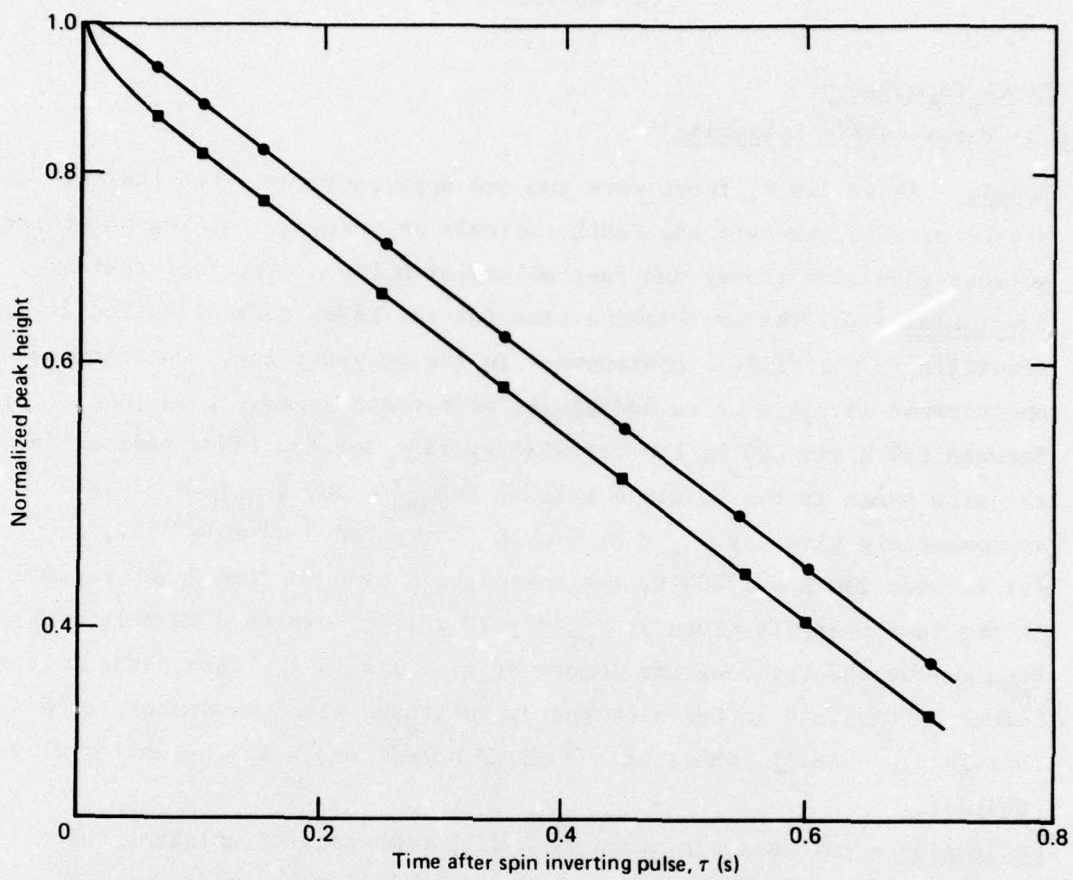
Figure 46 EPR spectra of the TANOL radical spin probe in samples of DER 332/DETA after complete cure (15 days): (a) taken at 77 K, (b) taken at 293 K, (c) taken at 373 K.

4.2 NMR Studies

Preliminary room-temperature NMR experiments were performed to determine the feasibility of using these techniques to study the effects of water in cured epoxy resins. The free-induction decay signal of a cured epoxy resin containing about 3 wt% water displayed two components similar to those seen in the block copolymer. One component, assigned to the protons in the rigid epoxy resin, was large in amplitude and had a spin-spin relaxation time T_2 of 8 μ s. The other component, assigned to the protons associated with the more mobile water, was small in amplitude and had a spin-spin relaxation time T_2 of 260 μ s. Observing the free-induction decay signal at various times after applying a 180° spin inverting pulse, to measure the spin-lattice relaxation time T_1 , showed that the two components had different T_1 's, but it was difficult to measure them independently with good precision.

To independently measure the T_1 's of the two components, two different types of spectra were obtained: 1) multiple-pulse, high-resolution, partially spin-lattice relaxed spectra, and 2) conventional, partially spin-lattice relaxed spectra. The multiple-pulse spectra did not resolve the two components, and the single peak obtained was dominated by the large signal with the T_2 of 8 μ s. On the other hand, the conventional, partially spin-lattice relaxed spectra are dominated by the small signal with the T_2 of 260 μ s. Figure 47 shows the normalized resonance peak heights obtained from these two different spectra at various times τ after the spin inverting pulse. These data show that the protons in the rigid epoxy are relaxing to the lattice slower than the protons associated with the water. The fact that the two curves become parallel to one another for $\tau > 0.05$ s indicates that the protons in the epoxy are coupled to those in the water.

The results show that it is possible to independently measure the spin-spin and spin-lattice relaxation times of the protons in the epoxy and the water. Also, the two-component nature of the free-induction decay signal can be used to measure the ratio of the rigid protons associated with the cured epoxy to the more mobile protons associated with the water in the same way as was done in Section 2.3.3 with the block copolymer. This should prove useful in detecting and monitoring reversion because the relative number of mobile protons increases as the reversion takes place.



GP77-0962-29

Figure 47 Spin-lattice relaxation of the epoxy (●) and water (■) protons in a moist, cured epoxy sample.

5. CONCLUSIONS

5.1 Block Copolymers

Electron Paramagnetic Resonance

- Result - Above 220 K, there were two and apparently only two radical phases present, wherein the TANOL radicals are undergoing slow molecular motions (the slow phase) and fast molecular motions (the fast phase).
Conclusion - (a) The correlation time for the TANOL radical motion is sensitive to the radical environment in the polymer, i.e., whether the environment is rigid or is undergoing main-chain segmental motions. (b) Between 230 K and 293 K, the correlation time for the TANOL radical in the slow phase in the 50 wt% copolymer ($\overline{DP}_{DMS} = 20$, $\overline{DP}_{BPAC} = 6$) is approximately given by $\tau_{cs} = 2.56 \times 10^{-10} \exp(10.5 \text{ kJ mole}^{-1}/RT) \text{ s}$. (c) Between 250 K and 300 K, the correlation time for the TANOL radical in the fast phase is given by $\tau_{cf} = 5.25 \times 10^{-12} \exp(9.3 \text{ kJ mole}^{-1}/RT) \text{ s}$.
- Result - α , the ratio of the number of radicals in the fast phase to the number of radicals in the slow phase, increased with temperature such that $\ln \alpha \propto -\Delta H/RT$, where $\Delta H = 20.5 \text{ kJ mole}^{-1}$ and R is the universal gas constant.

Conclusion - (a) This variation of α with temperature indicates that there is a distribution of segmental motional activity along the DMS blocks. (b) The radical is bound in the slow phase and 'free' in the fast phase so that when the radical environment undergoes segmental motions, the radical makes a discontinuous jump into the fast phase. Hence, as the temperature is increased, the region of segmental motional activity grows outwards from the centers of the DMS blocks and the number of radicals in the fast phase (and hence α) increases.

Nuclear Magnetic Resonance

- Result - The spin-lattice relaxation time T_1 and the spin-lattice relaxation time in the rotating frame $T_{1\rho}$ were observed to go through minima, and the spin-spin relaxation time T_2 was observed to go through a transition as the copolymer temperature was varied.

Conclusion - The correlation time for DMS motion in the 50 wt% copolymer with $\overline{DP}_{DMS} = 20$ and $\overline{DP}_{BPAC} = 6$ is given by $\tau_c = 4.19 \times 10^{-18} \exp(40.3 \text{ kJ mole}^{-1}/RT) \text{ s}$.

- Result - β , the ratio of the number of protons in the rubbery phase to those in the rigid phase, as determined from the free-induction decays, increased abruptly at the glass transition and then slowly increased as the temperature was increased.
Conclusions - A distribution of glass transition temperatures exists in the DMS component, and, as the temperature is increased, more of the DMS passes through its glass transition and contributes to the rubbery phase. Finally, as the temperature is further increased, some of the BPAC passes through its glass transition and contributes to the rubbery phase.
- Result - The broadline partially spin-lattice relaxed spectra of the DMS component displayed coincident upright and inverted spectral lines whose widths were a function of block length.
Conclusions - The DMS motion at the centers of the DMS blocks is less restricted than the motion at the ends of the DMS blocks, and the motion at the centers becomes less restricted as the DMS block length is increased.
- Result - The widths of the narrow inverted and upright broad resonances seen in the partially spin-lattice relaxed broadline spectra changed disproportionately as the temperature was varied.
Conclusions - As the temperature is increased from below the glass transition, extensive molecular motion occurs in a small region at the centers of the DMS blocks. As the temperature is increased further, this region of extensive motion grows from the centers to the ends of the DMS blocks and behaves as if a distribution of T_g existed along the DMS blocks, T_g being lowest at the centers of the DMS blocks.

5.2 Plasticizer Effects in Block Copolymers

Electron Paramagnetic Resonance

- Result - The EPR spectra of the TANOL spin probe changed upon addition of the perdeuterocyclohexane plasticizer, the most significant effect being that α was linearly proportional to plasticizer content up to 50 wt% amounts of plasticizer.
Conclusion - (a) The size of the DMS regions undergoing segmental motions increases with increasing amounts of perdeuterocyclohexane (i.e., these regions are plasticized), and hence the number of TANOL radicals which are 'free' and in the fast phase also increases. (b) The EPR spectra

could be used to measure plasticizer diffusion rates and plasticizer concentrations in copolymers.

Nuclear Magnetic Resonance

- Result - The presence of a perdeuterocyclohexane plasticizer in the copolymer reduced the NMR linewidth of both the aromatic and methyl proton resonances, but the area beneath the aromatic resonance peak was smaller than expected.

Conclusions - Molecular motion in all of the DMS component and 32% of the BPAC component is increased significantly by the addition of 59 wt% plasticizer.

5.3 Epoxy Resins

Electron Paramagnetic Resonance

- Result - The TANOL spin probe was stable in the DER 332/DETA epoxy resin system, and its EPR spectrum was temperature dependent.

Conclusion - Nitroxide radicals should be sensitive spin probes of glass transition phenomena in this epoxy matrix.

Nuclear Magnetic Resonance

- Result - A cured epoxy resin containing water was found to exhibit two spin-spin and spin-lattice relaxation times.

Conclusion - The moist epoxy is a two-phase system as opposed to a homogeneous system, and the NMR techniques used to study block copolymers will be useful in studying moist epoxy resins.

5.4 General

The conclusions of both the EPR and NMR experiments support the idea that there is a distribution of segmental motion along the DMS blocks and, as the temperature is increased, the segmental motional activity proceeds outward from the centers of the DMS blocks. This implies that the copolymers behave as though there is a distribution of glass transition temperatures associated with the different regions of the DMS blocks.

The values of the correlation times for DMS motion (τ_c), radical motion in the slow phase (τ_{cs}), and radical motion in the fast phase (τ_{cf}) are such that $\tau_{cf} < \tau_c < \tau_{cs}$, e.g., at 250 K $\tau_{cf} = 4.6 \times 10^{-10}$ s, $\tau_c = 1 \times 10^{-9}$ s and $\tau_{cs} = 4 \times 10^{-8}$ s. The relative order of these times is as expected since in the fast phase the radicals are 'free' to undergo end-over-end rotational

motions, and, in the slow phase, there are no segmental motions but only restricted radical motions.

The EPR results with varying composition described in Section 2.2.7 and also the NMR results with the plasticized samples described in Section 3.2 indicate that not all the BPAC blocks are associated into domains.

The results on epoxy resins indicate that further EPR and NMR measurements would provide information concerning the effects of water on glass transition phenomena in epoxy resins as well as plasticizer effects in other polymer systems.

To date, five papers²⁴⁻²⁸ have been presented at conferences which describe, in preliminary form, the work reported herein.

REFERENCES

1. H. M. McConnell, "Molecular Motion in Biological Membranes," Spin Labeling: Theory and Applications, (Academic Press, New York, 1974).
2. P. L. Kumler and R. F. Boyer, "ESR Studies of Polymer Transitions," Macromolecules 9, 903 (1976).
3. J. S. Waugh, L. M. Huber, and U. Haeberlen, "Approach to High Resolution in Solids," Phys. Rev. Letters 20, 180 (1968).
4. R. P. Kambour, "Microdomains in Alternating Block Polymers of Dimethylsiloxane and Bisphenol-A Carbonate," Polymer Letters 7, 573 (1969).
5. H. A. Vaughn, "The Synthesis and Properties of Alternating Block Polymers of Dimethylsiloxane and Bisphenol-A Carbonate," Polymer Letters 7, 569 (1969).
6. These copolymers were obtained from H. A. Vaughn and D. G. LeGrand of the General Electric Company.
7. I. M. Brown, "Electron Spin-Echo Envelope Decays and Molecular Motion: Rotational and Translational Diffusion," J. Chem. Phys. 60, 4930 (1974).
8. I. M. Brown, "Electron Spin Echoes and Spectral Diffusion in Organic Radical Solids," J. Chem. Phys. 55, 2377 (1971).
9. H. A. Resing, "Apparent-Phase-Transition Effect in the NMR Spin-Spin Relaxation Time Caused by a Distribution of Correlation Times," J. Chem. Phys. 43, 669 (1965)
10. D. G. LeGrand, "Mechanical and Optical Studies of Poly(Dimethylsiloxane) Bisphenol-A Polycarbonate Copolymers," Polymer Letters 7, 579 (1969).
11. P. Coffey, B. H. Robinson, and L. R. Dalton, "Rapid Computer Simulation of ESR Spectra," Chem. Phys. Letters 35, 360 (1975).
12. J. H. Freed, "Theory of Slow Tumbling ESR Spectra for Nitroxides," Spin Labeling: Theory and Applications, (Academic Press, New York, 1974).
13. D. Kivelson, "Electron Spin Relaxation in Liquids," Electron Spin Relaxation in Liquids, (Plenum Press, New York, 1972).
14. A. C. Lind, "A Programmable Digital Pulser for NMR," Rev. Sci. Inst. 43, 1800 (1972).
15. David W. McCall, "Nuclear Magnetic Resonance Studies of Molecular Relaxation Mechanisms in Polymers," Acc. Chem. Res. 4, 223 (1971).

16. J. G. Powles, A. Hartland, and J. A. E. Kail, "Proton Magnetic Resonance Relaxation in a Series of Dimethylsiloxane Polymers," *J. Polymer Sci.* 55, 361 (1961).
17. W. K. Rhim, D. D. Elleman, and R. W. Vaughan, "Enhanced Resolution for Solid State NMR," *J. Chem. Phys.* 58, 1772 (1973).
18. A. C. Lind and D. P. Ames, "Multiple-Pulse Reduction of Proton Dipolar Broadening in Solid Copolymers," *J. Polymer Sci. B* 12, 339 (1974).
19. A. C. Lind, "Spin Diffusion Effects in Partially Spin-Lattice Relaxed NMR Spectra of Solid Block Copolymers," *J. Chem. Phys.* 66, 3482 (1977).
20. D. W. McCall and D. R. Falcone, "Nuclear Magnetic Relaxation in Seven Polymers," *Trans. Faraday Soc.* 66, 262 (1970).
21. V. A. Kaniskin, A. Kaya, A. Ling, and M. Shen, "Mechanical and Dielectric Relaxations in Alternating Block Copolymers of Dimethylsiloxane and Bisphenol-A Carbonate," *J. Appl. Polymer Sci.* 17, 2695 (1973).
22. D. W. McCall and E. W. Anderson, "Molecular Motion in Polyethylene. III," *J. Polymer Sci., Part A*, 1, 1175 (1963).
23. D. G. LeGrand, "Molecular Motion in Block Copolymers," *Trans. Soc. Rheol.* 15, 541 (1971).
24. I. M. Brown, "Pulsed and cw EPR Studies of Spin Probes in Solid Polymers," *Bull. Am. Phys. Soc.* 22, 271 (1977).
25. A. C. Lind, "Nuclear Spin Diffusion Effects in Block Copolymers," *Bull. Am. Phys. Soc.* 22, 383 (1977)
26. I. M. Brown and A. C. Lind, "EPR and NMR Studies of Block Copolymers of Bisphenol-A Carbonate and Dimethylsiloxane," Navy Polymer Characterization Meeting, Washington, D.C., 17 May 1977.
27. I. M. Brown, "Spin-Probe EPR Studies in Solid Polymers," Sixth International Symposium on Magnetic Resonance, Banff, Canada, 21 - 27 May 1977.
28. A. C. Lind, "NMR: Spin Diffusion and Molecular Motional Effects," Sixth International Symposium on Magnetic Resonance, Banff, Canada, 21 - 27 May 1977.

DISTRIBUTION

	Copies		Copies
Commander, Naval Air Systems Command Department of the Navy Washington, DC 20361 Attn: AIR-52032F	5	Commanding Officer Naval Air Development Center Warminster, PA 18974 Attn: Code 606	2
Commander, Naval Air Systems Command Department of the Navy Washington, DC 20361 Attn: AIR-320A	1	Commander Naval Weapons Center China Lake, CA 93555 Attn: Code 605	1
Commander, Naval Air Systems Command Department of the Navy Washington, DC 20361 Attn: AIR-954 (for DDC)	10	Director, Naval Research Laboratory Washington, DC 20375 Attn: Code 6110 Code 6170	1 1
Commander, Naval Surface Weapons Center White Oak, Silver Spring, MD 20910 Attn: WR-31	2	Office of Naval Research 800 N. Quincy Street Arlington, VA 22217 Attn: Code 472	1
Commanding Officer Naval Ship R&D Center Annapolis Laboratory Annapolis, MD 21402	1	Stanford Research Institute 333 Ravenswood Avenue Menlo Park, CA 94025	1
Plastics Technical Evaluation Center Picatinny Arsenal Dover, NJ 07801 Attn: Code SMUPA-VP3	2	National Bureau of Standards Institute for Materials Research Washington, DC 20234 Attn: Dr. Leslie Smith	1
Army Materials & Mechanics Research Center Watertown, MA 02172 Attn: Dr. George Thomas	1	Goodyear Aerospace Corporation Akron, OH 44315 Attn: Hugh Boyd	1
Director, Air Force Materials Laboratory Wright Patterson AFB, OH 45433 Attn: AFML/MBE AFML/MXE AFML/MBC	1 1 1	W. E. Woolam Southwest Research Institute 1150 Connecticut Avenue Suite 613 Washington, DC 20036	1
		W. J. Verzino Aerospace Corporation P. O. Box 92957 Los Angeles, CA 90009	1

	Copies		Copies
Battelle Columbus Laboratories 505 King Avenue Columbus, OH 43201 Attn: R. J. Jakobsen	1	Vought Corporation Advanced Technology Center P. O. Box 6144 Dallas, TX 75222	1
Fred A. Keimel, President Adhesive & Sealants Newsletter P. O. Box 72 Berkely Heights, NJ 07922	1	Dr. J. O. Brittain Dept. of Materials Science & Engineering Northwestern University Evanston, IL 60201	1
D. R. Ulrich Air Force Office of Scientific Research Bolling AFB Washington, DC 20332	1	IIT Research Institute 10 W. 35th Street Chicago, IL 60616	1
Lockheed Missile and Space Company, Inc. P. O. Box 504 Sunnyvale, CA 94088 Attn: Clayton A. May	1	University of California Lawrence Livermore Laboratory P. O. Box 808 Livermore, CA 94550 Attn: T. T. Chiao	1
R. W. Lauver NASA Lewis Research Center Cleveland, OH 44135	1		
Boeing Aerospace Company Seattle, WA 98008 Attn: John Hoggatt	1		
Columbus Aircraft Division Rockwell International 4300 E. Fifth Avenue Columbus, OH 43216 Attn: J. Fasold	1		
General Electric R&D Center P. O. Box 8 Schenectady, NY 12301	1		
Office of Naval Research Boston Branch Office 495 Summer Street Boston, MA 02210 Attn: L. H. Peebles	1		
Vought Corporation Aeronautics Division P. O. Box 5907 Dallas, TX 75222 Attn: A. Hohman	1		